# Aspects of Confinement
# in Lattice Gauge Field Theory

**Dissertation**
zur Erlangung des Grades eines
Doktors der Naturwissenschaften

der Fakultät für Mathematik und Physik
der Eberhard-Karls-Universität zu Tübingen

vorgelegt von
**Jochen Gattnar**
aus Ruit auf den Fildern

2005

*Meinen Eltern und meiner Schwester*
*in Dankbarkeit gewidmet*

# Zusammenfassung

Bis zum heutigen Tag stellt das Phänomen des Farbeinschlusses (color confinement) in der Quantenchromodynamik (QCD) ein faszinierendes Problem dar. Der Zentrumsvortexmechanismus beschreibt eine mögliche Erklärung des Farbeinschlusses im rein gluonischen Anteil der QCD. In der vorliegenden Dissertation konzentrieren wir unsere Untersuchungen auf die Bedeutung der Zentrumsvortizes für die Physik im infraroten Bereich der $SU(2)$ Yang-Mills-Theorie mit Hilfe von Monte-Carlo-Simulationen der $SU(2)$ Gittereichtheorie.

Am Anfang geben wir einen kurzen Überblick über die Gittereichtheorie und die verwendeten numerischen Algorithmen, die für die Monte-Carlo-Simulationen notwendig sind. Anschließend führen wir das Bild der Zentrumsvortizes für den Farbeinschluß ein und erklären den Phasenübergang von der Confinementphase in die Deconfinementphase mittels des Perkolation-Deperkolation-Phasenübergangs der Zentrumsvortizes.

Durch einen Vergleich der räumlichen Stringtension sowohl der dreidimensionalen reinen Yang-Mills-Theorie als auch der dreidimensionalen Yang-Mills-Theorie gekoppelt an adjungierte Higgsfelder mit der Stringtension berechnet mit zentrumsprojizierten Linkvariablen, weisen wir nach, daß die räumliche Stringtension zentrumsdominant ist. Desweiteren finden wir eine Vortexflächendichte, die übereinstimmt mit den Ergebnissen aus der vierdimensionalen reinen Yang-Mills-Theorie. Beide Ergebnisse stützen das Zentrumsvortexbild der Hochtemperaturphase der vierdimensionalen Yang-Mills-Theorie.

Darauf folgend untersuchen wir die Bedeutung der Zentrumsvortizes für das Verhalten der Greenschen Funktionen, d.h. der Gluon- und Geistformfaktoren, im Infrarotbereich und ihren Einfluß auf den Farbeinschluß. Mit Hilfe von neuen numerischen Algorithmen berechnen wir direkt die Formfaktoren, die die Abweichung eines Propagators von einem freien Propagator angeben. Die Berechnungen der Formfaktoren werden in der Landaueichung vollzogen. Die in den Formfaktoren enthaltene Information über den Farbeinschluß wird extrahiert, indem die Zentrumsvortizes aus den Konfigurationen der Linkvariablen eliminiert werden. Dies führt auf ein Modell, das keinen Farbeinschluß besitzt.

In der vollständigen, farbeinschließenden Theorie besitzt der Gluonformfaktor ein ausgeprägtes Maximum im mittleren Impulsbereich, während das bekannte Ergebnis aus der Störungsrechnung bei hohen Impulsen reproduziert wird. Nahe den verschwindenden Impulstransfers zeigt der Gluonformfaktor ein von einer Masse dominiertes Verhalten. Betrachtet man das nicht-farbeinschließende Modell, so verliert der Gluonformfaktor im mittleren Impulsbereich an Wert und zeigt eine klare Abweichung von dem Verhalten des Gluonformfaktors der vollständigen Theorie. Desweiteren finden wir einen divergenten Geistformfaktor im Infrarotbereich. Unser Ergebnis stimmt mit der Gribov-Zwanziger-Bedingung für den Farbeinschluß überein. Diese Bedingung setzt die Divergenz des Geistformfaktors am Gribovhorizont in direkten Bezug zu dem Farbeinschluß. Betrachten

ii

wir das nicht-farbeinschließende Modell, so divergiert der Geistformfaktor im Infrarotbereich nicht mehr. Die im Geistformfaktor beinhalteten Signale des Farbeinschlusses gehen verloren, wenn der Beitrag der Zentrumsvortizes eliminiert wird.

Da die laufende Kopplung direkt aus den Gluon- und Geistformfaktoren berechnet werden kann, zeigen wir ihre Abhängigkeit von den Zentrumsvortizes im Infrarotlimes. Die laufende Kopplung der vollständigen Theorie und des nicht-farbeinschließenden Modells reproduzieren das perturbative Verhalten in dem Bereich, in dem die Störungsrechung gültig ist. Im Bereich der mittleren Impulse ist die laufende Kopplung des Modells stark unterdrückt und scheint im Infrarotlimes zu verschwinden, wohingegen die laufende Kopplung der vollständigen Theorie stark ansteigt und sich im Infrarotlimes einer nicht-verschwindenden Konstante anzunähern scheint.

Anschließend vergleichen wir unsere Meßdaten mit den Ergebnissen, die man aus dem Dyson-Schwinger-Zugang erhalten hat. Beide Resultate stimmen qualitativ gut überein. Auch werden die Formfaktoren bei endlichen Temperaturen berechnet. Unsere Resultate bei hohen Temperaturen stimmen ebenfalls mit einer nicht verschwindenden Stringtension überein. Abschließend betrachten wir den Einfluß der Gribovkopien auf die Formfaktoren in der Landaueichung. Die Formfaktoren sind qualitativ stabil gegenüber dem Gribovrauschen.

Schlußendlich konnten wir die Bedeutung der Zentrumsvortizes für das Infrarotverhalten der Greenschen Funktionen der reinen Yang-Mills-Theorie und für den Farbeinschluß aufzeigen. Unsere Resultate stellen eine Beziehung zwischen dem Confinementmechanisum der Zentrumsvortizes und dem Gribov-Zwanziger-Confinementkriterium her.

# Abstract

Down to the present day, the phenomenon of color confinement represents still a challenging problem of quantum chromodynamics. In the pure gluonic sector of QCD, the center vortex confinement mechanism describes a possible explanation of color confinement. In the present thesis, we concentrate our investigations on the relevance of center vortices for the infra-red physics of pure $SU(2)$ Yang-Mills theory by means of Monte-Carlo simulations of $SU(2)$ lattice gauge field theory.

At the beginning, we give a short review of lattice gauge field theory and of the numerical algorithms needed for our Monte-Carlo simulations. Subsequently, we introduce the center vortex mechanism of color confinement and we explain the confinement-deconfinement phase transition of pure Yang-Mills theory by the percolation-depercolation phase transition of center vortices.

By a comparison of the spatial string tension of the three-dimensional pure Yang-Mills theory as well as three-dimensional pure Yang-Mills theory coupled to adjoint Higgs fields with the value of the string tension obtained from the pure center vortex content, we show that the spatial string tension is center dominated. Furthermore, we find a vortex area density being in accordance with the vortex area density of the four-dimensional theory. Both findings support the center vortex picture of the high temperature phase of four-dimensional Yang Mills theory.

Afterwards, we investigate the relevance of center vortices for the behavior of Green's functions, i.e. the gluon and ghost form factors, in the infra-red region and their importance for color confinement. By using novel numerical algorithms, we measure directly the form factors giving the deviation of the propagators from the free ones. The calculations of the form factors were performed in Landau gauge. The information of color confinement encoded in the form factors is extracted by removing the center vortices from the ensemble of link variables by hand. This results in a non-confining model.

In the full, confining theory the gluon form factor has a rather pronounced peak in the medium momentum range, while at high momenta the result obtained by perturbative Yang-Mills theory is reproduced. Close to zero momentum transfer, the gluon form factor is mass dominated. Considering the non-confining model, the gluon form factor looses a good part of strength in the medium momentum range showing a clear deviation form the gluon form factor of the confining theory. Furthermore, we find a divergent ghost form factor in the infra-red region. Our result is in accordance with the Gribov-Zwanziger criterion for color confinement which directly relates the divergence of the ghost form factor at the Gribov horizon to color confinement. If we consider the non-confining model, the ghost form factor ceases to diverge in the infra-red limit. Hence, the signals of confinement encoded in the ghost form factor are lost when the center vortex content of the theory is eliminated.

iv

Using the fact that the running coupling constant can be obtained directly from the gluon and ghost form factors, we show its dependence on the center vortex content in the infra-red limit. The running coupling constants of the full theory and of the non-confining model reproduce nicely the perturbative running coupling constant in the region where perturbation theory holds. In the region of medium momenta, the strength of the running coupling of the non-confining model is strongly suppressed and seems to vanish in the infra-red limit, whereas the running coupling of the full theory increases and seems to reach a non-zero constant in the infra-red limit.

Subsequently, we compare our measured data with the results obtained by the Dyson-Schwinger approach. Both findings are in good agreement on a qualitative level. The form factors are also computed at finite temperatures. Our results at high temperatures agree with a non-vanishing spatial string tension. Finally, we consider the influence of Gribov copies on the form factors in Landau gauge. On a qualitative level, the form factors are stable against Gribov noise.

In conclusion, we have shown the relevance of center vortices for the infra-red behavior of Green's functions of pure Yang-Mills theory and for color confinement. Our results establish a connection between the center vortex mechanism of confinement and the Gribov-Zwanziger confinement criterion.

# Contents

# Chapter 1

# Introduction

At present, the Standard Model of Particle Physics molds our world view of the elementary constituents of matter and of the fundamental interactions in which they are involved. The Standard Model regards three of four fundamental interactions: strong interaction, electromagnetic and weak interaction. The latter two are unified to the Glashow-Salam-Weinberg theory of the electroweak interaction. The fourth and last fundamental interaction, gravitation, is negligible in particle physics[1] and is not incorporated into the standard model so far. The discovery that the variety of physical processes of the universe can be explained in terms of few elementary particles acting under the influence of a small number of fundamental forces is one of the most significant scientific progresses of the last century.

The quark model [GM64], [Zwe64] and the parton model [BP69], [Fey69] describe the known hadron spectrum by introducing quarks and gluons on a phenomenological basis. That hadrons have a substructure was shown in deep inelastic scattering experiments of leptons on hadrons [Bjo69]. From the experimental data one can conclude that the hadrons are a composite of point like particles. If the momentum transfer of the scattering leptons is large, the point particles of matter behave like free particles. This behavior is called asymptotic freedom. Quarks are spin-1/2 particles with fractional charges and they come in six different species, i.e. in six flavors. Assigning quarks to the fundamental representation of the $SU(3)_{\text{flavor}}$ group, one obtains the phenomenologically successful $SU(3)$ schemes for baryons and mesons. In the early days, the model seemed to have difficulties to reconcile Fermi statistics for quarks for all known hadrons, i.e. for the $\Delta^{++}$ particle. It has a charge of $+3/2$, a spin of $+3/2$ and consists of three up quarks violating the Pauli exclusion principle. This problem is resolved by postulating a new internal quantum number for quarks, the color quantum number. If a quark of each flavor has three color states, Fermi statistics is again fulfilled. The quarks are bound into hadrons by the strong interaction, which is

---

[1]Only at extremely high energy ($10^{19}$ GeV, the Planck energy), gravitation has to be considered.

1

mediated by the gluons being gauge bosons. A striking characteristic of quarks is that they are not observed as free particles up to now. They appear in color-less multiplets of $SU(3)_{\text{flavor}}$ transforming as singlets, octets or decouplets. The permanent embedding of quarks inside colorless bounded states is called color confinement.

Nowadays, the fundamental starting point of a theoretical description of hadronic physics are the symmetry principles. For instance, a quantum field theory has to respect Lorentz invariance restricting the form of the action to be a Lorentz-scalar. Lorentz invariance is a symmetry of space-time, but fields can also transform in an internal space. The Maxwell Lagrangian is invariant under local, continuous transformations of the Abelian group $U(1)$, (i.e. under gauge transformation $\Omega(x) \in U(1)$). The invariance under $U(1)$ transformations results in a conserved electric current which itself gives rise to conservation of electric charge. This is the so called Noether theorem. The Noether theorem states that a symmetry of the action of a theory leads to the conservation of a current. On the other hand, we can think of a conserved charge as the generator of the local, continuous transformation under which the Lagrangian of our theory should be invariant. This is the modern approach to construct a relativistic quantum field theory of the basic constituents of matter.

Within the standard model, quantum chromodynamics (QCD) is the quantum field theory describing the strong interactions of the fundamental building blocks of matter. Generally, it is assumed that the strong interactions act only on the color quantum numbers. Up to now, no flavor dependences of strong forces are known. All flavor-dependent effects can be explained by the quark mass differences. The basic degrees of freedom of QCD are thus quarks and gluons, since they are the only fundamental particles carrying the color quantum number. Treating color similarly to the electric charge in electrodynamics and having the Noether theorem in mind, the entire structure of QCD emerges from the requirement of local gauge invariance of the Lagrangian with respect to a phase rotation of the quark fields and from the requirement of renormalizability. Since in QCD we have three different colors, the gauge transformation $U$ becomes a (complex valued) unitary $(3 \times 3)$-matrix, i.e. $U^{\dagger}U = UU^{\dagger} = 1$, with $\det[U] = 1$. Hence, QCD is based on a non-Abelian gauge group $SU(3)$ and is thus called a non-Abelian gauge theory [YM54]. Non-Abelian gauge theories were established as possible candidates for the standard model by the discovery that non-Abelian gauge theories are renormalizable [tH71b], [tH71a], even if their symmetry group is spontaneously broken and the theory thus becomes massive. On this groundwork, the theory of the strong interactions is finally given by the Lagrangian

$$\mathcal{L} = -\frac{1}{4\,g^2}F^{\text{a}}_{\mu\nu}F^{\text{a}\,\mu\nu} + \bar{q}(i\gamma^{\mu}\mathsf{D}_{\mu} - m)q, \qquad (1.1)$$

with the covariant derivative $\mathsf{D}_{\mu} = \partial_{\mu} - iA_{\mu}$ and the coupling strength of the strong interaction $g$. As mentioned before, the gauge group is $SU(3)$ with the

quark fields $q$ in the fundamental representation whereas the flavor index of the quark fields is suppressed and $m$ is the quark mass. The quarks of different flavors have different masses.

The gluons are defined in the fundamental representation by the gauge fields $A_\mu = A_\mu^a \hat{T}^a$, where $\hat{T}^a$ are traceless hermitian $(3 \times 3)$-matrices. The matrices $\hat{T}^a$ are the generators of the $SU(3)$ gauge transformations. The gluon field strength tensor is given by

$$F_{\mu\nu} = \partial_\mu A_\nu - \partial_\nu A_\mu - i[A_\mu, A_\nu]. \tag{1.2}$$

The crucial difference between electrodynamics and QCD is the presence of the commutator on the r.h.s. of eq. (1.2). This commutator gives rise to the gluon-gluon interactions, since the gluons carry color charge and can therefore interact with each other. The color fields do not simply add like in electrodynamics. The QCD field equations are non-linear giving rise to a non-trivial dynamics of strong interactions.

From scattering experiments we know that quarks behave as free particles at high momentum transfers and accordingly at short distances. A striking discovery was that this property, called asymptotic freedom, only occurs in the presence of non-Abelian gauge theories [GW73], [Pol73]. The running coupling $g$ of the strong interaction decreases logarithmically at increasing momentum transfer, so that QCD appears to be a free theory in the high momentum regime. This is the phenomenon of scaling and indicates that quarks act as free particles at high momentum transfers. In this regime, observables calculated in perturbative series in $g$ agree with experimental data showing the validity of QCD in the high momentum regime. On the other hand, the running coupling increases at decreasing momentum transfers. A large coupling constant implies that the quarks bind more tightly together. This is called infrared slavery which is the flip side of asymptotic freedom. The problem of color confinement is not addressable by perturbation theory, since the running coupling becomes large in this domain and perturbative series with respect of the running coupling $g$ are not valid anymore.

Since perturbation theory cannot give evidence of the phenomenon of color confinement, a non-perturbative treatment is needed. Before one defines a non-perturbative approach it is reasonable to simplify the theory. The first approximation is that we only regard the pure gluonic sector of QCD, which defines the pure $SU(3)$ Yang-Mills theory. The masses of the dynamical quark fields are set to infinity so that they appear as static quarks which couple as colored background fields to the dynamical gluons. A potential can be defined between the statical quarks separated by a distance. A demonstrative picture thereof is that the streamlines of the gluonic fields are bundled into a color electric flux tube due to the self interaction of the gluons. If the static quark-antiquark potential rises linearly with distance, we say that the quarks are confined, since it would need an infinite amount of energy to separate the static quarks. The effect of spontaneous

dynamical quark-antiquark pair generation[2] is not included in pure Yang-Mills theory, because of the infinite mass of the quarks. The second approximation is performed by considering the $SU(2)$ group as the gauge group of our theory in contrast to the $SU(3)$ color gauge group of QCD. Despite this simplifications, it is believed that pure $SU(2)$ Yang-Mills theory is sufficient to understand the basic mechanism of color confinement.

In the following chapter we introduce a non-perturbative approach to pure Yang-Mills theory which is suitable to give insight in the color confinement problem: the $SU(2)$ lattice gauge field theory in quenched approximation. We show that the lattice gauge theory recovers the true pure $SU(2)$ Yang-Mills theory in the continuum limit and we show further how measurement data are related to continuum observables.

The third chapter covers how color confinement is related to the static quark antiquark potential and how color confinement appears in lattice gauge theory. Afterwards, we introduce the center vortex confinement mechanism [Man76], [MP79], [tH78] as a possible candidate of an explanation of color confinement. Since it is believed that there exists a phase transition from the confinement phase to a non-confining phase [Lin79], [Shu80], i.e. to the quark-gluon plasma, it is shown that the phase transition can be explained by a percolation-depercolation phase transition of center vortices [LTER99], [ELRT00].

In the next chapter, we address the dimensionally reduced $SU(2)$ pure Yang Mills theory on the lattice in three dimensions which can be viewed as the high temperature limit of the four dimensional theory. In particular, we want to know if the basic observables are dominated by the center vortex content of the gauge fields. If the measurement value of an observable stems mainly from the center of the gauge fields, we say that the observable is center dominant. Center dominance means that the relevant degrees of freedom for observables are center vortices.

In the last three chapters, we concentrate on the Green's function in Landau gauge of pure $SU(2)$ Yang-Mills theory on the lattice. They are of particular interest mainly because of two reasons: 1) We can compare our results with another non-perturbative approach to QCD: the Dyson-Schwinger equations. In this approach, Green's functions are the basic quantities. The Dyson-Schwinger approach suffers mainly from the highhanded truncation of the infinite Dyson-Schwinger series, whereas the lattice approach suffers from the finiteness of the lattice. Hence, a comparison of observables of both approaches is an exciting topic by itself. 2) The gluon and ghost propagators are the basic Green's functions of pure gauge theory. The relevance of center vortices on the behavior of Green's functions in the infra-red limit might shed light on the color confinement problem. Our investigations are extended to Green's functions of the three dimensional theory to achieve a complete view of the center vortex impact on confinement

---

[2]In the flux-tube picture, hadronization is considered as a breaking of the color electric flux tube. New quarks emerge at the ends of the flux tube forming new hadrons.

physics. Finishing, we address the ambiguities of the gauge fixing procedure, the Gribov copies. Gauge fixing is needed for the calculation of Green's functions and we investigated the importance of Gribov copies for the values of Green's functions measured in lattice simulations.

# Chapter 2

# Gauge Field Theory on the Lattice

## 2.1 The Partition Function and the Euclidean Path Integral

The close connection between quantum statistical mechanics and quantum field theory is based on the formulation of the Feynman path integral. This analogy is seen by comparing the quantum field theory in Euclidean path integral form with quantum statistical mechanics in the canonical ensemble, i.e. the path integral represents a canonical ensemble in d-dimensional space-time. Especially for lattice field theories, the two languages are absolute precisely equivalent.

The fundamental quantity of quantum statistical mechanics is the partition function of the theory under consideration:

$$
\begin{aligned}
\mathcal{Z}[\beta] &= \exp\left\{-F(\beta)\right\} \\
&= \mathsf{Tr}\left[\exp\left\{-\beta\mathsf{H}\right\}\right] = \sum_n \langle n | \exp\left\{-\beta\mathsf{H}\right\} | n \rangle,
\end{aligned}
\tag{2.1}
$$

where $F(\beta)$ is the free energy, $\mathsf{H}$ is an hermitian Operator representing the Hamiltonian of the theory and $\beta = 1/(\mathrm{k_B}T)$, with $T$ the temperature and $\mathrm{k_B}$ the Boltzmann's constant. The states $|n\rangle$ form a complete, orthonormal basis set and the sum is taken over all these states. The expectation value of some quantum mechanical operator $\hat{O}$ corresponding to an observable $O$ is given by

$$
\langle \hat{O} \rangle = \mathcal{Z}^{-1}\,\mathsf{Tr}\left[\hat{O}\exp\left\{-\beta\mathsf{H}\right\}\right] = \mathcal{Z}^{-1}\sum_n \langle n | \hat{O} \exp\left\{-\beta\mathsf{H}\right\} | n \rangle,
\tag{2.2}
$$

where the sum is taken again over all eigenstates of the Hamiltonian. In general, the eigenvalues of the Hamiltonian $\mathsf{H}$ are not known and we want to evaluate the trace of eq. (2.2) without diagonalizing $\mathsf{H}$. A modus operandi is given by the Euclidean path integral.

Consider a Hamiltonian $\mathsf{H}$ which is bounded from below. This operator is decomposed into two operators in the following way

$$\mathsf{H} = \mathsf{H}_0 + \mathsf{V},$$

where $\mathsf{H}_0$ is a free Hamiltonian and $\mathsf{V}$ is an interaction operator. With a continuous basis set $\{|\alpha\rangle\}$ of $\mathsf{H}$, the trace of the partition function eq. (2.1) becomes

$$
\begin{aligned}
\mathcal{Z}[\beta] &= \int \mathsf{d}\alpha \, \langle\alpha| \exp\{-\beta\mathsf{H}\} |\alpha\rangle = \int \mathsf{d}\alpha \, \langle\alpha| \exp\{-\beta(\mathsf{H}_0 + \mathsf{V})\} |\alpha\rangle \\
&= \lim_{N\to\infty} \int \mathsf{d}\alpha \, \langle\alpha| \left( \exp\left\{-\frac{\beta}{N}\mathsf{H}_0\right\} \exp\left\{-\frac{\beta}{N}\mathsf{V}\right\} \right)^N |\alpha\rangle, \qquad (2.3)
\end{aligned}
$$

where we used the exact Trotter product formula [Tro59], [Suz71] for two non-commuting operators $\mathsf{A}, \mathsf{B}$

$$\exp\{\mathsf{A} + \mathsf{B}\} \xrightarrow[N\to\infty]{} \left( \exp\left\{\frac{\mathsf{A}}{N}\right\} \exp\left\{\frac{\mathsf{B}}{N}\right\} \right)^N, \quad N \in \mathbb{N} \qquad (2.4)$$

and

$$\exp\left\{\frac{\mathsf{A}}{N} + \frac{\mathsf{B}}{N}\right\} \approx \exp\left\{\frac{\mathsf{A}}{N}\right\} \exp\left\{\frac{\mathsf{B}}{N}\right\} \exp\left\{-\frac{1}{2N^2}[\mathsf{A}, \mathsf{B}]\right\}.$$

From the last equation we see, that we make an error of the order $\mathcal{O}(1/N^2)$, if we neglect the last product on the right hand side. Especially, if the operators do commute up to a constant, $[\mathsf{A}, \mathsf{B}] \in \mathbb{C}$, the error made is only an irrelevant constant.

To convert this into a path integral, we insert the completeness relation

$$\int \mathsf{d}\alpha \, |\alpha\rangle\langle\alpha| = 1$$

between the individual products

$$\mathcal{Z}[\beta] = \lim_{N\to\infty} \int \mathsf{d}\alpha \int \prod_{j=1}^{N-1} \mathsf{d}\alpha_j \prod_{j=1}^{N} \langle\alpha_j| \exp\left\{-\frac{\beta}{N}\mathsf{H}_0\right\} \exp\left\{-\frac{\beta}{N}\mathsf{V}\right\} |\alpha_{j-1}\rangle, \quad (2.5)$$

where periodic boundary condition are imposed

$$|\alpha_{j=N}\rangle = |\alpha_{j=0}\rangle = |\alpha\rangle. \qquad (2.6)$$

The main point here is that we have defined the path integral Eq. (2.5) as a limiting procedure for $N \to \infty$.

If we interpret the inverse temperature $\beta$ as the Euclidean time[1] for a short time, the factor $\beta/N$ in the exponent can be seen as a small time slice $\epsilon$. The

---

[1]The relation between the inverse temperature and a (Euclidean) time stems from the analytical continuation (Wick-rotation) of the real world (Minkowski) time to imaginary time: $t \to -i\tau$ and $\beta = 1/k_\mathrm{B}T$. With imaginary time, the Schrödinger equation transforms into a diffusion equation, which is a typical thermodynamic equation.

integrand of eq. (2.5) becomes a time-like discretization of the transition amplitude

$$\langle \alpha_N | \exp\{-\beta \mathsf{H}\} |\alpha_0\rangle =$$
$$= \lim_{N\to\infty} \int \prod_{j=1}^{N-1} \mathsf{d}\alpha_j \prod_{j=1}^{N} \langle \alpha_j | \exp\{-\epsilon \mathsf{H}_0\} \exp\{-\epsilon \mathsf{V}\} |\alpha_{j-1}\rangle$$
$$= \lim_{N\to\infty} \int \prod_{j=1}^{N-1} \mathsf{d}\alpha_j \prod_{j=1}^{N} \langle \alpha_j | \exp\left\{-\frac{\epsilon}{2}\mathsf{V}\right\} \exp\{-\epsilon \mathsf{H}_0\} \exp\left\{-\frac{\epsilon}{2}\mathsf{V}\right\} |\alpha_{j-1}\rangle$$
$$= \lim_{N\to\infty} \int \prod_{j=1}^{N-1} \mathsf{d}\alpha_j \prod_{j=1}^{N} \langle \alpha_j | \mathsf{T} | \alpha_{j-1}\rangle$$

with the transfer matrix $\mathsf{T}$. An important property of the transfer matrix $\mathsf{T}$ is that it is a Hilbert-Schmidt operator, i.e $\mathsf{T}$ is a compact operator which has an orthonormal basis $\{\alpha\}$ with $\sum_\alpha \|\mathsf{T}|\alpha\rangle\|^2 < \infty$. With the help of the transfer matrix the calculation of the partition function of many physical problems reduces basically to the evaluation of the largest eigenvalue of the operator[2] $\mathsf{T}$.

Concluding, we may rewrite the partition function eq. (2.5) formally as

$$\mathcal{Z}[\beta] = \int [\mathsf{D}\alpha] \exp\{-\mathcal{S}_{\mathrm{E}}[\beta]\}, \tag{2.7}$$

which yields the Euclidean path integral with the Euclidean action

$$\mathcal{S}_{\mathrm{E}}[\beta] = \lim_{\substack{\epsilon\to 0 \\ N\epsilon=\beta}} \sum_{j=1}^{N} \epsilon \mathsf{H} = \int_0^\beta \mathsf{d}\tau' \, \mathsf{H}(\tau') \tag{2.8}$$

and with the functional integral measure

$$\lim_{N\to\infty} \prod_{j=1}^{N-1} \int \mathsf{d}\alpha_j = \int [\mathsf{D}\alpha].$$

As a next point, we want to discuss the relationship between thermal correlation functions, the basic quantities of statistical physics, and propagators (Green's functions), the basic observables of a quantum field theory. Thermal correlation functions can be derived from the generating functional $\mathcal{Z}[\beta, j]$ which is defined by

$$\mathcal{Z}[\beta, j] = \int [\mathsf{D}\alpha] \exp\left\{-\mathcal{S}_{\mathrm{E}}[\beta] + \int_0^\beta \mathsf{d}\tau \, j(\tau)\alpha(\tau)\right\}, \tag{2.9}$$

---

[2]This method calculates the free energy directly in terms of the largest eigenvalue of the large matrix $\mathsf{T}$.

where $j(\tau)$ is an appropriate source term for $\alpha$. Functional differentiation with respect to $j(\tau)$ gives the thermal average of the correlation functions in imaginary time

$$
\begin{aligned}
G^{(2)}(\alpha(\tau_1), \alpha(\tau_2)) \;\; &:= \;\; \langle \alpha(\tau_1)\alpha(\tau_2)\rangle = \frac{1}{\mathcal{Z}[\beta, j=0]}\frac{\delta^2\,\mathcal{Z}[\beta, j]}{\delta j(\tau_1)\,\delta j(\tau_2)}\bigg|_{j=0} \qquad (2.10) \\
&= \;\; \frac{1}{\mathcal{Z}[\beta, j=0]}\int [\mathsf{D}\alpha]\,\alpha(\tau_1)\alpha(\tau_2)\exp\left\{-\mathcal{Z}_{\mathrm{E}}[\beta, j=0]\right\}.
\end{aligned}
$$

The path integral in the equation above can now be identified as the thermal average (cf. eq. (2.2)) of time-ordered operators in the Heisenberg picture,

$$
\langle\mathsf{T}[\hat{\alpha}(-i\tau_1)\hat{\alpha}(-i\tau_2)]\rangle_\beta = \frac{1}{\mathcal{Z}[\beta]}\mathsf{Tr}\left[\exp\left\{-\beta\mathsf{H}\right\}\mathsf{T}[\hat{\alpha}(-i\tau_1)\hat{\alpha}(-i\tau_2)]\right]. \qquad (2.11)
$$

If we identify $\alpha$ as field variables, this equation defines the time ordered propagator of the corresponding fields.

From the cyclicity of the trace of thermal averages (i.e. $\mathsf{Tr}[\hat{A}\hat{B}] = \mathsf{Tr}[\hat{B}\hat{A}]$) or from the periodicity, cf. eq. (2.6), of the paths in the path integral formalism, the following property of the propagator is deduced

$$
\langle\mathsf{T}[\hat{\alpha}(-i\beta)\hat{\alpha}(-i\tau)]\rangle_\beta = \langle\mathsf{T}[\hat{\alpha}(0)\hat{\alpha}(-i\tau)]\rangle_\beta. \qquad (2.12)
$$

Furthermore, we can continue back from Euclidean space to Minkowski space (i.e. $-i\tau \to t$), if our theory obeys the Osterwalder-Schrader (reflection) positivity which involves time reflections and complex conjugations [OS73], [OS75]. Then we can define the two-point functions $\Delta^>(t_1, t_2)$ and $\Delta^<(t_1, t_2)$ with $t_1 > t_2$ as follows:

$$
\begin{aligned}
\Delta^>(t_1, t_2) \;\; &= \;\; \langle\hat{\alpha}(t_1)\hat{\alpha}(t_2)\rangle_\beta \qquad\qquad\qquad\qquad (2.13) \\
\Delta^<(t_1, t_2) \;\; &= \;\; \langle\hat{\alpha}(t_2)\hat{\alpha}(t_1)\rangle_\beta = \Delta^>(t_2, t_1). \qquad\quad (2.14)
\end{aligned}
$$

If a complete set of eigenvectors of the Hamiltonian is inserted in the equations above and the condition of their convergence is taken into account, then it follows that $\Delta^>(t_1, t_2)$ is defined for $-\beta \le \mathfrak{Im}(t_1 - t_2) \le 0$ while $\Delta^<(t_1, t_2)$ is defined for $\beta \ge \mathfrak{Im}(t_1 - t_2) \ge 0$. Booth functions can be defined as distributions on the boundary of their domain. If the fact is used that $U_\beta := \exp\{-\beta\mathsf{H}\}$ is an evolution operator in imaginary time, $U_\beta^\dagger\hat{\alpha}(t)U_\beta = \hat{\alpha}(t + i\beta)$, and the cyclicity of the trace is used, the Kubo-Martin-Schwinger relation is derived [LB96]

$$
\Delta^>(t_1, t_2) = \Delta^<(t_1 + i\beta, t_2). \qquad (2.15)
$$

If we go back to imaginary times, we can now release the restriction that $\tau$ has to lie in the interval $[0, \beta]$. We may identify the imaginary time propagator with

$$
\Delta(\tau) = \begin{cases} \Delta^>(-i\tau, 0) \text{ for } \tau \in [0, \beta] \\ \Delta^<(0, -i\tau) \text{ for } \tau \in [-\beta, 0] \end{cases} \qquad (2.16)
$$

Because of the Kubo-Martin-Schwinger relation (2.15) and with periodic boundary conditions (i.e. $\tau - \beta = \tau$) the propagator obeys the periodicity condition

$$\Delta(\tau - \beta) = \Delta(\tau). \tag{2.17}$$

Hence, even if we calculate propagators in the Euclidean space with the restriction of $\tau$ to the interval $\tau \in [0, \beta]$, we can extend the interval of $\tau$ to negative values and we can relate our results to propagators calculated in continuous Minkowski space.

In conclusion, the partition function eq. (2.1) of the theory under consideration can be written as the Euclidean path integral

$$
\begin{aligned}
\mathcal{Z}[\alpha] &= \lim_{\beta \to \infty} \lim_{\substack{\epsilon \to 0 \\ N\epsilon = \beta}} \int [\mathsf{D}\alpha] \exp\left\{ -\mathcal{S}_{\mathrm{E}}[\beta] \right\} \\
&= \int [\mathsf{D}\alpha] \exp\left\{ -\int_0^\beta \mathsf{d}\tau' \, \mathsf{H} \right\}.
\end{aligned}
\tag{2.18}
$$

The partition function of a continuum quantum field theory in Euclidean space is derived, if we first take into account the Kubo-Martin-Schwinger relation eq. (2.15) so that we can extend the interval of possible values of $\tau$ to $\tau \in [-\beta, \beta]$. Secondly, we have to take a two-fold limit. The first limit describes the infinite volume limit, i.e. $t \to \infty$. The second limit is the continuum limit $\epsilon \to 0$. Finally, the partition function for a continuum theory in real time is given by

$$\mathcal{Z}[t] = \lim_{t \to \infty} \lim_{\substack{\epsilon \to 0 \\ N\epsilon = \beta}} \int [\mathsf{D}\alpha] \exp\left\{ -i \int_{-t}^t \mathsf{d}t' \, \mathsf{H} \right\}. \tag{2.19}$$

The generalization from one variable to four dimensional space-time is straight forward.

The expectation value of an observable is also given by a two-fold limit process

$$\langle O[\alpha] \rangle = \lim_{t \to \infty} \lim_{\substack{\epsilon \to 0 \\ N\epsilon = T}} \int [\mathsf{D}\alpha] \, O[\alpha] \, \exp\left\{ -i \int_{-t}^t \mathsf{d}t' \, \mathsf{H} \right\}. \tag{2.20}$$

If the Hamiltonian $\mathsf{H}$ of the discretized theory respects the Osterwalder-Schrader positivity property, then we can in principle perform a Wick rotation back to real times, $-i\tau \to t$, so that the propagators of the theory being calculated in Euclidean space are recovered in Minkowski space.

Motivated by our preliminary remarks, we can give a prescription for defining a quantum field theory on a discrete space-time lattice and subsequently taking the physical continuum limit so that the connection to the corresponding continuum quantum field theory is evident. First, we have to define the lattice version of the action of the continuum $SU(2)$ Yang-Mills theory (this will be done in the next section) and afterwards we have to discuss the (physical) continuum limit of lattice measurements gaining access to continuum observables.

## 2.2    Pure Yang-Mills Theory on the Lattice

After the technical remarks above about the relationship between quantum statistical mechanics and quantum field theory, we want to define the lattice version of pure $SU(2)$ Yang-Mills action. A motivation for introducing a discrete space-time lattice was the possibility of numerical simulation with the Monte-Carlo method. The paradigm of a Monte-Carlo lattice simulation is the Ising spin model. This model was the starting point of the first lattice gauge field theory which was introduced by F. Wegner [Weg71]. He looked for models, which could not magnetize but would have nontrivial phase diagrams. Additionally, those models should have phase transitions without local order parameters as opposed to the Ising model where the expectation value of the spin variables can be used as an order parameter. Hence, the task was to formulate a theory having no local order parameters and to find a symmetry of the model which can distinguish two (or more) phases. A solution was the extension of the Ising spin model to a lattice gauge model.

In contrast to the spin model, where the spins sit on space-time points (sites), the spins of the gauge model sit on connecting passages between two neighboring sites (links). The local, nearest neighbor spin interaction of the Ising spin model is replaced by a local four spins interaction on plaquettes, see fig. (2.1) (In the following, we restrict ourselves to planar models.). This means that the local interaction is a product of four spins around the smallest rectangle of four links. The lattice gauge model is additionally provided with a local gauge group. That is a spin flipping operator $\Omega(x)$, which forbids the occurrence of magnetization, since a local gauge symmetry cannot break down by Elitzur's theorem [Eli75].

For a detailed derivation of the lattice version of $SU(2)$ Yang-Mills theory with a close connection to spin systems see also [Kog79].

### 2.2.1    The Gauge Model of Wegner

From the start, we consider a cubic lattice in $d$-dimensional Euclidean space-time with a side length of $L$. The points of the discrete lattice, from now on called sites, are labeled by $x$ and they are subject to periodic boundary conditions $x + L = x$. The distance between two neighboring sites is set by the lattice constant $a$. In isotropic lattices this constant is the same in all directions and we want to restrict ourselves to isotropic lattices $\mathbf{\Lambda}$ in the following,

$$\mathbf{\Lambda} := \{x = (an_0, a\vec{n}) \,|\, n_\mu \in \mathbb{N}, \, a \in \mathbb{R}\} \text{ and } x_\mu + L = x_\mu.$$

The shortest connections between two neighboring sites are the links of the lattice, those are labeled by a site vector $x$ and by the label $\mu$ for the corresponding direction

$$\text{link: } l(x, \mu) = l(x + \hat{\mu}, -\mu), \tag{2.21}$$

PSfrag replacements

$s(x + \hat{\nu})$

$s(x)$  $s(x + \hat{\mu})$

$$\mathcal{S}^{\text{local}}_{\text{ising}}[s(x)] = J\, s(x) \cdot \sum_{\hat{l} \in \{\pm\hat{\mu}, \pm\hat{\nu}\}} s(x + \hat{l})$$

$s_\nu(x - \hat{\nu})$

$s_\mu(x - \hat{\nu})$

$$\mathcal{S}^{\text{local}}_{\mathbb{Z}_2}[s_\mu(x)] = J\big(s_\nu(x)s_\mu(x + \hat{\nu})s_\nu(x + \hat{\mu}) + \\ + s_\nu(x - \hat{\nu})s_\mu(x - \hat{\nu})s_\nu(x - \hat{\nu} + \hat{\mu})\big) \cdot s_\mu(x)$$
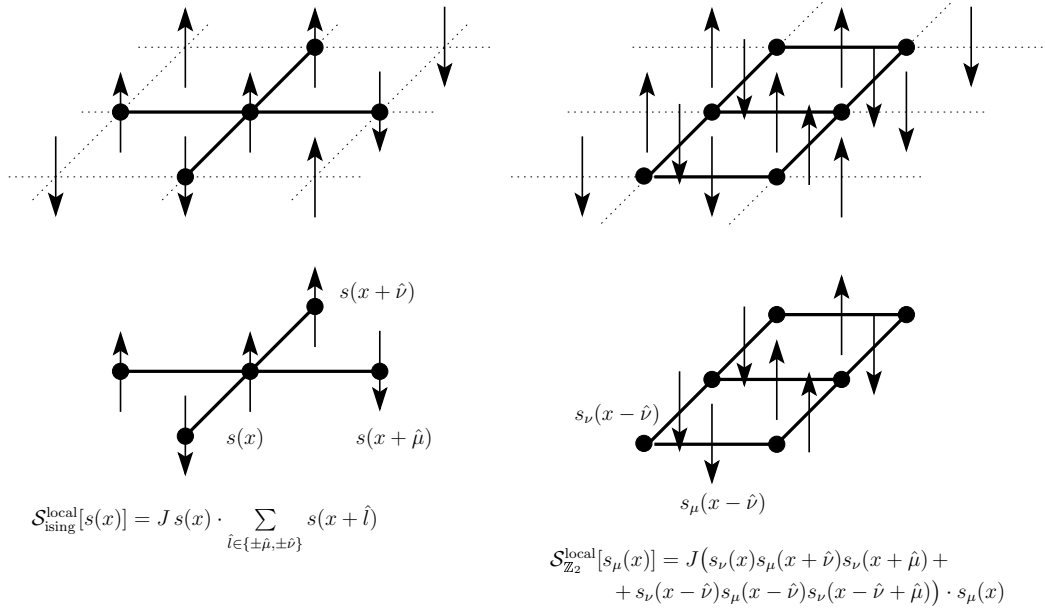
Figure 2.1: In the left panel the local action of a spin variable of the Ising model, in the right panel local action of a spin variable of the $\mathbb{Z}_2$ gauge model of Wegner are shown.

where $\hat{\mu}$ denotes the unit lattice vector in $\mu$-direction. The spin degrees of freedom $s(l) = s(x, \mu) = s_\mu(x) = \pm 1$ are placed on the links $l(x, \mu)$. The local plaquette variable $\mathsf{P}_{\mu\nu}(x)$ is defined as an ordered product of the spin variables $s_\mu(x)$ around an elementary cell,

$$\mathsf{P}_{\mu\nu}(x) = s_\nu(x)s_\mu(x + \hat{\nu})s_\nu(x + \hat{\mu})s_\mu(x). \tag{2.22}$$

The plaquettes can take the values

$$\mathsf{P}_{\mu\nu}(x) = \pm 1.$$

and thus, the partition function for the $\mathbb{Z}_2$-gauge model is given by

$$\mathcal{Z}_{\text{W}} := \sum_{\{S_i\}} \exp\left\{ +J \sum_{x, \mu < \nu} \mathsf{P}_{\mu\nu}(x) \right\}, \tag{2.23}$$

where the sum over $\{S_i\}$ is taken over all possible lattice spin configurations $S_i = \{s_\mu(x)\}_i \, \forall l(x, \mu)$. The parameter $J$ is the interaction constant of the model.

A local gauge transformation is implemented by the spin flip operator $\Omega(x) = \Omega^{-1}(x) = -1$ sitting on the site $x$. All spins connected to site $x'$ are flipped

together. The spins transform under such a operation as

$$s_\mu(x) \to \Omega^{-1}(x + \hat{\mu})s_\mu(x)\Omega(x). \qquad (2.24)$$

We see that a plaquette $\mathsf{P}_{\mu\nu}(x)$ associated with $x$ is invariant under such a spin flip transformation, since a spin flip operator $\Omega(x)$ changes always two spin variables of a plaquette:

$$\mathsf{P}_{\mu\nu}(x) \to \Omega(x)^{-1}\mathsf{P}_{\mu\nu}(x)\Omega(x) = (-1 \cdot s_\nu(x))s_\mu(x+\hat{\nu})s_\nu(x+\hat{\mu})(s_\mu(x) \cdot -1) = \mathsf{P}_{\mu\nu}(x).$$

The relative orientation of the spins is left invariant by the gauge transformation $\Omega(x)$, but not the orientation of the individual spins. Since the action is defined only in terms of plaquette variables $\mathsf{P}_{\mu\nu}(x)$ which are gauge invariant under the local gauge transformation $\Omega(x)$. The gauge symmetry of the action follows automatically.

As in contrast to the Ising model, the spin variable $s_\mu(x)$ cannot be used as a local order parameter for a magnetization phase transition. Spontaneous magnetization of this model vanishes for all temperatures $T$, $\langle s_\mu(x)\rangle = 0 \,\forall\, T$, as a result of the local gauge symmetry due to Elitzur's theorem [Eli75]. Still, the $\mathbb{Z}_2$-gauge model has a non-trivial phase structure which can be labeled by a non-local order parameter. A possible gauge-invariant correlation function is the product of spin variables around a closed path of links $\mathsf{W}[\mathcal{C}] = \prod_{l\in\mathcal{C}} s(l)$ [Weg71], where $\mathcal{C}$ is a closed path. The expectation value of $\mathsf{W}[\mathcal{C}]$ will depend on the characteristics of the closed path $\mathcal{C}$, particular the loop has a perimeter $d$ and a minimal enclosed surface area $A$. At high temperature, the expectation value of $\mathsf{W}[\mathcal{C}]$ falls off exponentially with the area $A$ (area law), $\langle\mathsf{W}[\mathcal{C}]\rangle \propto \exp\{-A\}$, whereas it falls off exponentially with the perimeter $d$ at low temperature, $\langle\mathsf{W}[\mathcal{C}]\rangle \propto \exp\{-d\}$ (perimeter law). This shows that the $\mathbb{Z}_2$-gauge model has distinct high- and low-temperature phases, see [Weg71], [Kog79], [CJR83].

## 2.2.2  The Generalization to $SU(2)$ Yang-Mills Theory

Our goal is to define the proper lattice version of $SU(2)$ Yang-Mills theory. To accomplish this, we first generalize the spin gauge model of Wegner to the case of continuous, Abelian groups [Wil74], [Pol75] see also [Kog79].

### Abelian Field Theory on the Lattice

For an Abelian theory, e.g. QED, the spin variables $s_\mu(x)$ have to correspond to gauge vector fields $A_\mu(x)$ and the plaquette variables of the spin variables should be analogous to the curl of the gauge fields, $\mathsf{P}_{\mu\nu}(x) \to \partial_\mu A_\nu(x) - \partial_\nu A_\mu(x)$. At first, the spin degrees of freedom are enlarged in such a way, that the action has a global Abelian symmetry group. The spin variables sitting on the sites are

thereby parameterized as

$$\vec{s}(x) = \begin{pmatrix} \cos\left(\theta(x)\right) \\ \sin\left(\theta(x)\right) \end{pmatrix},$$

where $\theta(x)$ is an angle variable. The action results from the usual nearest neighbor interaction of the spin variables

$$\mathcal{S}_{\text{ab.is.}} = -J \sum_{x,\mu} \vec{s}(x) \cdot \vec{s}(x+\hat{\mu}) = -J \sum_{x,\mu} \cos\left(\Delta_\mu \theta(x)\right), \qquad (2.25)$$

with the usual forward differential operator $\Delta_\mu$, eq. (A.9), and the coupling constant $J$. This action posses a global, continuous gauge symmetry[3]. The transition to a local gauge symmetry on a space-time lattice is done in an analogous manner as in the transition from the Ising spin model to the $\mathbb{Z}_2$-gauge model. The spin degrees of freedom are moved from the sites to the links, $\theta_\mu(x)$, and a lattice version of the curl is defined by the tensor $\theta_{\mu\nu}(x)$

$$\theta_{\mu\nu}(x) = \Delta_\mu \theta_\nu(x) - \Delta_\nu \theta_\mu(x) = (\theta_\nu(x+\hat{\mu}) - \theta_\nu(x)) - (\theta_\mu(x+\hat{\nu}) - \theta_\mu(x)), \quad (2.26)$$

which is invariant under gauge transformations $\Omega(x)$ sitting on arbitrary sites. The action may now defined in accordance with eq. (2.25) as

$$\mathcal{S} = J \sum_{x,\mu<\nu} \left(1 - \cos\left(\theta_{\mu\nu}(x)\right)\right), \qquad (2.27)$$

where the summation runs over all lattice sites and over all surfaces in positive directions. The cosine term in the action above may be rewritten in the following way

$$
\begin{aligned}
\cos\left(\theta_{\mu\nu}(x)\right) &= \frac{1}{2}\left(e^{-i\theta_\nu(x)}\, e^{-i\theta_\mu(x+\nu)}\, e^{i\theta_\nu(x+\mu)}\, e^{i\theta_\mu(x)} + \text{c.c.}\right) \\
&= \frac{1}{2}\left(s_\nu^\dagger(x) s_\mu^\dagger(x+\nu) s_\nu(x+\mu) s_\mu(x) + \text{c.c.}\right) \\
&= \frac{1}{2}\left(\mathsf{P}_{\mu\nu}(x) + \mathsf{P}_{\mu\nu}^\dagger(x)\right),
\end{aligned}
$$

where the link variables are given by

$$s_\mu(x) = \exp\left\{i\theta_\mu(x)\right\}. \qquad (2.28)$$

This shows explicitly the path ordered product around an elementary cell giving the plaquette variable $\mathsf{P}_{\mu\nu}(x)$ and the action can be expressed in those plaquette variables

$$\mathcal{S} = J \sum_{x,\mu<\nu} \left(1 - \frac{1}{2}\left(\mathsf{P}_{\mu\nu}(x) + \mathsf{P}_{\mu\nu}^\dagger(x)\right)\right). \qquad (2.29)$$

---

[3]If all spins are rotated by the same arbitrary angle $\alpha$, the action still remains unchanged.

Discrete $\mathbb{Z}_N$ Abelian gauge theories can be defined, if the values of the angular variable $\theta_\mu(x)$ are given by the set $\theta_\mu(x) \in \{2\pi n/N | n \in \{0, 1, \ldots, N-1\}\}$. Continuous $U(1)$ Abelian gauge theory can be formulated by allowing the angular variable to take continuous values , i.e. $-\pi < \theta_\mu(x) < \pi$.

The affinity of the above lattice model to continuum electrodynamics becomes obvious in the naive continuum limit, where the lattice spacing $a = \beta/N$ goes to zero: $a \to 0$. In this limit the spin variables $\theta_\mu(x)$ are expected to be smooth, slowly changing functions and the plaquettes can be expanded by its series

$$\mathsf{P}_{\mu\nu}(x) = \exp\{i\theta_{\mu\nu}(x)\} = 1 - i\theta_{\mu\nu}(x) - \frac{1}{2}\theta_{\mu\nu}^2(x) \pm \ldots.$$

and the action can be approximated by

$$\mathcal{S} = J \sum_{x,\mu<\nu} \left(1 - \frac{1}{2}\left(2 - \theta_{\mu\nu}^2(x) \pm \ldots\right)\right) \approx J \sum_{x,\mu<\nu} \frac{1}{2}\theta_{\mu\nu}^2(x). \qquad (2.30)$$

If we replace the discrete sum over the plaquettes in the action eq. (2.29) by the integral over space

$$\sum_x \to \int \frac{\mathrm{d}x}{a^4},$$

with $a$ the lattice constant (in the previous section the parameter $\epsilon$ corresponded to the lattice constant a). If we perform the limit $a \to 0$ and replace the angular variables $\theta$ by

$$\theta_\mu(x) \to -ag_eA_\mu(x), \qquad (2.31)$$

where $g_e$ represents the electric coupling constant (i.e. charge $e$) and $A_\mu(x)$ are the gauge potentials, the continuum action of electrodynamics with zero mass photons is recovered

$$\mathcal{S}_{\mathrm{QED}} \approx J \int \frac{\mathrm{d}x}{a^4}\frac{1}{2}\theta_{\mu\nu}^2(x) = J \int \frac{\mathrm{d}x}{a^4}\frac{a^4g_e^2}{2}F_{\mu\nu}^2(x) = \frac{1}{4}\int \mathrm{d}x\, F_{\mu\nu}^2(x) \qquad (2.32)$$

with the field strength tensor

$$F_{\mu\nu}(x) = \partial_\mu A_\nu(x) - \partial_\nu A_\mu(x).$$

The interaction coupling $J$ was replaced by $J = 1/2g_e^2$. If we introduce integer valued sources $j_\mu(x)$ sitting on the sites and obeying the current conservation, the gauge invariance is preserved and the partition function is given by

$$\mathcal{Z}_{\mathrm{QED}}^{\mathrm{lat.}}[j_\mu(x)] = \prod_{x,\mu}\int_{-\pi}^{+\pi} \mathrm{d}\theta_\mu(x)\exp\left\{-\mathcal{S}_{\mathrm{QED}} + \sum_x j_\mu(x)\theta_\mu(x)\right\}.$$

Completing this derivation, the partition function of quantum electro dynamics is recovered without fermions. The limit $a \to 0$ by constant space-time extension

is only achieved if $N \to \infty$, and this is exactly the needed limit for the Euclidean path integral

$$\mathcal{Z}_{\text{QED}}[j_\mu(x)] \simeq \int\limits_{\forall\,\text{paths}} [\mathrm{D}A] \exp\left\{ -\frac{1}{4} \int \mathrm{d}^4 x \left( \frac{1}{4} F_{\mu\nu}^2 - e J_\mu A_\mu \right) + \text{ g.f. } \right\}, \quad (2.33)$$

where g.f. is an abbreviation for the gauge fixing term. This defines the free Maxwell theory[4], with zero mass photons.

**Pure $SU(2)$ Yang-Mills Theory on the Lattice**

Finally, we want to deal with non-Abelian gauge theories describing the purely gluonic domain of Quantum Chromodynamics, i.e. $SU(N)$ gauge theory on the lattice in quenched approximation. For this purpose, we replace the spin variables with generators of the gauge group under consideration with an additional unit element. In the following, we restrict us to the gauge group $SU(2)$, the generalization to $SU(N)$ gauge groups is straight forward. The generators are then the Pauli matrices $\sigma_i$ and the additional unit element is the $(2 \times 2)$ unit matrix $\mathbb{1}_2$. The $SU(2)$ gauge group is obtained, if each element of the generators and the unit element is multiplied by an arbitrary real number $u^{\text{a}}$. The index $\text{a} = 0, 1, 2, 3$ labels the color quantum number, whereby the constraint $u^{\text{a}} u^{\text{a}} = 1$ is additionally imposed. One combines subsequently all four matrices to the link variable $U_\mu(x)$

$$U_\mu(x) := s_\mu(x) \in \left\{ \mathbb{1} u_0 + i\vec{u} \cdot \vec{\sigma} \,\Big|\, \sum_{\text{a}=0}^{3} (u^{\text{a}})^2 = 1 \right\}, \quad (2.34)$$

which is a usual $SU(2)$ matrix in fundamental representation. The link variable $U_\mu(x)$ behaves under a gauge transformation $\Omega(x) \in SU(2)$ like

$$U_\mu(x) \to \Omega^\dagger(x + \hat{\mu}) U_\mu(x) \Omega(x), \quad (2.35)$$

where the gauge transformations $\Omega(x)$ reside again only on the sites of the lattice. The plaquette variable is a path ordered product of the link variables around the smallest loop of the lattice

$$\mathsf{P}_{\mu\nu}(x) = U_\nu^\dagger(x) U_\mu^\dagger(x + \hat{\nu}) U_\nu(x + \hat{\mu}) U_\mu(x), \quad (2.36)$$

where the negative oriented link variables, e.g. the oriented link $l(x + \hat{\nu}, -\nu)$ from $x + \nu$ to $x$, carry the inverse matrix $U_\nu^\dagger(x)$

$$U_{-\nu}(x + \hat{\nu}) \equiv U_\nu^\dagger(x). \quad (2.37)$$

---

[4]On the lattice, the term $\cos(e_0 a^2 F_\mu \nu)$ induces non-trivial self interactions causing the Coulomb's weak coupling phase to give way to a confining strong coupling phase by magnetic flux condensation.

The plaquette variable $\mathsf{P}_{\mu\nu}(x)$ is a special case of the Wilson loop $\mathsf{W}[R,T]$ [Wil74]. For the definition of the Wilson loop we consider a rectangular closed path $\mathcal{C}$ in four-dimensional Euclidean space-time, with a space-like extension of $R$ and a time-like extension $T$. The Wilson loop is defined for a general path $\mathcal{C}$ as the path order product of link variables belonging to the path $\mathcal{C}$:

$$\mathsf{W}[\mathcal{C}] := \frac{1}{2}\mathsf{Tr}\left[U[\mathcal{C}]\right] = \frac{1}{2}\mathsf{Tr}\left[\mathsf{P}\left[\prod_{l_\mu \in \mathcal{C}} U(l_\mu)\right]\right], \tag{2.38}$$

with $l_\mu = (x,\mu)$, $U(l_\mu) = U_\mu(x)$ and $\mathsf{P}[U]$ denotes the path ordering of the link variables. For $SU(N)$ pure gauge theory the expectation value of a Wilson loop $\langle \mathsf{W}[\mathcal{C}] \rangle$ is given by the expectation value of $1/N\,\mathsf{Tr}\left[U[\mathcal{C}]\right]$, where $U[\mathcal{C}]$ is the path ordered product of the link variables $U_\mu(x)$ along the closed path $\mathcal{C}$ in the fundamental representation of the gauge group. The Wilson loop and its special cases play an important role for investigations of confinement in pure Yang-Mills theories which is the subject of the next chapter.

With the plaquette variables eq. (2.36) and motivated by the action eq. (2.29) of lattice QED, a most local, gauge invariant choice for the lattice version of the pure $SU(2)$ Yang-Mills action , the Wilson action [Wil74], is given by

$$\mathcal{S}_{SU(2)}^{\text{lat.}}\left[U_\mu(x)\right] = \beta \sum_{x,\mu<\nu} \left(1 - \frac{1}{4}\mathsf{Tr}\left[\mathsf{P}_{\mu\nu}(x) + \mathsf{P}_{\mu\nu}^\dagger(x)\right]\right), \tag{2.39}$$

where $\beta$ is the only free parameter of the theory. This parameter plays later an important role for the continuum limit and may not be confused with the inverse temperature.

Finally, if we introduce sources $j_\mu(x)$ sitting on the sites, the lattice generating functional is given by

$$\mathcal{Z}_{SU(2)}^{\text{lat.}}\left[j_\mu(x)\right] = \int [\mathsf{d}U_\mu(x)]\exp\left\{-\mathcal{S}_{SU(2)}^{\text{lat.}}\left[U_\mu(x)\right] + \sum_{x,\mu} j_\mu(x)U_\mu(x)\right\}, \tag{2.40}$$

where the integration measure $[\mathsf{d}U_\mu(x)]$ is given by

$$\int [\mathsf{d}U_\mu(x)] = \prod_{x,\mu}\int \mathsf{d}U_\mu(x). \tag{2.41}$$

This is the Haar measure being an invariant measure under the action of a topological group. This measure meets the following properties:

normalization $\quad\quad\quad \int[\mathsf{d}\Omega] = 1$
right & left invariance $\quad \int[\mathsf{d}(\Omega\Omega')]f(\Omega) = \int[\mathsf{d}(\Omega'\Omega)]f(\Omega) = \int[\mathsf{d}\Omega]f(\Omega)$ $\quad$ (2.42)

where $\Omega$ is an element of a topological[5] group $\Gamma$, $\Omega \in \Gamma$.

The Haar measure is a more general and an abstract extension to the Lebesgue measure. However in most cases it can be shown that it leads to a measure that is different from the Lebesgue measure by only a factor of proportionality. Nowadays, it is the most used measure for probability measures, because it allows existence and uniqueness proofs in a fairly general setting. We do not want to go into details, the important point is that it can be used as a probability measure with the properties above, which allows us to use statistical physics and its probabilistic language for compact groups like $SU(2)$. Note that the Haar measure also emerges in the partition function of the continuum pure Yang-Mills theory [Rei96].

The next step is to show that our lattice action $\mathcal{S}^{\text{lat.}}_{SU(2)}[U_\mu(x)]$, eq. (2.39), produce the continuous $SU(2)$ Yang-Mills theory in the naive continuum limit. As in the Abelian theory, the plaquette variable can be expanded as (compare with eq. (2.30))

$$\mathsf{P}_{\mu\nu}(x) = \mathbf{1} - a^2 g F_{\mu\nu}(x) + \frac{1}{2}a^4 F^{\text{a}}_{\mu\nu}(x)\tau^{\text{a}}F^{\text{b}}_{\mu\nu}\tau^{\text{b}} \pm \ldots, \qquad (2.43)$$

with the following representation for the link variables

$$U_\mu(x) = \exp\left\{-agA_\mu(x)\right\} = \exp\left\{-agA^a_\mu(x)\tau^a\right\}, \qquad (2.44)$$

with $\tau^a = i\sigma^a$. The field strength is then defined as

$$F_{\mu\nu} = \frac{i}{g_0}\left[\mathsf{D}_\mu, \mathsf{D}_\nu\right] = \partial_\mu A_\nu - \partial_\nu A_\mu - ig_0\left[A_\mu, A_\nu\right], \qquad (2.45)$$

with the covariant derivative $\mathsf{D}_\mu = \partial_\mu - ig_0 A_\mu$. The continuous parameters are the gluon gauge field $A_\mu = \frac{1}{2}\tau^a A^a_\mu$ living in the Lie algebra of color $SU(2)$. Respecting the trace of the plaquettes, this leads to the following action of the pure $SU(2)$ Yang-Mills theory

$$\beta \sum_{x,\mu<\nu}\left(1 - \frac{1}{4}\mathsf{Tr}\left[\mathsf{P}_{\mu\nu}(x) + \mathsf{P}^\dagger_{\mu\nu}(x)\right]\right) \xrightarrow[a\to0]{} -\beta\int \mathsf{d}^4x \frac{g^2}{16}F_{\mu\nu}(x)^{\text{a}}F^{\text{a}}_{\mu\nu}(x),$$

where the trace of the plaquettes has been taken into account. If we identify the lattice parameter $\beta$ with the coupling constant $g$, $\beta = 4/g^2$, the action reduces to the usual Yang-Mills action for the $SU(2)$ gauge group. Hence, the lattice action $\mathcal{S}^{\text{lat.}}_{SU(2)}[U_\mu(x)]$ corresponds to the continuum $SU(2)$ Yang-Mills theory. Furthermore, it was shown that the Wilson action fulfills reflection positivity condition [Sei82], [OS78] which allows the analytical continuation back from Euclidean time to Minkowski time, see also [MM], [Roe].

---

[5]A topological group is a continuous group which posses a Hausdorff topology, e.g. Lie-groups.

## 2.3   The Continuum Limit and Renormalization

In the preceding sections, we have shown the relationship between statistical physics and quantum field theory on the lattice. It was emphasized that the true partition function of a quantum field theory is obtained in the continuum limit $a \to 0$ and in the thermodynamic (the infinite volume) limit $\mathsf{Vol}[\Lambda] \to \infty$. In the following we want to address the correlation between the expectation values of an observable $\hat{O}_{\text{lat}}$ on the lattice and its corresponding continuum observable $\hat{O}_{\text{phys}}$. The lattice expectation value of an observable is given by

$$\langle \hat{O}_{\text{lat.}}[U] \rangle = \mathcal{Z}_{SU(2)}^{-1} \int [\mathsf{d}U] \, O[U] \, \exp\left\{ -\beta \, \mathcal{S}_{SU(2)}^{\text{lat.}}[U] \right\}, \tag{2.46}$$

where $\mathcal{Z}_{SU(2)}$ is the partition function of the Wilson action. The continuum value of an observable $\hat{O}$ is obtained by taking the following limits

$$\langle \hat{O}[U] \rangle = \lim_{\mathsf{Vol}[\Lambda] \to \infty} \lim_{\substack{a \to 0 \\ Na=l}} \langle \hat{O}_{\text{lat.}}[U] \rangle, \tag{2.47}$$

where we consider a cubic discrete space-time lattice $\Lambda$ with extension $l$. The lattice value of an observable is extrapolated to the physical continuum if we take the thermodynamic limit by inserting more and more lattice points into the lattice volume. The continuum limit is taken by tuning the $\beta$-parameter in an appropriate manner. The $\beta$-parameter is the only free parameter of the pure $SU(2)$ lattice gauge field theory. We know that the $\beta$-parameter is related to the coupling, $\beta = 4/g$ for $SU(2)$ Yang-Mills theory. The strength of the coupling $g$ depends on the momentum and thus it depends on distance via Fourier transformation. This means that by changing the $\beta$-parameter, we choose our scale of length and hence the lattice spacing $a$. Additionally, the space-time lattice $\Lambda$ provides the field theory with a momentum cut-off $\pi/a$ rendering the possible infinities of momentum loop-integrals finite. By implementing the continuum limit $a \to 0$ the cut-off goes to infinity and divergences in observables are generally produced in the case of a four dimensional field theory. As a consequence thereof, we have to renormalize our lattice theory to obtain finite results for physical quantities.

### The Continuum Limit of a Lattice Observable

At the beginning, we consider the Ising model which is a mathematical model for a ferromagnet. At high temperatures, the magnetic spin variables of a ferromagnet have random spin orientations and the average magnetization vanishes. If the temperature drops below a critical temperature $T_{\text{c}}$, the Curie temperature, a phase transition occurs The spins prefer to align themselves in one direction and a net magnetization appears. For a characterization of the phase transition, we

introduce the connected spin-spin correlation function

$$G(r) = \langle s(r)s(0)\rangle - \langle s(r)\rangle\langle s(0)\rangle. \tag{2.48}$$

The correlation function depends only on the distance $r$ between the two spins, since translation invariance holds. The connected correlation function is a measure for information transport of the spins over a distance $r$. It can be shown that the correlation function is well represented for large $r$ by [LB88], [Lan02]

$$G(r) = \frac{g(r/\xi)}{r^{d+\eta-2}}, \text{ with } g(r/\xi) \sim \exp\{-r/\xi\} \text{ for } r \gg \xi, \tag{2.49}$$

where $d$ is the number of space dimensions and $\eta$ is the anomalous dimension. The correlation length $\xi$ represents the characteristic length scale of spin-spin correlations which specifies the size of spin clusters. If the critical temperature $T_c$ is approached, the correlation length diverges indicating a second order phase transition,

$$\xi \propto |T - T_c|^{-\nu} \text{ for } T \sim T_c, \tag{2.50}$$

with the critical index $\nu$ being equal to one for the two-dimensional Ising model.

On the other hand, the mass spectrum of a pure gauge theory, like in quantum mechanics, is measured by the connected Green's functions of appropriate plaquette operators

$$G(\tau) = \langle O_{\mathsf{P}}(\tau)O_{\mathsf{P}}(0)\rangle - \langle O_{\mathsf{P}}(\tau)\rangle\langle O_{\mathsf{P}}(0)\rangle = \sum_{n \neq 0} |\langle 0|\hat{O}|n\rangle|^2 \exp\{-(E_n - E_0)\tau\}, \tag{2.51}$$

where $E_n$ are the eigenvalues of the Hamiltonian of the theory and $E_0$ is the eigenvalue of the ground state. The mass spectrum is expected to begin with a first state above the vacuum and having a positive definite mass $m_1$ which is called the mass gap of the theory. It represents basically the mass of a well defined excitation being like a particle. For $\tau$ sufficiently large the connected Green's function decays exponentially like

$$G(\tau) \xrightarrow[\tau \to \infty]{} \exp\{-(E_1 - E_0)\tau\} = \exp\{-m_1(g)\tau\} = \exp\{-\tau/\xi_{\text{phys}}\}. \tag{2.52}$$

By comparison with the spin-spin correlation function, it is apparent that the correlation length $\xi_{phys}$ is given by the inverse of the mass gap

$$\xi_{\text{phys}} = m_1^{-1}(g) = (E_1 - E_0)^{-1}. \tag{2.53}$$

If we go over to lattice units, we have $\tau = an$ and $\tau/\xi = n/\xi_{\text{lat}}$. Since $\xi_{\text{phys}} = m_1^{-1}(g)$ is a physical quantity with a dimension of length, it must remain finite in the continuum limit $a \to 0$. This implies that the lattice correlation length has to diverge. The divergence of the correlation length $\xi_{\text{lat}}$ is the trademark of a second (or higher) order phase transition. Thus, the non-trivial continuum

limit is reproduced in the limit $a \to 0$ if and only if the $\beta$-parameter can be tuned in such a manner so that $\xi_{\mathrm{phys}}$ is kept constant. Adjusting the $\beta$-parameter corresponds to tuning the running coupling constant $g$ because of $\beta = 4/g^2$ for the $SU(2)$ gauge group. Consequently, the lattice action $\mathcal{S}^{\mathrm{lat.}}_{SU(2)}[U_\mu(x)]$ eq. (2.39) can only describe continuum pure $SU(2)$ Yang-Mills theory if a critical value $g_{\mathrm{c}}$ exists in such a way that the correlation length $\xi_{\mathrm{lat}}(g)$ diverges,

$$\lim_{g \to g_{\mathrm{c}}} \xi_{\mathrm{lat}}(g) = \infty, \ \ \text{so that} \ \ a\, \xi_{\mathrm{lat}}(g) = \text{const} = \xi_{\mathrm{phys}}. \tag{2.54}$$

On the other hand, if the lattice action does not exhibit a critical value $g_{\mathrm{c}}$ for the running coupling, then this action cannot describe any quantum field theory.

Generally, the expectation value $O$ of a physical observable $\hat{O}$ having a mass dimension of $d_{\hat{O}}$ is related to corresponding lattice quantity $O_{\mathrm{lat.}}(g)$ by

$$\langle \hat{O} \rangle(g, a) = \left( \frac{1}{a} \right)^{d_{\hat{O}}} \langle O_{\mathrm{lat.}} \rangle(g) \tag{2.55}$$

The lattice observable is a function of the dimensionless coupling $g$ only. The behavior of $g(a)$ is determined by the requirement that an arbitrary lattice observable $O_{\mathrm{lat}}$ assumes its physical value $O_{\mathrm{phys}}$ in the continuum limit

$$\langle \hat{O} \rangle(g, a) \xrightarrow{a \to 0} O_{\mathrm{phys}}.$$

With the help of eq. (2.55), the needed relation for lattice quantities is obtained

$$\langle O_{\mathrm{lat}} \rangle(g) \xrightarrow{a \to 0} a^{d_{\hat{O}}} O_{\mathrm{phys}}.$$

As noted above, the inverse of the lattice constant represents the momentum cut-off $\Lambda$. If we consider perturbation theory then performing the continuum limit means to move the momentum cut-off to infinity and the occurring of divergences are absorbed in the bare coupling so that physical observables obtain finite values. Fixing the value of $O_{\mathrm{phys}}$ corresponds to choose a scale $\mu = O_{\mathrm{phys}}^{1/d_{\hat{O}}}$ (in perturbation theory this is equivalent to defining the renormalization point).

A functional relation between the coupling constant $g$ and the lattice constant $a$, i.e. $g = g(a)$, has to be available for the existence of the physical limit of an observable. The functional behavior of $g(a)$ has to fulfill another two requirements: 1) The running coupling $g(a)$ has to feature scaling properties. This means that the function $g(a)$ extracted with the help of an arbitrary observable has to hold in the limit $a \to 0$ for all well-defined physical observables having finite values in the continuum limit. 2) There may exist several possible values for the critical point $g_{\mathrm{cr}}$ for a variety of correlation lengths by which phase transitions of the lattice theory occur. Thus there are possibly zero, one or several continuum field theories contained in a single lattice theory. For this reason the true critical point has to be found which describes the features of QCD in quenched approximation. In particular, the weak coupling limit should be present, where perturbation theory is valid.

## Renormalization and the Running Coupling

In order that our lattice theory represents pure $SU(2)$ Yang-Mills theory, we require that the continuum limit, which is now given by $g(a) \to g_{\mathrm{cr}}$, corresponds to the weak coupling expansion exhibiting an asymptotically free theory[6] at short distances [GW73],[Pol74]. Divergences occur generally in higher order perturbation theory of QCD. They can be removed by either introducing a cutoff momentum scale $\Lambda_{\mathrm{co}}$ or by analytically continuing the number of space-time dimensions away from four $(d \to 4 - \varepsilon)$, i.e. performing a dimensional regularization, subsequently followed by a charge, mass and wave function renormalization. We use the first method for regularization and consider unrenormalized functions describing vertices and self-energies involving $n_{\mathrm{B}}$ external boson lines and $n_{\mathrm{F}}$ external fermion lines. They are defined in terms of the momentum cutoff $\Lambda_{\mathrm{co}} = \pi/a$ and the bare coupling constant $g_0$ by

$$\Gamma^{\mathrm{u}}_{n_{\mathrm{B}}, n_{\mathrm{F}}} = \Gamma^{\mathrm{u}}_{n_{\mathrm{B}}, n_{\mathrm{F}}}(p_i, g_0, \Lambda_{\mathrm{co}}), \tag{2.56}$$

where $p_i$ denotes the external momenta. The renormalized functions $\Gamma^{\mathrm{r}}$ are given in terms of a scale parameter $\mu$, a renormalized coupling constant $g(g_{\mathrm{cr}}, \Lambda_{\mathrm{co}}/\mu)$ and renormalization constants $Z_{\mathrm{B}}(\Lambda_{\mathrm{co}})$ and $Z_{\mathrm{F}}(\Lambda_{\mathrm{co}})$ for external boson and fermion wave functions respectively by

$$\Gamma^{\mathrm{r}}_{n_{\mathrm{B}}, n_{\mathrm{F}}}(p_i, g, \mu) \equiv \lim_{\Lambda_{\mathrm{co}} \to \infty} (Z_{\mathrm{B}}(\Lambda_{\mathrm{co}}))^{n_{\mathrm{B}}} (Z_{\mathrm{F}}(\Lambda_{\mathrm{co}}))^{n_{\mathrm{F}}} \Gamma^{\mathrm{u}}_{n_{\mathrm{B}}, n_{\mathrm{F}}}(p_i, g_{\mathrm{cr}}, \Lambda_{\mathrm{co}}). \tag{2.57}$$

The scale $\mu$ is utilized by demanding that $\Gamma^{\mathrm{r}}$ be equal to some predetermined function at an Euclidean momentum $p^2 = -\mu^2$. Thus for a one-boson and two fermion vertex we obtain

$$\Gamma^{\mathrm{r}}_{1,2}(0, p, -p)\big|_{p^2 = -\mu^2} = \lim_{\Lambda \to \infty} Z_{\mathrm{F}}^2 Z_{\mathrm{B}} \Gamma^{\mathrm{u}}(0, p, -p)\big|_{p^2 = -\mu^2} \equiv g(g_{\mathrm{cr}}, \Lambda_{\mathrm{co}}/\mu), \tag{2.58}$$

where the unrenormalized function $\Gamma^{\mathrm{u}}$ is independent of $\mu$, while the renormalized function $\Gamma^{\mathrm{r}}$ and the renormalization constants, $Z_{\mathrm{B}}(\Lambda)$ and $Z_{\mathrm{F}}(\Lambda)$, will depend on the scale $\mu$. By differentiating eq. (2.57) with respect to $\mu$, subsequently multiplying both sides with scale parameter $\mu$ and performing some transformation, see e.g. [Col98], we obtain the renormalization group equation

$$\left( \mu \frac{\partial}{\partial \mu} + \beta^{\mathrm{RG}}(g) \frac{\partial}{\partial g} + n_{\mathrm{B}} \gamma_{\mathrm{B}}(g) + n_{\mathrm{F}} \gamma_{\mathrm{F}}(g) \right) \Gamma^{\mathrm{r}}(p_i, g, \mu) = 0, \tag{2.59}$$

where the renormalization group functions are given by

$$\beta^{\mathrm{RG}}(g) = \mu \frac{\partial g}{\partial \mu}, \quad \gamma_{\mathrm{B}}(g) = -\frac{\mu}{Z_{\mathrm{B}}} \frac{\partial Z_{\mathrm{B}}}{\partial \mu}, \quad \gamma_{\mathrm{F}} = -\frac{\mu}{Z_{\mathrm{F}}} \frac{\partial Z_{\mathrm{F}}}{\partial \mu}. \tag{2.60}$$

---

[6]The short distance properties of QCD are the correct explanation of large momentum physics.

The behavior of any generalized vertex function $\Gamma^r$ under a change of scale $\mu \to \lambda\mu$ is governed by these universal functions.

The $\beta^{\mathrm{RG}}$-function has to be evaluated to higher orders in perturbation theory because the perturbative expansion coefficient is not particularly small. The series is usually written as

$$\beta^{\mathrm{RG}}(g) = -\beta_0^{\mathrm{RG}} \frac{g^3}{16\pi^2} - \beta_1^{\mathrm{RG}} \frac{g^5}{(16\pi^2)^2} + \dots, \tag{2.61}$$

with the coefficients[7]

$$\beta_0^{\mathrm{RG}} = \frac{11}{3} \mathsf{C}_2(A) = \frac{22}{3} \tag{2.62}$$

$$\beta_1^{\mathrm{RG}} = \frac{34}{3} \left( \mathsf{C}_2(A) \right)^2 = \frac{136}{3}, \tag{2.63}$$

where only the contributions of the gauge bosons were considered. The contributions from spin-$\frac{1}{2}$ fermions and scalars are neglected since we analyze pure $SU(2)$ Yang-Mills theory. The fermionic or scalar dynamical degrees of freedom are not considered in pure $SU(2)$ Yang-Mills theory. The relation between the $\beta^{\mathrm{RG}}$-function and the lattice constant $a$ is seen if we take into account the constancy of a physical observable in the continuum limit with respect to a change in scale (see also eq. (2.60))

$$a \frac{\mathsf{d}}{\mathsf{d}a} O_{\mathrm{phys}} = a \frac{\mathsf{d}}{\mathsf{d}a} a^{-d_{\hat{O}}} \langle O_{\mathrm{lat}} \rangle(g) = 0 \quad \Leftrightarrow \quad \frac{\mathsf{d} \ln\langle O_{\mathrm{lat}} \rangle(g)}{\mathsf{d}g} \cdot \beta^{\mathrm{RG}}(g) = -d_{\hat{O}},$$

$$\beta^{\mathrm{RG}}(g) \equiv -\mu \frac{\mathsf{d}g}{\mathsf{d}\mu} = -a \frac{\mathsf{d}g}{\mathsf{d}a}. \tag{2.64}$$

We investigate now the behavior of the $\beta^{\mathrm{RG}}$-function under a change of scale, $a \to \lambda a$. With new variables $t = \ln \lambda$ and $\bar{g}(g,t) = g(g_0, \Lambda_{\mathrm{co}}/\lambda a)$, the relation for the $\beta^{\mathrm{RG}}$-function can be written as

$$\frac{\mathsf{d}\bar{g}(g,t)}{\mathsf{d}t} = \beta(\bar{g}), \quad \bar{g}(g,0) = g(g_0, \Lambda_{\mathrm{co}}/\mu) = g. \tag{2.65}$$

The behavior of $\bar{g}$ with increasing $t$ describes the region of large momentum scales and depends on the sign of $\beta^{\mathrm{RG}}(g)$. Consider $\beta^{\mathrm{RG}}(0) = 0$ and suppose that $\beta^{\mathrm{RG}}$ assumes a value of zero at the points $\bar{g} = 0, g_1, g_2, \dots$. Under the assumption that $\beta(\bar{g}) > 0$, $\bar{g}$ increases from its $t = 0$ value $\bar{g} = g$ until a zero $g_i$ of $\beta^{\mathrm{RG}}(\bar{g})$ is encountered: $\bar{g} \to g_i$ as $t \to \infty$. On the other hand, if $\beta^{\mathrm{RG}}(\bar{g}) < 0$, then $\bar{g}$ decreases from $\bar{g} = g$ at $t = 0$ until again a zero $g_i$ of $\beta^{\mathrm{RG}}(\bar{g})$ is encountered. Hence, in either case, the coupling $\bar{g}$ approaches a zero of the $\beta^{\mathrm{RG}}$-function. Those zeros are fixed points since $\mathsf{d}\bar{g}/\mathsf{d}t = 0$.

---

[7]The quantity $\mathsf{C}_2(A)$ represents the quadratic Casimir operator for the adjoint representation of the gauge group $G$.

If $\beta'_{\mathrm{RG}}(\bar{g}) < 0$ as $t \to \infty$, an ultraviolet fixed point is approached, if $\beta'_{\mathrm{RG}} > 0$ an infrared fixed point is approached for $t \to -\infty$. This is the domain of small momentum scales and accordingly the domain of large distance scale. If an ultraviolet fixed point is at the origin ($\beta^{\mathrm{RG}}(0) = 0$ and $\beta'_{\mathrm{RG}}(0) < 0$) then perturbation theory gets better and better for $t \to \infty$ since $\bar{g}(t) \to 0$. A theory featuring this behavior is called asymptotically free which is a characteristic of pure $SU(2)$ gauge theory and has to be reproduced by our lattice theory.

The differential equation (2.64) can be solved for $a(\beta)$ (here $\beta$ is our free parameter of the lattice theory) with the eq. (2.61) for $\beta^{\mathrm{RG}}(g)$

$$a^2(\beta) = a^2_{\mathrm{fix}}(\beta_{\mathrm{fix}}) \exp\left\{-\frac{6\pi^2}{11}(\beta - \beta_{\mathrm{fix}})\right\} \tag{2.66}$$

where the relation between the lattice $\beta$ parameter and the coupling constant $g$ was used. The value of the integration constant $a_{\mathrm{fix}}(\beta_{\mathrm{fix}}) = (\langle O_{\mathrm{lat}}\rangle(\beta_{\mathrm{fix}})/O_{\mathrm{phys}})^{1/d_{\hat{O}}}$ has to be determined by choosing a physical value $O_{\mathrm{phys}}$ for an arbitrary observable $\hat{O}$.

The favored observable $O_{\mathrm{phys}}$ which is used to fix the scale is the string tension $\sigma$. This quantity is defined as the limit

$$\lim_{T \to \infty} \chi(\hat{R}, \hat{T}) = \sigma a^2, \tag{2.67}$$

where $\hat{R}$ and $\hat{T}$ are space-like and time-like extensions respectively. The functions $\chi(\hat{R}, \hat{T})$ are the Creutz ratios [Cre80] being defined by

$$\chi(\hat{R}, \hat{T}) = -\ln\left\{\frac{\mathsf{W}(\hat{R}, \hat{T})\mathsf{W}(\hat{R} - 1, \hat{T} - 1)}{\mathsf{W}(\hat{R}, \hat{T} - 1)\mathsf{W}(\hat{R} - 1, \hat{T})}\right\} \tag{2.68}$$

and $\mathsf{W}(\hat{R}, \hat{T})$ are rectangular Wilson loops eq. (2.38). The dependence of the lattice spacing and the $\beta$-parameter is approximated by

$$\sigma a^2(\beta) \simeq 0.12 \exp\left\{-\frac{6\pi^2}{11}(\beta - 2.3)\right\}, \quad \sigma := (440\mathrm{MeV})^2; \tag{2.69}$$

for an improved relation see [BCLM04]. Figure (2.2) shows different Creutz ratios in dependence of the $\beta$-parameter and the scaling function (2.69). For a detailed discussion of the scaling property of the Creutz ratio and the extraction of the string tension from measurement data see [GM84].

The range of the $\beta$-values has to be set to $\beta \in [2.1, 2.6]$ which defines the scaling window. In this range, our simulations can be related to perturbation theory. The lower bound is set because of discretization errors occurring by large distances of the sites. The upper bound is set because of the size of the lattice which would be to small for higher values of $\beta$ with respect to the number of lattice sites used on our simulations.
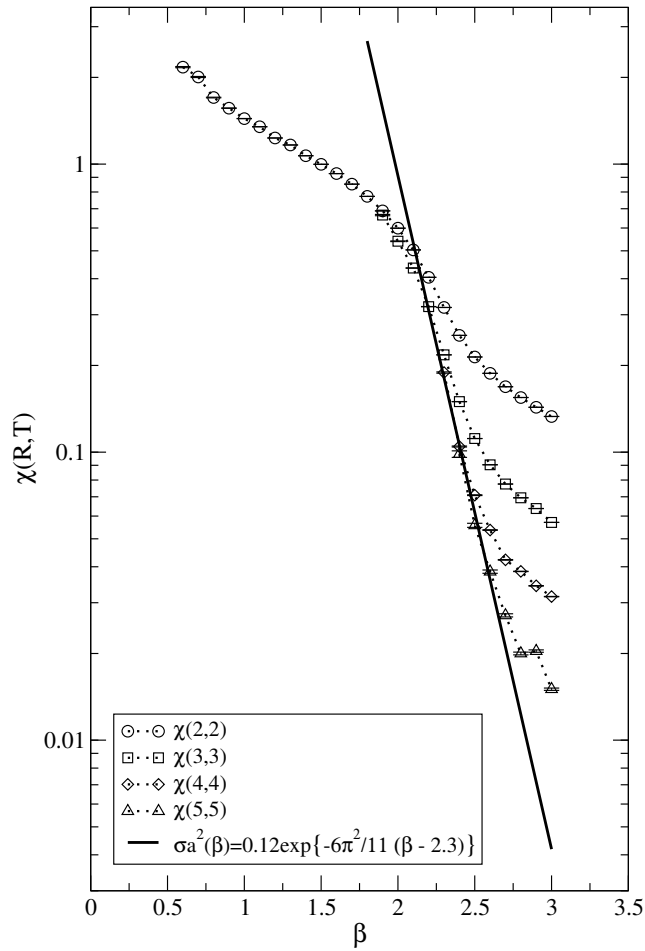
Figure 2.2: Creutz ratios and scaling function for $SU(2)$ Yang-Mills theory. The scaling window is given by the range $\beta \in [2.1, 2.6]$ where the scaling function $\sigma a^2(\beta)$ coincides with the Wilson loops and in this range the proper scaling behavior is given. The Creutz ratios were calculated on a $12^4$ lattice.

## 2.4 The Monte Carlo Method

In this section, we want to explain the basic numerical methods used in lattice Yang-Mills field theories. Our starting point is a discrete four, dimensional space-time lattice $\mathbf{\Lambda} = \{x = (an_0, a\vec{n}) | n_\mu \in \mathbb{N}, a \in \mathbb{R}^+\}$ with periodic boundary conditions $n_\mu + L_\mu = n_\mu$ where $L_\mu$ is the number of sites in direction $\mu$ of the lattice. At each link between two sites resides a link variable $U_\mu(x)$. A configuration of link variables $\mathbf{U}$ is defined as the set of all link variables $U_\mu(x)$ residing on the links of the lattice. When evaluating expectation values eq. (2.46) of an observable $\langle O[U] \rangle$, a single measured value of $O[\mathbf{U}]$ should be weighted according to the Boltzmann factor

$$\rho(\mathbf{U}) \propto \exp\left\{-\mathcal{S}_{SU(2)}^{\text{lat.}}[\mathbf{U}]\right\}. \tag{2.70}$$

We can generate random configurations $\mathbf{U}$ and accept them with probability $\rho(\mathbf{U})$ and sum over the number of configurations to obtain averages of observables. Since the number of configurations with a particular energy increases exponentially with energy, most of our randomly generated configurations will have a very high energy. Consequently, those configurations have a vanishingly small probability of acceptance and most of the time spent to produce configurations is for naught which is obviously very inefficient.

A possible solution is to abandon the idea of constructing statistically independent configurations. A new configurations $\mathbf{U}_\tau$ is constructed against the probability distribution of the antecedent configuration $\mathbf{U}_{\tau-1}$. This new sequence of configuration is called a Markov chain and the index $\tau$ represents the Markov time at which the configuration is constructed. An ergodic Markov chain is defined as an ensemble of configurations satisfying basically two conditions: 1) Every configuration included in the ensemble should be producible from every other configuration within a finite number of steps (connectedness or irreducibility). 2) After visiting a particular configuration, it should not be possible to return to the same configuration except after $t = nk$ steps, where $k$ is fixed and $n \in \mathbb{N}$. For an ergodic Markov chain, the Boltzmann distribution becomes independent of $t$ for large $t$.

### 2.4.1 The Metropolis Monte Carlo Algorithm

Our goal has to be to find an ergodic Markov chain of configurations $\{\mathbf{U}\} = \{\mathbf{U}_1, \mathbf{U}_2, \ldots, \mathbf{U}_N\}$ which produces the required Boltzmann distribution $\rho(\mathbf{U})$, eq. (2.70). We must therefore find a transition probability $P(\mathbf{U}'|\mathbf{U})$ from configuration $\mathbf{U}$ to configuration $\mathbf{U}'$ which leads to the given Boltzmann distribution $\rho(\mathbf{U})$. The transition probabilities are additionally normalized:

$$\sum_{\mathbf{U}'} P(\mathbf{U}'|\mathbf{U}) = 1. \tag{2.71}$$

If a new configuration is chosen, the change in the distribution function is basically determined by two processes: 1) Going from configuration $\mathbf{U}_\tau$ at Markov step $\tau$ to $\mathbf{U}'_{\tau+1}$ at $\tau + 1$ leads to a decrease of $\rho(\mathbf{U})$ and 2) going from $\mathbf{U}'_\tau$ at step $\tau$ to $\mathbf{U}_{\tau+1}$ at step $\tau + 1$ increases the value of the Boltzmann weight. These mechanisms can be summarized in the master equation

$$\rho_{\tau+1}(\mathbf{U}) - \rho_\tau(\mathbf{U}) = -\sum_{\mathbf{U}'} P(\mathbf{U}'|\mathbf{U})\,\rho_\tau(\mathbf{U}) + \sum_{\mathbf{U}'} P(\mathbf{U}|\mathbf{U}')\,\rho_\tau(\mathbf{U}'). \qquad (2.72)$$

Since we are interested in stationary distribution (i.e. $\tau$ independent, $\rho_{\tau+1}(\mathbf{U}') = \rho_\tau(\mathbf{U})$), we can give a particular solution to the master equation

$$P(\mathbf{U}'|\mathbf{U})\,\rho(\mathbf{U}) = P(\mathbf{U}|\mathbf{U}')\,\rho(\mathbf{U}'), \qquad (2.73)$$

which holds for all pairs of configurations. This identity is called the detailed balance solution[8] of the master equation.

The transition amplitude may now be written as the product of two factors

$$P(\mathbf{U}'|\mathbf{U}) = T(\mathbf{U}'|\mathbf{U})\,p_a(\mathbf{U}'|\mathbf{U}). \qquad (2.74)$$

The first factor $T$, the so called trial step probability, on the right hand side of eq. (2.74) is the probability that the system travels from the configuration $\mathbf{U}$ to the configuration $\mathbf{U}'$. Furthermore, the trial probability is symmetric, i.e. $T(\mathbf{U}'|\mathbf{U}) = T(\mathbf{U}|\mathbf{U}')$, and satisfies $0 \le T(\mathbf{U}'|\mathbf{U}) \le 1$ and $\sum_{\mathbf{U}'} T(\mathbf{U}'|\mathbf{U}) = 1$. The second factor $p_a(\mathbf{U}'|\mathbf{U})$ of eq. (2.74) is the probability of accepting the new configuration $\mathbf{U}'$. The acceptance probability may assume values between zero and one, $p_a(\mathbf{U}'|\mathbf{U}) \in [0, 1]$

Substituting eq. (2.74) into the detailed balance solution eq. (2.73) of the master equation (2.72) leads to a detailed balance relation for the acceptance probability $p_a(\mathbf{U}'|\mathbf{U})$

$$\frac{p_a(\mathbf{U}'|\mathbf{U})}{p_a(\mathbf{U}|\mathbf{U}')} = \frac{\rho(\mathbf{U}')}{\rho(\mathbf{U})}. \qquad (2.75)$$

Consequently, the algorithm is divided into two stages. In the first stage, a new configuration $\mathbf{U}'$ is generated from $\mathbf{U}$ with probability $T(\mathbf{U}'|\mathbf{U})$. In the second stage, the Boltzmann factors of both configurations are compared. If $\rho(\mathbf{U}') > \rho(\mathbf{U})$ then $p_a(\mathbf{U}'|\mathbf{U})$ is chosen to be one. On the other hand, if $\rho(\mathbf{U}') < \rho(\mathbf{U})$ then $p_a(\mathbf{U}'|\mathbf{U})$ is to be chosen as the quotient of both distributions $\rho(\mathbf{U}')/\rho(\mathbf{U})$. The new configuration is accepted and replaces the old one if a random variable is smaller than $p_a(\mathbf{U}'|\mathbf{U})$.

---

[8]This means physically that a statistical system is in equilibrium.

This results in the Metropolis algorithm [MRR$^+$53] as follows

$$P(\mathbf{U}'|\mathbf{U}) = T(\mathbf{U}'|\mathbf{U})\, p_a(\mathbf{U}'|\mathbf{U}); \tag{2.76}$$

$$\sum_{\mathbf{U}'} T(\mathbf{U}'|\mathbf{U}) = 1, \quad T(\mathbf{U}'|\mathbf{U}) = T(\mathbf{U}|\mathbf{U}'); \tag{2.77}$$

$$T(\mathbf{U}'|\mathbf{U}) > 0, \quad \forall\, \mathbf{U}, \mathbf{U}'; \tag{2.78}$$

$$\text{if } \rho(\mathbf{U}') < \rho(\mathbf{U}) \text{ then } p_a(\mathbf{U}'|\mathbf{U}) = \frac{\rho(\mathbf{U}')}{\rho(\mathbf{U})},$$

$$\mathbf{U}' \text{ is accepted if a random variable } r \leq p_a(\mathbf{U}'|\mathbf{U})$$

$$\text{if } \rho(\mathbf{U}') > \rho(\mathbf{U}) \text{ then } p_a(\mathbf{U}'|\mathbf{U}) = 1,$$

$$\mathbf{U}' \text{ is automatically accepted.}$$

A disadvantage of the Metropolis algorithm is that the sequence of configurations $\mathbf{U}_{\tau+1}, \mathbf{U}_{\tau+2}, \ldots$ is strongly correlated. This holds especially for the beginning of a sequence, since it is difficult to choose a starting configuration $\mathbf{U}_0$ being a proper member of the sequence. To obtain a proper sequence of configurations, one chooses an arbitrary starting configuration $\mathbf{U}_0$ and discards it together with the first few generated configurations from it, this is sometimes called thermalizing the distribution $\rho(\mathbf{U})$. A certain number of configurations between two configurations $\mathbf{U}$ and $\mathbf{U}'$ are additionally discarded so that autocorrelations are reduced.

## 2.4.2 The Heat-bath Algorithm for $SU(2)$ Yang-Mills Theory

For the simulation of lattice $SU(2)$ Yang-Mills theory, a variant of the Metropolis algorithm is generally used: the heat-bath algorithm [Cre80],[CJR83]. In this algorithm, the fact is adopted that an update step involves one or a few degrees of freedom and the remaining ones are kept fixed. This can be read off directly from the Boltzmann factor of $SU(2)$ Yang-Mills theory. If the link variable $U_{\mu'}(x')$ is updated, the Boltzmann factor factorizes into two parts, one containing $U_{\mu'}(x')$ and one without $U_{\mu'}(x')$:

$$\exp\left\{-\mathcal{S}_{SU(2)}^{\text{lat.}}[\mathbf{U}]\right\} = \exp\left\{-\tilde{\mathcal{S}}_{SU(2)}^{\text{lat.}}[U_{\mu'}(x')]\right\} \cdot \exp\left\{-\mathcal{S}_{SU(2)}^{\text{lat.}}[\mathbf{U}/U_{\mu'}(x')]\right\} \tag{2.79}$$

with

$$\tilde{\mathcal{S}}_{SU(2)}^{\text{lat.}}[U_{\mu'}(x')] = \beta \sum_{\nu}\left(1 - \frac{1}{4}\mathsf{Tr}\left[\mathsf{P}_{\mu'\nu}(x') + \mathsf{P}_{\mu'\nu}^{\dagger}(x')\right]\right),$$

with $\{\nu \,|\, \nu \in \{\pm 0, \pm 1, \pm 2, \pm 3\} \wedge \nu \neq \pm\mu'\}$ and the action $\mathcal{S}_{SU(2)}^{\text{lat.}}[\mathbf{U}/U_{\mu'}(x')]$ contains only those plaquettes which do not contain the link variable $U_{\mu'}(x')$. Since the acceptance probability of the new variable depends only on the six plaquettes containing the particular link, one needs only to consider their contribution

to the action. The new link is accepted with the same prescription as in the Metropolis method with the sole difference that $\rho(\mathbf{U}')$ depends only on the link variable $U_{\mu'}(x')$ because the other link variables are kept fixed. The heat-bath algorithm satisfies the detailed balanced condition and is equivalent to applying successively an infinite number of Metropolis steps to $U_{\mu'}(x')$ with $\mathbf{U}/U_{\mu'}(x')$ kept fixed.

For the numerical implementation, see also [CJR83], we parameterize the $SU(2)$-link variables as in eq. (2.34)

$$U_\mu(x) = \left\{ \mathbb{1}\,u_0 + i\vec{u}\cdot\vec{\sigma} \,\middle|\, \sum_{\mathrm{a}=0}^{3} u_{\mathrm{a}}^2 = 1 \right\}. \tag{2.80}$$

The normalized, invariant Haar measure takes the form (see appendix (A.3))

$$\mathsf{d}U = \frac{1}{2\pi^2}\delta(1 - u^2)\mathsf{d}^4 u = \frac{1}{4\pi^2}\sqrt{(1 - u_0^2)}\,\mathsf{d}u_0\,\mathsf{d}\Omega, \tag{2.81}$$

where the vector $\vec{u}$ was parameterized in spherical coordinates $(r, \vartheta, \phi)$ and the $r$ integration was performed, $\mathsf{d}\Omega$ represents the differential solid angle of $\vec{u}$. The contribution of link variable $U_{\mu'}(x')$ to the action can be written as

$$\mathcal{S}\left[U_{\mu'}(x')\right] = -\frac{1}{2}\mathsf{Tr}\left[U_{\mu'}(x')\sum_\nu B(\nu, x', \mu')\right] \tag{2.82}$$

$$\text{with } \{\nu|\nu \in \{\pm 0, \pm 1, \pm 2, \pm 3\} \wedge \nu \neq \pm\mu'\}, \tag{2.83}$$

where the bails $B(\nu, x', \mu')$ are given by

$$B(\nu, x', \mu') = U_\nu(x' + \mu')\,U_{\mu'}^\dagger(x' + \nu)\,U_\nu^\dagger(x'). \tag{2.84}$$

The sum over the six bails yields a $SU(2)$ matrix up to a constant

$$\bar{B} := \sum_\nu B(\nu, x', \mu') = k\,\bar{U}, \text{ with } \bar{U} \in SU(2) \text{ and } k = \sqrt{\mathsf{det}[\bar{B}]}. \tag{2.85}$$

The Boltzmann factor takes the form

$$\mathsf{d}U'\,\rho(U') \propto \exp\left\{\frac{\beta\,k}{2}\,\mathsf{Tr}\left[U'\bar{U}\right]\right\}\mathsf{d}U', \tag{2.86}$$

where we have set $U' := U_{\mu'}(x')$. With the variable substitution $V = U'\bar{U}$ we obtain

$$\mathsf{d}(V\bar{U}^\dagger)\,\rho(V\bar{U}^\dagger) \propto \exp\left\{\frac{\beta\,k}{2}\,\mathsf{Tr}\left[V\right]\right\}\mathsf{d}(V\bar{U}^\dagger)$$

$$\propto \frac{1}{2}\sqrt{1 - v_0^2}\,\exp\left\{\beta\,k\,v_0\right\}\mathsf{d}v_0\,\mathsf{d}\Omega, \tag{2.87}$$

where the right invariance of the Haar measure $\mathsf{d}(V\bar{U}^{\dagger}) = \mathsf{d}V$ and the parameterization of appendix (A.3) were used. A new link variable $U'$ is generated by choosing randomly $v_0$ from the interval $[-1, 1]$ with the weight factor

$$\mathsf{d}\rho(v_0) \propto \sqrt{1 - v_0^2} \, \exp\{\beta\,k\,v_0\} \, \mathsf{d}v_0. \tag{2.88}$$

In order to simplify the distribution, we set $\eta = \exp\{\beta\,k\,v_0\}$. The random variable $\eta$ is uniformly generated in the interval $\eta \in [\exp\{-2\beta\,k\}, \exp\{2\beta\,k\}]$ and the new value of $v_0$ is accepted with the probability $p_a(v_0) = (1 - \ln^2(\eta)/(\beta\,k)^2)^{1/2}$. The direction of $\vec{v}$ is selected randomly on the 3-sphere, with $\cos(\vartheta) \in [-1, 1]$ and $\varphi \in [0, 2\pi]$ and $|\vec{v}| = (1 - v_0^2)^{1/2}$. This completes the generation of $V$. Finally, we have to recover the link variable $U'$:

$$U' = V\,\bar{U}^{\dagger}. \tag{2.89}$$

# Chapter 3

# Confinement of Quarks on the Lattice

As mentioned in the introduction, the hypothesis of confinement in quantum chromodynamics lacks a thorough explanation and derivation from first principles. The color confinement problem was defined as the absence of colored states built together of quarks and gluons in the spectrum of QCD, i.e. all asymptotic particle states are color singlets.

It is general believed that the confinement problem can be completely addressed without dynamical fermions and that it can be entirely solved in terms of pure Yang-Mills gauge theory. Consequently, the fermionic degrees of freedom do not appear as integration variables but they can be introduced as external sources. Those sources can be used to probe the ground state of pure Yang-Mills theory. A similar definition of color confinement for pure gauge theory is given by the Wilson criterion [Wil74] which states that the potential between static colored sources rises to infinity when the separation between the sources increases. Suppose we have a very heavy quark and anti-quark pair being a color-neutral, bounded system. On a qualitative level, we can assume that color electric fluxes emanating from the quarks are squeezed into string-like configurations (flux tubes) with a constant energy density per unit length. Since string breaking and thus hadronization are forbidden by the restriction of the quenched approximation of QCD, the potential between the constituents rises with their distance. This means that the energy of free quarks is infinite, i.e. free quark states are not present in the spectrum.

It has been a cornerstone of lattice pure gauge field theory that quark confinement is verifiable by calculating the static quark and anti-quark potential ($q\bar{q}$-potential) in computer simulations [Cre80]. In the following we give the relation between the static $q\bar{q}$-potential and the fundamental observable on the lattice, the Wilson loop [Wil74]. Afterwards, we work out the relation of the string tension $\sigma$ to the $q\bar{q}$-potential.

So far, we mentioned the definition and the detection of color confinement

but not why it exists. Motivated by lattice investigations, the current point of view is that quark confinement is produced by some special class of gauge field configurations, e.g. instantons, Abelian monopoles or center vortices, which dominate in the vacuum state on large distance scales. In this thesis we want to concentrate on the center vortex picture of confinement and discuss its relevance for the confinement mechanism.

## 3.1   The Wilson Loop and the $q\bar{q}$-Potential

First, we want to give the relation between the Wilson loop eq. (2.38) and the static $q\bar{q}$-potential. For detailed derivations see [BW79], [Pol78], [LSG91], we give here only a short, qualitative version. For this we consider the energy of a system composed of a quark $q$ at $x = (t, \mathbf{0})$ and an anti-quark $\bar{q}$ at $x(t, \mathbf{r})$. The $q\bar{q}$-state at time $t$ can be written as

$$|q(t, \mathbf{0})\, \bar{q}(t, \mathbf{r})\rangle = \sum_{\forall \mathcal{C}_{(t,\mathbf{0})}^{(t,\mathbf{r})}} C(\mathcal{C}_{(t,\mathbf{0})}^{(t,\mathbf{r})})\, \mathsf{S}[\bar{q}(t,\mathbf{r}), q(t,\mathbf{0}), \mathcal{C}_{(t,\mathbf{0})}^{(t,\mathbf{r})}]\, |0\rangle, \tag{3.1}$$

where $\mathcal{C}_{(t,\mathbf{0})}^{(t,\mathbf{r})}$ is a path joining $\mathbf{0}$ and $\mathbf{r}$ at the same time $t$ and $C(\mathcal{C}_{(t,\mathbf{0})}^{(t,\mathbf{r})})$ is a complex number depending on the path $\mathcal{C}$. We have defined the path ordered, gauge invariant operator as

$$\mathsf{S}[\bar{q}(t,\mathbf{r}), q(t,\mathbf{0}), \mathcal{C}_{(t,\mathbf{0})}^{(t,\mathbf{r})}] = \bar{q}(t,\mathbf{r}) U(\mathcal{C}_{(t,\mathbf{0})}^{(t,\mathbf{r})}) q(t,\mathbf{0}) = \bar{q}(t,\mathbf{r})\, \mathsf{P} \left[ \prod_{l_\mu^0 = (t,\mathbf{0})}^{l_\mu' = (t,\mathbf{r})} U(l_\mu) \right] q(t,\mathbf{0}),$$
$$\tag{3.2}$$

where $\mathsf{P}[U]$ is the path ordering operator. The operator $\mathsf{S}[\bar{q}(t,\mathbf{r}), q(t,\mathbf{0}), \mathcal{C}_{(t,\mathbf{0})}^{(t,\mathbf{r})}]$ has a nonzero matrix element between the vacuum and the quarkonium state[1] involving a pair of classical heavy quarks separated at the distance $r$ as well as gluon fields generated by these sources. Next, we consider the overlap between $|q\bar{q}\rangle$ at $t = 0$ and the $|q\bar{q}\rangle$ at $t = T$,

$$M(R,T) = \langle 0|\mathsf{S}[\bar{q}(0,\mathbf{R}), q(0,\mathbf{0}), \mathcal{C}_{(t,\mathbf{r})}^{(t,\mathbf{0})}]\, \mathsf{S}[\bar{q}(T,\mathbf{R}), q(T,\mathbf{0}), \mathcal{C}_{(t,\mathbf{0})}^{(t,\mathbf{r})}]|0\rangle. \tag{3.3}$$

If we insert a complete set of energy eigenstates and take the limit for large $T$, then the smallest energy eigenstate will dominate. The smallest energy eigenvalue corresponds to the potential energy of the $q\bar{q}$-state separated by a distance $R$

$$\lim_{T \to \infty} M(R,T) \propto \exp\left\{-V(R)T\right\}. \tag{3.4}$$

---

[1]We consider here the ground state of a Hamiltonian involving only relatively light gluon degrees of freedom, while the heavy quark degrees of freedom and the distance between the quarks are frozen.

Since the quark state is a heavy quark state, the quark fields can be regarded as external sources probing the vacuum. The quark propagator can be expressed as

$$\langle 0|q(t', \mathbf{x})\bar{q}(t, \mathbf{x})|0\rangle \propto U\left[\mathcal{C}_{(t,\mathbf{x})}^{(t',\mathbf{x})}\right] \exp\left\{-m|t-t'|\right\}, \tag{3.5}$$

where the gluon fields were treated as background fields. Inserting the explicit quark representation of $\mathsf{S}[\bar{q}(t, \mathbf{r}), q(t, \mathbf{0}), \mathcal{C}_\mathbf{0}^\mathbf{r}]$ eq. (3.2) into eq. (3.3) and using the quark propagator eq. (3.5), we obtain

$$
\begin{aligned}
M(R, T) &= \langle 0|\bar{q}(0, \mathbf{R})U[\mathcal{C}_{(0,\mathbf{0})}^{(0,\mathbf{R})}]q(0, \mathbf{0})\,\bar{q}(T, \mathbf{0})U[\mathcal{C}_{(T,\mathbf{R})}^{(T,\mathbf{0})}]q(T, \mathbf{R})|0\rangle \\
&\propto \langle 0|\mathsf{Tr}\left[U[\mathcal{C}_{(0,\mathbf{R})}^{(T,\mathbf{R})}]U[\mathcal{C}_{(0,\mathbf{0})}^{(0,\mathbf{R})}]U[\mathcal{C}_{(T,\mathbf{0})}^{(0,\mathbf{0})}]U[\mathcal{C}_{(T,\mathbf{R})}^{(T,\mathbf{0})}]\right]|0\rangle]\exp\left\{-2mT\right\} \\
&\propto \langle 0|\mathsf{W}[R, T]|0\rangle \exp\left\{-2mT\right\}, \tag{3.6}
\end{aligned}
$$

with the Wilson loop $\mathsf{W}[R, T]$ which was defined in eq. (2.38). Hence, in the limit of large separation, the expectation value of the Wilson loop $\langle W(R, T)\rangle$ describes the change in the vacuum to vacuum transition amplitude induced by the presence of an external quark current (apart from the constant factor $2m_q$). This represents the creation of a quark-antiquark pair in the limit of infinite quark mass at time $T$ and with a spacial separation of a distance $R$. This two sources propagate for a certain time interval and subsequently annihilate.

A comparison of eq. (3.6) with eq. (3.4) provides the relation between the static $q\bar{q}$-potential and the expectation value of the Wilson loop

$$V(R) = -\lim_{T\to\infty}\frac{1}{T}\ln\left\{\langle\mathsf{W}(\mathsf{R}, \mathsf{T})\rangle\right\}. \tag{3.7}$$

We say that the theory is confining, if the Wilson loop decays according to an area law, i. e.

$$\langle W(R, T)\rangle \propto \exp\left\{-\sigma RT\right\}, \tag{3.8}$$

then we have an asymptotically, linearly increasing potential

$$V(R) \propto \sigma R. \tag{3.9}$$

The constant $\sigma$ is the string tension $\sigma$ and may be read off by such a decay rate. On the other hand, if the Wilson loop falls off according to a perimeter decay law,

$$\langle W(R, T)\rangle \propto \exp\left\{-\epsilon(R + T)\right\}, \tag{3.10}$$

then the resulting $q\bar{q}$-potential is constant $V(R) \propto \epsilon$. This describes the self-energy of the created sources. Such a theory ceases to confine the sources and would describe free particles.

Furthermore, there exists a theorem [Sei78], [Bac86] denoting that the force between a static quark and anti-quark is everywhere attractive and that the force cannot increase with distance,

$$\frac{\mathsf{d}V(R)}{\mathsf{d}R} > 0 \text{ and } \frac{\mathsf{d}^2V(R)}{\mathsf{d}R^2} \leq 0. \tag{3.11}$$

The proof is given in lattice gauge theory and holds for any gauge group and for any number of space-time dimensions. This theorem inflicts that the upper bound for the $q\bar{q}$-potential is given by a straight line. The slope of the straight line is the value of the string tension $\sigma$ which can only be asymptotically reached in $R$. On the other hand, the $q\bar{q}$-potential has a lower bound, since large Wilson loops can be bounded from above by a perimeter law decaying exponentially [SY82], so that the $q\bar{q}$-potential is bounded from below by a Coulomb type potential. The static $q\bar{q}$-potential is shown in fig.(3.1) which is taken from [BSS95].
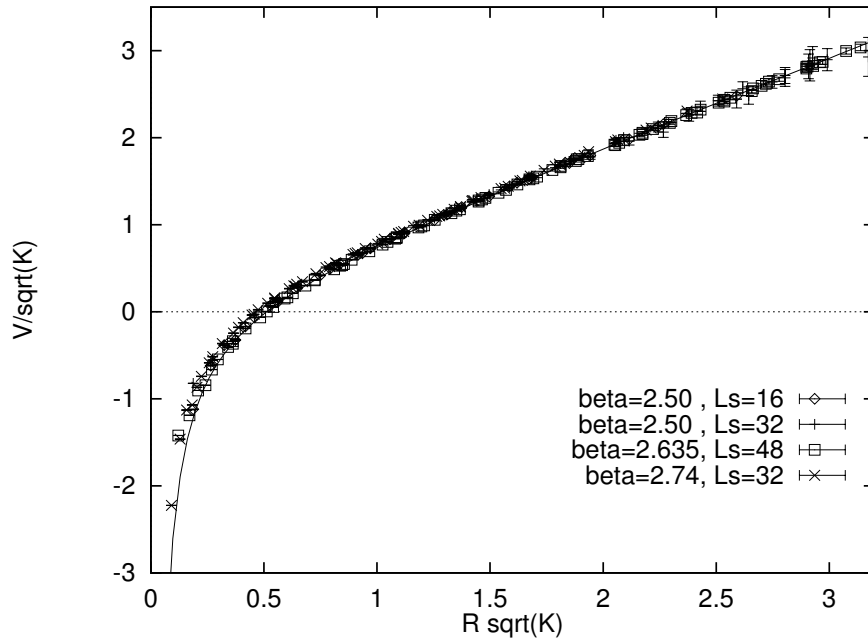


Figure 3.1: The static $q\bar{q}$-potential of $SU(2)$ Yang-Mills theory. The picture is taken from [BSS95] and $K$ is the string tension.

If we take into account the self energy contributions of the sources, we assume that the expectation value of the Wilson loop decays according to

$$\langle \mathsf{W}(R,T) \rangle = \exp\left\{-(\sigma T R + \epsilon(R+T) - \gamma)\right\}, \qquad (3.12)$$

where $\gamma$ represents sub-leading terms which are neglected in all following considerations. The self energy term competes with the term proportional to the area law and for the extraction of the string tension one wants to eliminate the terms proportional to the perimeter decay law. For this reason one measures the Creutz ration [CJR83]

$$\chi(R,T) = -\ln\left\{\frac{\langle \mathsf{W}(R,T) \rangle \langle \mathsf{W}(R-1,T-1) \rangle}{\langle \mathsf{W}(R,T-1) \rangle \langle \mathsf{W}(R-1,T) \rangle},\right) \qquad (3.13)$$

which eliminates the terms proportional to the perimeter of the Wilson loop and the string tension is isolated by studying these Creutz ratios. If the expectation value of the Wilson loop depends on $R, T$ in the way described above, the Creutz ratios $\chi(R, T)$ will be independent of these variables and will coincide with the string tension

$$\lim_{T \to \infty} \chi(R, T) = \sigma a^2(\beta). \tag{3.14}$$

As mentioned in the chapter before, only numbers are measured. The Creutz ratio will not directly produce the string tension but a dimensionless function being related to the renormalization group equation (2.66).

Concluding, we want to emphasize that the string tension $\sigma$ is a constant which is the slope of the linear rising $q\bar{q}$-potential in the limit of large distance between the quark sources.

## 3.2 The Phase Structure of $SU(2)$ Yang-Mills Theory

It is generally believed that a phase transition occurs from the confinement phase to a deconfinement phase at high temperatures and/or at high densities. In the deconfinement phase the quarks and gluons are not confined to hadrons anymore but they constitute a quark-gluon plasma. This phase transition can also occur in a pure gauge field theory at finite temperature and is seen in Monte Carlo simulations. It is generally believed that strongly interacting matter changes its behavior drastically at extreme temperatures and/or densities (e.g. big bang, super nova or neutron star). It was argued [CP75] that hadronic matter appears as an asymptotically free gas of quarks and gluons, the quark-gluon plasma. The qualitative differences of the quark-gluon plasma at asymptotically high energy and hadronic matter at low energy indicates that a phase transition occurs from the confinement phase to a deconfinement phase at high temperatures and/or at high densities. The existence of a phase transition was shown in the strong coupling limit of lattice QCD [Pol78], [Sus79].

The phase transition can be verified by the structure of the correlation function of two Polyakov loops. The Polyakov loop is defined by the trace of a Wilson line whose path winds around once through the lattice in periodic time direction:

$$\mathsf{P}(\mathbf{x}) = \mathsf{Tr} \left[ \prod_0^{n_t} U(\mathbf{x}, t) \right], \tag{3.15}$$

with $n_t$ the extension in the time direction. The time ordered product is closed because of the periodic boundary condition. In a lattice field theory, the temperature is given by the inverse of the extent of the lattice in time direction $T = 1/(a(\beta) n_t)$. A characterization of the different phase can be the broken

or unbroken realization of a global symmetry[2] of the Lagrangian. The action of a pure $SU(N)$ gauge theory is invariant under the global center symmetry transformation on a finite periodic lattice

$$U_0(\mathbf{x}, t_0) \rightarrow z U_0(\mathbf{x}, t_0), \quad z \in \mathbb{Z}_N, \quad \forall \mathbf{x}, \tag{3.16}$$

where $\mathbb{Z}_N$ is the subgroup composed of all center elements of the gauge group and only the links in time direction are transformed. Because the factors $z$ and $z^{-1}$ cancel each other in time-like closed loop, the time-like plaquette variable $\mathsf{P}_{\mu\nu}(x)$ and therefore the action are invariant under this symmetry transformation.

However, there exist gauge-invariant operators being changed by such a global symmetry transformation and one of them is the Polyakov loop which transforms under (3.16) like

$$\mathsf{P}(\mathbf{x}) \rightarrow z\mathsf{P}(\mathbf{x}). \tag{3.17}$$

The global center symmetry can now be realized in one of two ways

$$\langle \mathsf{P}(\mathbf{x}) \rangle = \begin{cases} 0 & \text{unbroken center symmetry phase} \\ \neq 0 & \text{broken center symmetry phase} \end{cases} \tag{3.18}$$

A comparison of the definition of the static $q\bar{q}$-potential with the expectation value of the correlation function of two Polyakov loops separated by a distance shows that one Polyakov loop can be interpreted as a massive static quark at a spatial position $\mathbf{x}$ propagating only in the time direction. In this picture, the expectation value of the Polyakov loop decays accordingly to

$$\langle \mathsf{P}(\mathbf{x}) \rangle \propto \exp\left\{ -\frac{1}{T} F \right\},$$

where $F$ is the free energy of the isolated quark. The free energy of an isolated quark is finite in the deconfinement phase, i.e. $\langle \mathsf{P}(\mathbf{x}) \rangle \neq 0$, whereas the free energy is infinite in the confinement phase, i.e. $\langle \mathsf{P}(\mathbf{x}) \rangle = 0$. Therefore, we have a direct relation between the realization of the global center symmetry and the confinement phase:

**unbroken center symmetry $\Leftrightarrow$ confinement phase**

and thus confinement holds for a vacuum state which is invariant under a global center symmetry transformation [Pol78]. Finally, the confinement-deconfinement phase transition is associated with the breaking of the global center symmetry which originates from the fact that the Polyakov is a true disorder parameter (zero in the confinement (low-temperature) phase, non-zero in the deconfinement (high temperature) phase).

---

[2]A local symmetry like the gauge symmetry cannot by broken due to Elitzur's theorem.

# 3.3 The Center Vortex Picture of Confinement

In the previous section it was shown that confinement may be indeed a property of QCD. An explanation from first principle would be desirable and some possible mechanisms of confinement were suggested. One particular example is confinement due to the effects of Abelian monopoles and the picture of the dual superconductor [tH75], [Man76], [Par75]. This proposal is based on the physics of a type II superconductor in which magnetic fields are squeezed into flux tubes and all other magnetic fields are piled out by the Meissner effect. Because the roles of electric and magnetic fields of QCD are interchanged with regard to a type II superconductor, one refers to the dual superconductor and to the dual Meissner effect.

A second possible explanation is given by the center vortex mechanism [tH78], [Mac], [NO79], [AO80]. A possible definition for a center vortex in three-dimensions is a closed tube which has a finite thickness and carries a quantized magnetic flux. This means that a Wilson loop being non-trivially pierced by a center vortex obtains a factor proportional to a nontrivial center element of the gauge group because of the magnetic flux carried by the center vortex. The center $\mathbb{Z}$ of a group $G$ is defined as the set of all elements of $G$ which commute with every element of $G$. The center $\mathbb{Z}$ of the group $SU(N)$ is the cyclic group $\mathbb{Z}_N$ which is defined as

$$\mathbb{Z}_N := \{\exp\{i\, 2\pi k/N\}|k \in \mathbb{N}\}\,. \tag{3.19}$$

Random fluctuations of the number of vortices piercing a Wilson loop result in an area law and consequently to confinement [ACY78], [ELRT98].

## 3.3.1 Center Vortices and Their Properties

We want to give a detailed description of the center vortex mechanism for confinement. Let us consider firstly a $\mathbb{Z}_2$ lattice gauge field configuration which may be produced by the Wegner action, eq. (2.23) introduced in [Weg71]. The link variables can take the values $\mathbb{Z}_2 = \pm 1$ and hence the plaquettes can take the values $\mathsf{P}_{\mu\nu}(x) = \pm 1$. If a plaquette consists of an odd number of negative links, it will be negative and it is said to be pierced by a (magnetic) center vortex:

**center vortex pierces plaquette** $\Leftrightarrow \mathsf{P}_{\mu\nu}(x) = -1.$

The vortices are the only non-trivial configurations of a $\mathbb{Z}_2$ theory and every $\mathbb{Z}_2$-configuration is characterized by its vortex content up to a $\mathbb{Z}_2$ gauge transformation which leaves the value of the plaquettes unchanged.

The center vortices are easily detected in a $\mathbb{Z}_N$ theory since the degrees of freedom of the link variables are all elements of the center group and hence the plaquettes can take only values corresponding to the factor product group. Considering pure Yang-Mills theory again, we first have to detect the center

vortices in a $SU(N)$ lattice gauge theory. A possible procedure was proposed in [DDFG$^+$98], [DDFGO98], [DDFGO97b]. Note that the dynamics of the resulting $\mathbb{Z}_N$ configurations is governed by the $SU(N)$ action. The revitalization of the center vortex picture, which was first suggested at the end of the seventies and in the beginning of the eighties [tH78], [Mac], [NO79], [AO80], came with the proof that the pure vortex vacuum produces the full string tension and has the right scaling behavior towards the continuum limit [LRT98].

The localization of center vortices is achieved by fixing the link configuration to a certain gauge and by a following center projection. A configuration of link variables $\{U_\mu(x)\}$ is transformed into a certain gauge by using gauge transformations $\Omega(x)$ with the constraint that some functional $\mathsf{F}\left[\{U_\mu^\Omega(x)\}\right]$ is zero or extremal which defines the gauge. We want a gauge which leaves the residual $Z_N$ part of the link variable in the fundamental representation unchanged. The fundamental representation of a link variable may be decomposed into its center part $Z_\mu(x)$ and its coset part $\tilde{U}_\mu(x) \in SO(3) \cong SU(2)/\mathbb{Z}_2$ as follows

$$U_\mu(x) = Z_\mu(x)\tilde{U}_\mu(x). \tag{3.20}$$

We use the (direct) maximal center gauge with the following gauge fixing condition

$$\mathsf{F}\left[\{U_\mu^\Omega(x)\}\right] = \sum_{x,\mu} \mathsf{Tr}\left[U_\mu(x)\right]^2 \rightarrow \ \ \max. \tag{3.21}$$

This gauge tries to move the full link variables $U_\mu(x)$ via gauge transformations $\Omega(x)$ as close as possible to the center elements $Z_\mu(x)(\in \mathbb{Z}_2 = \{\pm 1\}$ for $SU(2)$ theory). The effect of this gauge condition is that one concentrates as much as possible of the information being relevant for confinement contained in the link configurations on particular collective degrees of freedom, in our case magnetic vortices. With this procedure we hope to get a good approximation of the dynamics by neglecting the residual deviations away from those collective degrees of freedom, i.e. we subsequently conduct the center projection being defined by

$$Z_\mu(x) = \text{sign}\left[\mathsf{Tr}\left[U_\mu^\Omega(x)\right]\right] \quad \text{for} \quad SU(2) \tag{3.22}$$

and thus the center gauge fixed links $U_\mu^\Omega(x)$ are projected onto the nearest center element $Z_\mu(x)$ of the group. Again, we say that a plaquette is pierced by a center vortex if the product of its center projected fields $Z_\mu(x)$ bordering the plaquette multiply to $\mathsf{P}_{\mu\nu}(x) = -1$.

The center vortices carry a flux proportional to a non-trivial center element of the gauge group and hence contribute an equivalent factor to any Wilson loop whose minimal area is pierced by a vortex. This factor is $-1$ for both the $\mathbb{Z}_2$ theory and for the center projected $SU(2)$ pure Yang-Mills theory. If we consider a Wilson loop $\langle \mathsf{W}(\mathcal{C})\rangle$ made up of links $l = \pm 1$ which forms the closed path $\mathcal{C}$ enclosing an area $\mathcal{A}$ which contains plaquettes $p = \pm 1$ then the expectation

value of the Wilson loop is given by the product of the plaquettes $p$ it encloses or equivalently, by the product of the links $l$ along the boundary (Stokes' law):

$$\langle W(\mathcal{C}) \rangle = \prod_{l \in \mathcal{C}} l = \prod_{p \in \mathcal{A}} p. \tag{3.23}$$

Hence, the Wilson loop measures the magnetic flux through its enclosing area and consequently the Wilson loop receives a factor $-1$ from every vortex piercing the area $\mathcal{A}$.

The magnetic vortices live on a dual lattice with the same lattice spacing $a$. They are closed lines in a three-dimensional space time or equivalently closed two-dimensional surfaces in four-dimensional space-time. If we consider a elementary cell in three dimensions, then every link contributes to two plaquettes of this elementary cell and thus the product of all plaquettes of the elementary cell is one since this product contains every link twice. This is the manifestation of the Bianchi identity and implies that every such cube has an even number of vortices piercing its surface.

The next step is, to show that the collective degrees of freedom contain the relevant physical information. This is empirically tested and the success depends on the observables under consideration. We conduct a Monte Carlo experiment with the full Yang-Mills action as weight and measure an observable (e.g. Wilson loop) using either the full lattice configurations $\{U_\mu(x)\}$ or the center projected ones $\{Z_\mu(x)\}$. If both results agree, then the collective degrees of freedom are the physically relevant ones for this observable and we speak of center dominance for the particular observable. Center Dominance was shown for a variety of variables [DDFG$^+$98], first of all for large Wilson loops which is seen as evidence that direct center gauge fixing with subsequently center projection concentrates the physical information being relevant for confinement onto the vortex configurations. Additional signs for the relevance of the vortices is given by the center dominance of the string tension. The asymptotic string tension calculated from vortex configurations agrees within reasonable limits with the string tension calculated from full configurations. It is possible to remove the center vortex degrees of freedom from the full configurations. First one performs the direct maximal center gauge followed by the center projection. The located center degree of freedoms are now used to eliminate the vortex configurations:

$$\{U_\mu(x)\} \xrightarrow{\text{DMCG}} \{U_\mu^\Omega(x)\} = \{Z_\mu(x)\tilde{U}_\mu(x)\}$$
$$\{Z_\mu(x) \cdot U_\mu^\Omega(x)\} = \{\underbrace{Z_\mu(x)^2}_{=1}\tilde{U}_\mu(x)\} = \{\tilde{U}_\mu(x)\}.$$

The string tension calculated from configurations $\{\tilde{U}_\mu(x)\}$ disappears [DDFGO97a], [DDFG$^+$98]. In other words, the configurations $\{\tilde{U}_\mu(x)\}$ are incapable to produce a linearly rising potential. Thus, $SU(2)$ Yang-Mills theory without center vortex degrees of freedom ceases to have confinement and results in a non-confining

theory which must not be confused with a theory in the deconfinement phase. From this it follows that the vortex configurations are accountable for the linearly rising part of the $q\bar{q}$-potential.

There exists more evidence for the relevance of the center vortices: the vortex density scales, i.e the variation of the vortex density with the coupling $\beta$ goes as expected for a physical quantity with dimensions of inverse area [LRT98]; the $0^{++}$ and $2^{++}$ glueball masses are vortex dominant [LS00a]. Further results are reported in [DDFGO97b] and [FGO98].

### 3.3.2   The Center Vortex Percolation Transition

A model of color confinement has also to give access to the explanation of the phase transition to the deconfinement phase. A possible explanation of deconfinement is the center vortex percolation model which was considered in [ELRT98], [ELRT00] and which is now introduced. For this we consider a two-dimensional slice of our four-dimensional lattice with an area of $L^2 = L_\mu \times L_\nu$ which contains a Wilson loop with an area of $\mathcal{A}$. A generic vortex will pierce the slice at a point or not at all, but not in a line. If we assume $N$ of these points to be randomly distributed on the slice $L^2$ then the probability of finding $n$ such points inside the Wilson loop area $\mathcal{A}$ is given by a binomial distribution:

$$P_N(n) = \binom{N}{n} \left(\frac{\mathcal{A}}{L^2}\right)^n \left(1 - \frac{\mathcal{A}}{L^2}\right)^{N-n} \tag{3.24}$$

and the expectation value of the Wilson loop is given by

$$\langle W \rangle = \sum_{n=0}^{N} (-1)^n P_N(n) = \left(1 - \frac{2\rho\mathcal{A}}{N}\right)^N \xrightarrow[N\to\infty]{} \exp\left\{-2\rho\mathcal{A}\right\}, \tag{3.25}$$

where the planar density of the intersection points $\rho = N/L^2$ is kept constant as $N \to \infty$. Hence, an area law is achieved with the string tension $\sigma = 2\rho$ suggesting color confinement. An important point is that the Wilson loop has to be pierced sufficiently randomly by the vortices to generate confinement.

Consider now the same setting as before, but with an upper bound $d$ to the space-time extension of single vortices or of vortex networks. Then the intersection points of vortices with a slice $L^2$ always comes paired with another intersection point a finite distance apart, due to the closed character of the vortices precluding an area law. With this additional constraint for the vortices, the intersection points of vortices with a two-dimensional planar Wilson loop come in pairs at most a distance $d$ apart. To contribute a factor $-1$ to a planar Wilson loop, the midpoints lie in a strip of width $d$ centered on the trajectory of the loop. Let $p$ be the probability[3] that a pair which satisfies the condition above

---

[3]This probability includes all geometrical factors (e.g. distances of the midpoints of the

actually does contribute a factor $-1$. The probability $p$ does not depend on the macroscopic extension of the Wilson loop. A pair being placed randomly on a slice of the universe of area $L^2$ has a probability $p\mathcal{A}/L^2$ of contributing a factor $-1$ to a Wilson loop, where $\mathcal{A}$ is the area of the strip of width $d$ centered on the Wilson loop trajectory. To leading order we have $\mathcal{A} = Pd$, where $P$ is the perimeter of the Wilson loop and sub-leading corrections are induced by the local loop geometry.

Placing $N$ pairs on a slice of the universe of area $L^2$ at random, the probability that $n$ of them contribute a factor $-1$ to the Wilson loop is given by

$$P_{N_{\text{pairs}}}(n) = \binom{N_{\text{pairs}}}{n} \left(\frac{p\,P\,d}{L^2}\right)^n \left(1 - \frac{p\,P\,d}{L^2}\right)^{N_{\text{pairs}}-n}, \qquad (3.26)$$

the expectation value of the Wilson loops yields

$$\langle W \rangle = \sum_{n=0}^{N_{pairs}} (-1)^n P_{N_{pairs}}(n) \xrightarrow[N \to \infty]{} \exp\{-\rho p P d\} \qquad (3.27)$$

in the limit of a large universe. The quantity $\rho = 2N_{pairs}/L^2$ is now the planar density of the intersection points. This is a perimeter law showing that the theory does not have confinement, if the space-time extension of vortices or vortex networks is bounded. From this it follows that the vortices or networks of vortices (vortices are not forbidden to self-intersect) have to extend over the entire universe, i.e. to percolate, in order to realize confinement.

Conversely, the deconfinement transition in the vortex picture results, if the vortices cease to be of arbitrary length, i.e. cease to percolate in the deconfinement phase. The deconfinement transition can be characterized as a vortex percolation transition. Numerical analysis [ELRT00] abets the explanation of the deconfinement phase transition at a temperature around $T = 220MeV$ via the picture of a vortex percolation transition. As mentioned before, the expectation value of Polyakov loops does not vanish anymore which is a signature of the deconfinement phase. In the confinement phase the vortices or vortex networks extending usually over the whole universe, whereas in the deconfinement phase they constitute only small loops.

Space-like Wilson loops, however, show an area law behavior at all temperatures $T$. If we take a spatial-slice at a fixed time, the vortices still percolate in the space-like hypercube of the universe even at high temperatures.

---

pairs from the Wilson loop, their angular orientations, the distribution of separations between their points making up the pairs, and the local geometry of the Wilson loop up to the scale $d$) and forms an appropriate average thereof.

### 3.3.3   Comments on Center Vortices

The characteristics and physical relevance of center vortices are multifarious and to mention all facts would go beyond the scope of this work. For an extensive review see [Gre03] and the references therein. In the following we want to concentrate on the facts being relevant for our investigations and for the discussions of our results.

In the continuum theory, the center vortices can be created on a given background by performing a singular gauge transformation with a discontinuity [tH78]. Center vortices produced by such transformation are called thin center vortices. If the thin center vortices are smeared out into a surface-like region with a finite thickness and finite field strength, we have thick center vortices. In Hamiltonian formulation, an explicit construction of an operator creating a thin center vortex is given in [Rei03].

On the other hand, in lattice simulations we have to locate the center vortices in a given ensemble of link variables. This is performed by the method of center projection in an adjoint gauge. An adjoint gauge is a complete gauge-fixing condition for link variables which leaves a residual center symmetry for the link variables. The center projection is well defined, whereas the gauge-fixing procedure is firstly dependent on the gauge-fixing algorithm used and is secondly influenced by Gribov copies, i.e. it is not possible to find the global maximum of the gauge-fixing functional. Here we take the point of view that the gauge is not only defined by the gauge-fixing functional but also by the algorithm used and results should not really be compared between different algorithms. In practice, however, there exist no big difference between results of different algorithms. In the following, we only use the direct maximal center gauge algorithm (DMC). The center vortices in lattice gauge theory are also called P-vortices, but we generally speak of center vortices.

After this technicalities, we want to give an abbreviated overview of physical facts being related to center vortices.

- In gauge-fixed and unfixed frameworks, the absence of vortices implies absence of confinement.

- In zero temperature lattice calculations using DMC, the planar density $\rho_{\mathbb{Z}_2}$ of intersection points of center vortices with a given surface was shown to be a renormalization group invariant which defines $\rho_{\mathbb{Z}_2}$ as a physical quantity in $SU(2)$ Yang-Mills theory [LRT98]. Also a radial distribution function of these intersection points on a plane is a renormalization group invariant.

- If the thickness of center vortices is considered, Casimir scaling of the string tension is obtained [Bal00].

- A modified $SU(2)$ lattice ensemble in which all center vortices had been removed showed that the chiral symmetry is restored [dFD99] and all con-

figurations turn out to belong to the topologically trivial sector. The fact that the topological charge vanishes for a configuration without center vortices suggests that the topological charge might be carried by the center vortex background. The origin of topological charge in a center vortex setting was discussed in [ER00a], [ER00b] and [Rei02]. Topological charges emerge from intersection points of the center vortices. Additionally, it was shown [RSTZ02], [Rei02] that topological charge of center vortices can be linked to the density of zero modes of the Dirac operator being relevant for the chiral condensate.

# Chapter 4

# Vortices in the Limit of High Temperatures

The vortex percolation model for the confinement-deconfinement phase transition was introduced in section (3.3) and it was shown that the vortex picture also provides an appealing picture of the deconfinement phase transition at finite temperatures. The vortex ensemble undergoes a phase transition from a phase of percolating vortices at low temperatures (the confinement phase) to a phase of small vortex clusters ceasing percolation at high temperatures (the deconfinement phase). In fact, this depercolation transition is seen in a (2+1)-dimensional space-time slice of the 4-dimensional lattice universe. At a temperature below the critical temperature $T_{\mathrm{crit}}$, most of the vortices form a vortex cluster which has an extension of the lattice universe; when the temperature rises above $T_{\mathrm{crit}}$, however, the maximal extension of most of the vortex clusters is well below the extension of the lattice. In these space-time slices, the vortices partially align parallel to the time axis [LTER99], [ELRT00]. On the other hand, pure space-like Wilson loops show an area law behavior at all temperatures. This is an indication that vortices detected in a spatial hypercube at a given time are still percolating.

In this chapter we will concentrate on the high temperature behavior of the vortices and their properties. The physics of the high temperature phase of a Yang-Mills theory is of special interest, since one hopes to understand signatures of the quark-gluon plasma in heavy ion collisions which should occur in the deconfinement phase of the theory under certain circumstances. First experiments providing evidence for a quark-gluon plasma were performed at RHIC [Hei03] and should be supported by future collider experiments at LHC.

## 4.1   Dimensionally Reduced Yang-Mills Theory

At high temperature, the Euclidean time extension gets arbitrarily small and it was expected in the early eighties [AP81] that renormalizable four-dimensional

field theories reduce to effective three-dimensional models. At first a complete dimensional reduction was supposed, since the degrees of freedom in the temporal direction which are the non-static modes decouple resulting in a three-dimensional model of the theory. This approach to the high temperature phase is mainly based on the Ambjørn-Appelquist-Carazzone theorem which states that the heavy fields decouple from the low energy sector of the theory [Amb79], [AC75], [CK83]. This is seen in a perturbative treatment of a thermal field theory in imaginary times, where free Matsubara propagators occur of the form $(\mathbf{k}^2 + \omega_n^2 + m^2)^{-1}$ with the Matsubara frequencies $\omega_n = 2\pi nT$. The frequency $\omega_n$ acts like a mass, so that in the high temperature limit, $T \to \infty$, only the static modes ($n = 0$) should survive and the non-static modes ($n \neq 0$) are strongly suppressed. Thus, the non-static modes decouple and the resulting theory is completely reduced to three dimensions.

However, there exists an important objection to a complete dimensional reduction of a theory in general: at finite temperature heavy masses are generated thermally. The Ambjørn-Appelquist-Carazzone theorem holds up to terms of order $\mathbf{p}/T$ and $m/T$. A partial dynamical mass $m(T) \propto g^n T, n > 0$, is generated by the effective three-dimensional theory. Thus, a dimensional reduction takes only place to terms of order $g^n$ even at zero momentum [Lan89]. The correction terms to dimensional reduction do not vanish in the infinite temperature limit as they do in case of the decoupling of heavy particles at zero temperature in the four-dimensional theory. This happens, since in the zero temperature case a small mass $m$ is an input parameter which does not grow with the mass of a decoupled heavy field, whereas the mass $m$ at finite temperature acquires a $T$-dependent contribution. From this it follows that a complete dimensional reduction cannot take place in general [Lan89] and at least non-static residual interactions are induced in the static sector. Consequently, it was shown that four-dimensional pure Yang-Mills theory reduces to a three-dimensional theory being the purely static part of the original four-dimensional Yang-Mills theory coupled to a Higgs field in the adjoint representation [LMR92],[KLM$^+$94] at asymptotic temperatures. The Higgs field originates from the fourth, the temporal, component of the gauge field.

Starting from the Euclidean action of a pure Yang-Mills theory one can perform a perturbative treatment of the non-static modes, because at high temperature the coupling $g(T)$ becomes small due to asymptotic freedom. If the gauge fields are expanded into Fourier series in the temporal direction and the non-static modes are integrated out, the static modes are kept, one obtains a three dimensional effective action $\mathcal{S}_{\mathrm{eff}}[A, \phi]$ in which the gauge field is minimally coupled to a Higgs field

$$\mathcal{S}_{\mathrm{eff}}\left[A, \phi\right] = \mathcal{S}_{\mathrm{YM,3d}}\left[A\right] + \mathcal{S}_{\mathrm{adj}}\left[A, \phi\right] + \mathcal{S}_2\left[\phi\right] + \mathcal{S}_4\left[\phi\right], \qquad (4.1)$$

where $A$ are the space-like gauge fields and $\phi = A_0$ is the Higgs field in the adjoint

representation. The three dimensional pure Yang-Mills action is given by

$$\mathcal{S}_{\text{YM,3d}}[A] = \frac{1}{2g_3^2} \int \mathsf{d}^3 x \, \mathsf{Tr}\left[F_{ij}(x) F_{ij}(x)\right], \tag{4.2}$$

with $g_3^2 = Tg^2(T)$ the temperature dependent coupling constant of the three dimensional theory and $g(T)$ is the usual $T$-dependent coupling of the four dimensional theory. An important point is that the coupling constant $g_3$ has a dimension of temperature as opposed to the dimensionless coupling $g$ in four dimensions.

The second term in the equation above describes the kinetic term of the static adjoint Higgs field $\phi$:

$$\mathcal{S}_{\text{adj}}[A, \phi] = \int \mathsf{d}^3 x \, \mathsf{Tr}\left[([\mathsf{D}_i, \phi])^2\right]. \tag{4.3}$$

The last two terms of eq. (4.2) are the actions of the quadratic and quartic self-interactions of the Higgs field obtained by integrating out the non-static degrees of freedom in a one-loop approximation [Lan89] of the perturbative expansion in the temporal direction:

$$\mathcal{S}_2[\phi] = m_D^2 \int \mathsf{d}^3 x \, \mathsf{Tr}\left[\phi^2\right] \quad \text{and} \quad \mathcal{S}_4[\phi] = \lambda \int \mathsf{d}^3 x \, \mathsf{Tr}\left(\left[\phi^2\right]\right)^2, \tag{4.4}$$

with the Debye mass $m_D$ and the quartic coupling $\lambda$. Extending the calculation to two-loop results into small corrections of the parameters $g_3$, $m_D$ and $\lambda$ [KLRS97], e.g. the coupling constant $g_3$ comes by a correction term of the fourth order in $g$:

$$g_3^2 = Tg^2(T)\left(1 + \mathcal{O}\left(g^4\right)\right). \tag{4.5}$$

Up to now we have worked in continuous space-time and with this preparing work we may define our theory on a discrete space lattice. The lattice action corresponding to eq.4.2 can be written as

$$\mathcal{S}_{\text{YM,3d}}^{\text{lat}}[U, \phi] = \mathcal{S}_{\text{W}}^{\text{lat}}[U] + \mathcal{S}_{\text{hop}}[U, \phi] + \mathcal{S}_{\text{int}}[\phi], \tag{4.6}$$

where $U = U_i(x)$ are the space-like link variables and the Higgs field in adjoint representation is given by

$$\phi(x) = A_0^a(\vec{x})\tau^a \quad A_0^a(x) \in \mathbb{R}, \tag{4.7}$$

where the Higgs fields are located on the sites of the lattice. The standard Wilson gauge field action $\mathcal{S}_{\text{W}}[U]$ is given by

$$\begin{aligned}
\mathcal{S}_{\text{W}}[U] &= \beta \sum_{\vec{x}, i<j} \left(1 - \frac{1}{2}\mathsf{Tr}\left[U_i(\vec{x})U_j(\vec{x}+\hat{i})U_i^{-1}(\vec{x}+\hat{j})U_j^{-1}(\vec{x})\right]\right), \\
&= \beta \sum_{\vec{x}, i<j} \left(1 - \frac{1}{2}\mathsf{Tr}\left[\mathsf{P}_{ij}(\vec{x})\right]\right),
\end{aligned} \tag{4.8}$$

the gauge invariant action $\mathcal{S}_{\text{adj}}[U, \phi]$ denotes the kinetic (hopping) term

$$\mathcal{S}_{\text{hop}}[U, \phi] = \frac{\beta}{2} \sum_{\vec{x}, i} \mathsf{Tr}\left[\phi(\vec{x}) U_i(\vec{x}) \phi(\vec{x} + \hat{\imath}) U_i^\dagger(\vec{x})\right], \tag{4.9}$$

while the pure scalar part of the action $\mathcal{S}_{\text{int}}[\phi]$ summing up the actions $\mathcal{S}_2$ and $\mathcal{S}_4$ of eq. (4.1) becomes

$$\mathcal{S}_{\text{int}}[\phi] = -\frac{\beta}{2} \sum_{\vec{x}} \left( (3 + \frac{1}{2}h) \mathsf{Tr}\left[\phi(\vec{x})^2\right] + \frac{1}{4} K \mathsf{Tr}\left[\phi(\vec{x})^2\right]^2 \right), \tag{4.10}$$

where the parameters $h$ and $K$ are related to $\kappa$ and $\lambda$ of the continuum theory as follows

$$\frac{1 - 2\lambda}{\kappa} = 3 + \frac{1}{2}h \quad \text{and} \quad \frac{\lambda}{\kappa^2} = \frac{K}{2\beta}.$$

A comparison with the continuum theory yields the lattice constant $a$ in terms of the $\beta$-parameter

$$a = \frac{4}{g_3^2 \beta}. \tag{4.11}$$

Before we start our investigations of the vortex physics at high temperature, we have to say some words about the phase structure of the $SU(2)$ adjoint Higgs model which has some special features [Nad90] in three dimensions. This latter model possesses by a $SU(2)$ symmetric and a $U(1)$ symmetric phase, also called the confined and Higgs phase respectively, and we have to choose the phase corresponding to the deconfined phase of the $SU(2)$ gauge theory in four dimensions. It was shown by P. Lacock et. al. [LMR92] using an investigation of the one-loop effective potential and by L. Kärkkäinen et. al. [KLM$^+$94] using Monte-Carlo simulations that the physical relevant phase is the $SU(2)$ symmetric one and the corresponding values of the parameters $h, K$ are given in table (4.1) in section (3.4). In addition, it was shown that the spatial string-tension $\sigma_{\text{s}}$ of four-dimensional Yang-Mills theory scales with the dimensional parameter $g_3^4 = g^4(T) T^2$ and a large scale numerical analysis [Tep99] yields

$$\sigma_{\text{s}}(T) = c\, g_3^4 = c\, g^4(T)\, T^2, \qquad c = 0.136 \pm 0.011, \tag{4.12}$$

which supports the statement that the confining phase of the effective three-dimensional theory is the physical one.

## 4.2  Center Projection in the High Temperature Limit

To identify and investigate the vortex structure in four space-time dimensions, we apply (direct) maximal center gauge fixing followed by center projection

[DDFGO97a], [DDFG$^+$98]. The (direct) maximal center gauge condition in four dimensions is defined by maximizing the functional

$$\mathsf{F}\left[\{U_\mu(x)\}\right] = \sum_{x,\mu}\mathsf{Tr}\left[U_\mu^\Omega(x)\right]^2 \to \max, \qquad (4.13)$$

$$U_\mu^\Omega(x) = \Omega(x)U_\mu(x)\Omega^\dagger(x+\mu)$$

with respect to $\Omega(x)$. To maximize this functional for a given link configuration $\{U_\mu(x)\}$, we evaluate the gauge matrices $\Omega(x)$ by using an iteration over-relaxation algorithm [DDFGO97a], [DDFG$^+$98]. Here we assume that the naive iteration over-relaxation algorithm is capable to filter out the essential physics of the center vortex vacuum and that the Gribov problem plays a subordinate role which may be neglected. After the gauge fixing procedure is completed, we replace the gauge field link variables by their nearest center element, i.e. we perform the center-projection $SU(2) \to Z_2$:

$$U_\mu^\Omega(x) \to \mathsf{sign}\left[\mathsf{Tr}\left[U_\mu^\Omega(x)\right]\right] \in \{-\mathbb{1}_{2\times2}, +\mathbb{1}_{2\times2}\} . \qquad (4.14)$$

If we decompose the functional eq. (4.13) in a part concerning only the space-like link variables and in a part with only time-like link variables

$$\mathsf{F}\left[\{U_\mu(x)\}\right] = \sum_{x,i}\left(\mathsf{Tr}\left[U_i^\Omega(x)\right]\right)^2 + \sum_x\left(\mathsf{Tr}\left[U_0^\Omega(x)\right]\right)^2 , \quad i=1\ldots3 , \quad (4.15)$$

and using the fact that the trace of time-like gauge fields $\mathsf{Tr}\left[U_0(x)\right]$ is invariant under time independent gauge transformations, then the four dimensional maximum center gauge at a time slice corresponds exactly to the maximal center gauge condition for a three dimensional theory

$$\mathsf{F}^{3d}\left[\{U_i(\vec{x})\}\right] = \sum_{\vec{x},i}\mathsf{Tr}\left[U_i^\Omega(x)\right]^2 \to \max , \quad i=1\ldots3 , \quad \Omega = \Omega(\vec{x}). \quad (4.16)$$

Thus, we have established a relation between the closed vortex surfaces of the four dimensional theory at high temperatures and the closed vortex loops of the three-dimensional theory. The vortex loops of the three dimensional theory are identical to the vortex loops of the four dimensional theory at high temperatures at a constant time slice.

## 4.3 Three-dimensional Pure $SU(2)$ Gauge Theory

In a first step, we will neglect the coupling to the adjoint Higgs field $\phi$ and its self-couplings. We consider three-dimensional pure Yang-Mills theory with the Wilson action $\mathcal{S}_\mathrm{W}[U]$, see eq. (4.8). This is an approximation to the dimensionally reduced four-dimensional Yang-Mills theory, but it will still deliver insight into the color confinement mechanism with an emphasis on the center vortex picture of confinement.

### 4.3.1   The Center Dominance of the Static $q\bar{q}$-Potential

By calculating the Creutz ratios eq. (2.68) in the full and in the center projected theory, we obtain the expectation values of the first derivative of the static $q\bar{q}$-potential. The expectation values are extrapolated afterwards to the continuum limit. The numerical analysis was carried out on a $20^3$ lattice, the (direct) maximum center gauge was performed with the iteration over-relaxation algorithm, whereby three attempts were made to find the global maximum of the gauge fixing functional eq. (4.13). Our measured data for the full and center projected theory are presented in figure (4.1) as functions of the distance r for $\beta \in [3.0, 11.0]$. Drawing a comparison with the ansatz $V'(r) = \sigma_3 + \alpha/r$ for the first derivative of the potential yields a string tension of

$$\sigma_3 \;\approx\; 0.11\,g_3^4\,, \quad \text{(pure 3d YM-theory)}\,, \tag{4.17}$$

for the full theory. For three-dimensional pure Yang-Mills theory, the correlations of Polyakov-loops were measured in high statistics Monte-Carlo simulations [Tep99] and the following functional behavior of the spatial string tension with respect to the $\beta$-parameter was found

$$\sigma_s\,a^2 \;=\; \frac{1.788}{\beta^2}\left(1\,+\,\frac{1.414}{\beta}\,+\,\dots\right) \quad \text{for} \quad \beta \geq 3\,. \tag{4.18}$$

If we replace the $\beta$-parameter with the lattice constant, see eq. (4.11), we obtain for the three dimensional string tension

$$\sigma_3\,a^2 \;\approx\; 0.112\,g_3^4\,a^2, \tag{4.19}$$

which agrees with our result eq. (4.17). Both values are remarkably in good agreement to the value (4.12) obtained by a large scale simulation of the full four-dimensional theory [BSF+93], [BFH+93].

   This supports the point of view that space-like Wilson loops are dominated by the three-dimensional Yang-Mills theory. The $q\bar{q}$-potential depends on time-like Wilson loops, thus it appears that the string tension of the four-dimensional Yang-Mills theory is related to correlations of the adjoint Higgs field at high temperatures, i.e. its behavior depends strongly on the time component $A_0$ of the gauge fields and thus its sensitivity on the Higgs gauge field couplings [LMR92].

   In a next step, we consider the center projected theory and the first derivative of the potential thereof. First, we see a slight increase of the projected potential with increasing $r$. In the limit of large distances $r$, the (spatial) string tension obtained from the center projected potential is in good accordance to the full (spatial) string tension within statistical errors, whereas the short distance behavior due to gluon radiation is changed by center projection, see fig. (4.1). This behavior is qualitatively the same as seen in the case of the four-dimensional theory. Finally, we may draw the conclusion that the static $q\bar{q}$-potential is center
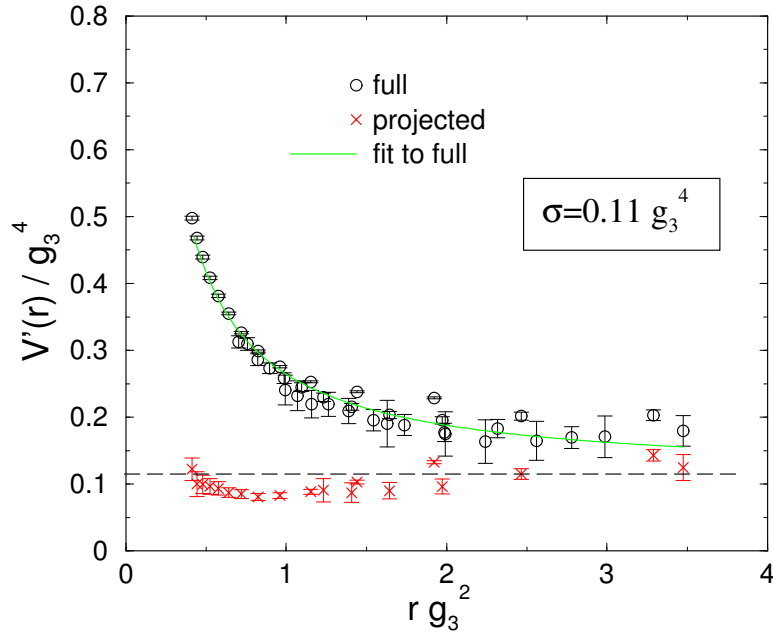
Figure 4.1: The derivative of the static $q\bar{q}$-potential calculated from configurations of the full three-dimensional Yang-Mills theory and calculated from configurations of the center projected theory.

dominant indicating that, if we restrict ourselves to maximal center gauge, the relevant degrees of freedom for color confinement are the center elements of the gauge group $SU(2)$.

## 4.3.2  The Vortex Area Density

Now we want to address the center projected gauge theory in terms of center vortices. As mentioned before, we say that a plaquette of the $\mathbb{Z}_2$-theory is pierced by a center vortex, if its value is $-1$. The center vortices form closed loops in three dimensions and accordingly closed surfaces in four dimensions due to the $\mathbb{Z}_2$ Bianchi identity. Since we want to establish the center vortex model as a possible explanation for color confinement, we have to show that vortices of the projected theory are in accordance with physical quantities of the full theory. For this we investigate whether the center vortices extrapolate to the continuum limit $a \to 0$ by considering the dimensionless vortex area density $\hat{\rho} = \rho\, a^2$ for large values of $\beta$. The vortex area density is defined as the fraction of negative plaquettes of a section through the lattice. An evidence would be the correct scaling behavior of the vortex area density in units of the lattice spacing in the continuum limit according to eq. (4.11). Thereby, a physical vortex area density $\rho$ would be given in the continuum. The scaling behavior is shown by calculating the ratio of the vortex area density and the derivative of the projected potential $V'_{\text{proj}}(r)$
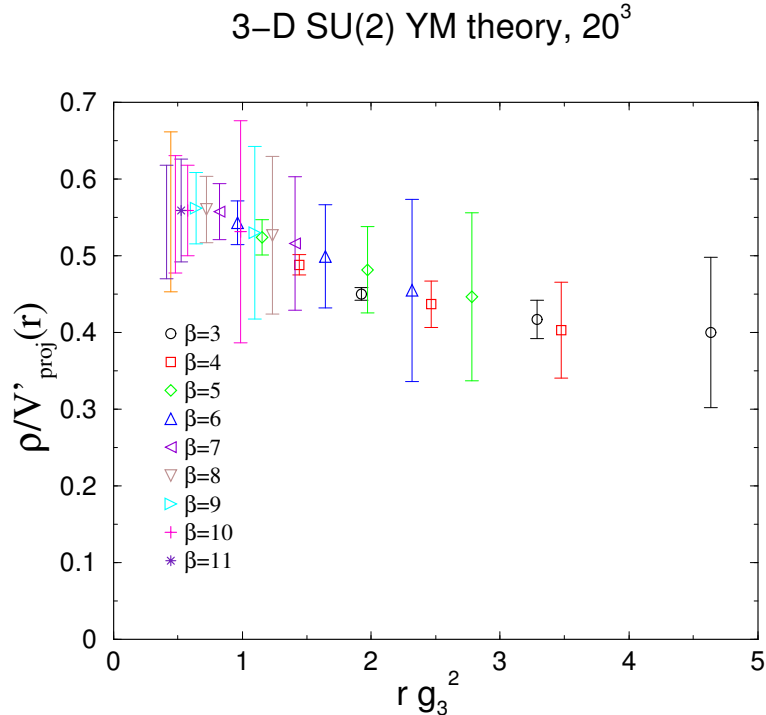
Figure 4.2: The ratio of the vortex area density $\rho$ and the derivative of the projected $q\bar{q}$-potential for several values of $\beta$.

as a function of distance $r$, since this potential extrapolates to the value of the full string tension, see figure (4.1). Our measured data of the ratio $\rho/V'_{\text{proj}}(r)$ are shown in figure (4.2).

The data of the ratio are slightly decreasing for increasing distance $r$. This behavior agrees with the slight increase of the derivative of the projected potential $V'_{\text{proj}}(r)$, see figure (4.1). The ratio $\rho/V'_{\text{proj}}(r)$ seems to approach a constant value in the region $r\,g_3^2 > 3$ and we conclude that a finite vortex area density exists in the continuum limit. As a last topic, we compare the asymptotic value of that ratio with the corresponding value of the ratio of the spatial vortex area density to the spatial string tension which are calculated in four-dimensional Yang-Mills theory at temperature $T \approx 2T_{\text{crit}}$

$$\frac{\rho}{\sigma_{\text{s}}} \approx 0.33, \qquad \text{4d Yang-Mills theory,} \quad T \approx 2T_{\text{crit}}. \qquad (4.20)$$

From this follows that the ratio eq. (4.20) is in good agreement with our ratio calculated of the three-dimensional theory within the statistical errors.

# 4.4 Three-dimensional $SU(2)$ Adjoint Higgs theory

Finally, we want to address the adjoint Higgs model. As mentioned at the beginning of this chapter, the static $q\bar{q}$-potential of the high temperature phase of four-dimensional Yang-Mills theory is well reproduced by the effective three-dimensional adjoint Higgs model with the action

$$\mathcal{S}_{\text{eff}}[U, \phi] = \mathcal{S}_{\text{YM}}[U] + \mathcal{S}_{\text{hop}}[U, \phi] + \mathcal{S}_{\text{int}}[\phi] , \qquad (4.21)$$

where $\mathcal{S}_{YM}$ is the 3-dimensional Wilson action eq. (4.8), $\mathcal{S}_{\text{hop}}[U, \phi]$ is the action of the kinetic hopping term eq. (4.9) and $\mathcal{S}_{\text{int}}[\phi]$ is the self interaction term of the Higgs field. The dimensionally reduced theory is thus described by the partition function

$$Z_{\text{eff}}[U, \phi] = \int [\mathsf{D}\, U] \, [\mathsf{D}\phi] \, \exp\left\{-\mathcal{S}_{\text{eff}}[U, \phi]\right\} . \qquad (4.22)$$

The integration over the link variables $U$ (on a three-dimensional lattice) takes into account the Haar measure, while the integration over the $\phi = \phi^a t^a$ field, which lives in the $\mathfrak{su}(2)$ algebra, is carried out with a flat measure. The Higgs field $\phi$ corresponds to the time component $A_0$ of the gauge field in the continuum. The alert reader might notice that the Higgs field is not sensitive of the center of the time like link variable $U_0$ and might suppose this as a contradiction. But it was shown [LTER99], [ELRT00] that the diameter of the vortices are small at high temperature. They align themselves in the time direction due to the short extent of the time direction and are generally closed due to periodic boundary conditions. The vortices become straight lines along the time direction in the limit of asymptotically high temperatures and plaquettes with a time and space component cannot be pierced by such vortices. Therefore we can neglect the center content of the link variable $U_0$ and the vortex picture is still consistent.

|       | $T/T_c$ | $\beta_4$ | $\beta$ | $h$    | $\kappa$ |
|-------|---------|-----------|---------|--------|----------|
| set 1 | 2.0     | 2.50      | 12.25   | $-.30$ | 0.106    |
| set 2 | 3.5     | 2.80      | 13.54   | $-.26$ | 0.094    |
| set 3 | 6.0     | 3.00      | 14.48   | $-.24$ | 0.086    |

Table 4.1: Parameter sets of the effective dimensionally reduced theory for a $24^3$ lattice taken from [LMR92].

To perform our numerical analysis in the physical phase of the effective model, we set the effective couplings $\beta, h, \kappa$, so that we choose the $SU(2)$ symmetric phase of the effective adjoint Higgs model which corresponds to the high temperature phase of four-dimensional Yang-Mills theory. The values for the simulation parameters are taken from [LMR92], [KLM$^+$94] and they are given in table (4.1).

### 4.4.1 The Static $q\bar{q}$-Potential of the Adjoint Higgs Model

Again we calculate the first derivative of the (spatial) static $q\bar{q}$-potential and the measured data are shown in fig.(4.3) for the parameters given in table (4.1). The spatial string tension $\sigma_\mathrm{s}$ is obtained for asymptotic values of the distance $r$. But we have to interpret one direction of the three-dimensional space of the effective field theory as time-like, so that the measured quantity calculated from spatial Wilson loops could be interpreted as the (spatial) static $q\bar{q}$-potential. The derivative of this potential yields the spatial string tension. Our result of the full effective theory is compared with both the result calculated with center projected configurations and with the result obtained from the three-dimensional pure Yang-Mills theory, see section (4.3.1) and fig.(4.1). First we note that the spatial string tensions calculated from the full and center projected configurations agree within statistical errors. Furthermore, we find that our results of the spatial string tensions coincide with the value (4.12) of the four-dimensional theory. Secondly, we observe that the values of the string tensions calculated in the three-dimensional pure Yang-Mills theory and in three-dimensional adjoint Higgs model are in good accordance. From this it follows that the adjoint Higgs field yields minor corrections to the spatial static potential and it is hoped the effect of the adjoint Higgs field can be neglected in future investigations.
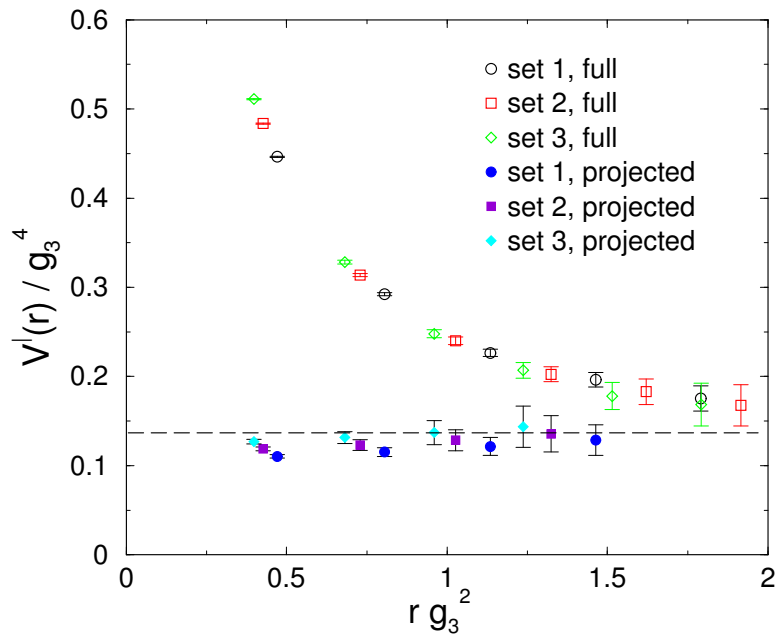


Figure 4.3: The derivative of the spatial static quark potential calculated with the dimensionally reduced theory. The dashed line indicates the spatial string tension (4.12) of the full 4-dimensional theory.

## 4.4.2   The Vortex Area Density in the Adjoint Higgs Model

Finally, we have calculated the ratio of vortex area density and spatial string tension for the adjoint Higgs model at temperatures provided by the parameter sets of table (4.1). The result is shown in figure (4.4). Comparing the scale of the horizontal axis in figure (4.2) and figure (4.4), we conclude that the above ratio has not yet reached its asymptotic value for the parameters given in table (4.1).
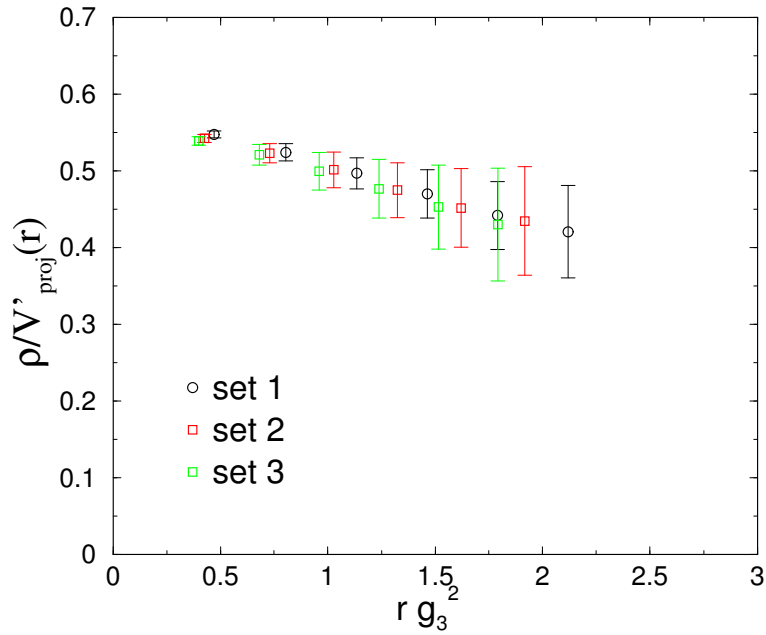


Figure 4.4: The ratio of the vortex area density $\rho$ and the derivative of the projected quark anti-quark potential at several temperatures (see table 4.1).

# Chapter 5

# Propagators in $SU(2)$ Yang-Mills Lattice Gauge Theory

In the preceding chapters we investigated the influence of center vortices on the static $q\bar{q}$-potential and their influence on the phase structure of pure Yang-Mills theory, whereby the maximal center gauge was used. It was shown that the vortex content of the theory is relevant for the linear increase of the potentials in four dimensions as well as in three dimensions due to center dominance of these observables. Furthermore, evidence was given that a percolation of center vortices is a possible candidate for the mechanism of quark confinement.

Despite the success of numerical simulations of lattice gauge field theory concerning color confinement, this method has some grave insufficiencies. Simulations of realistic $SU(3)$ quantum field theory with dynamical quarks are still cumbersome mainly because of the fermion doubling problem which enforces the usage of non-local actions. These actions are time consuming in numerical calculations even if improved algorithms [Kap92], [NN93], [Vra01] are used and the computational power has been increased over the past years. In addition, if the high temperature phase of Yang-Mills theory is addressed to shed some insight to signatures of the quark gluon plasma hopefully produced by collider experiments at RHIC and LHC, systems of finite baryon densities have to be considered. But these systems are hardly accessible in the realistic case of a $SU(3)$ gauge group [Bar98] in the lattice approach in spite of the recent success [EKKL99], [LS00b]. The fundamental problem of QCD at finite densities is that the effective action becomes complex after a Grassmann integration over the fermionic fields, because of the introduction of the chemical potential in the Dirac matrix. This prohibits the use of standard Monte-Carlo algorithms for the lattice simulations with dynamical fermions [BMK$^+$98].

A second non-perturbative method to treat Yang-Mills theory is the approach by Dyson-Schwinger equations (DSE). In contrast to LGT, the fermionic degrees of freedom can be easily incorporated, an extension to finite baryon densities is possible [RS00] and the study of hadron phenomenology [RW94] is possible

by DSE. For a recent review see [AvS01]. But the DSE approach requires a truncation of the infinite series of equations. This approximation is difficult to control and to improve systematically. Additionally, the DSE approach uses gluon and ghost propagators as integral parts. Since propagators are only defined in a certain gauge of the theory, gauge-fixing is needed. The gauge fixing is usually done in continuum field theory by the Faddeev-Popov procedure. But in contrast to the Abelian case, gauge-fixing is not unique in the non-Abelian case. There exist different gauge fields satisfying the gauge condition and they are related by a gauge transformation. These are the so-called Gribov copies. It seems to be that Gribov copies can be neglected in the area of validity of perturbation theory of QCD [Wil03], but they may be relevant in the non-perturbative regime which is the relevant domain for the confinement problem. Since the gluon and ghost propagators can be measured in simulations of LGT, the investigation of these propagators is a natural way for testing both methods. With a comparison of the results of both methods, we can check the performance of the truncation of the infinite Dyson tower of equations and the influence of Gribov copies on propagators in the non-perturbative regime.

Furthermore, it is a matter of common knowledge that all Green's functions carry all information about the physical and mathematical structure of the quantum field theory under consideration. The relevance of center vortices on the infrared behavior of the propagators is by itself of particular interest. In the following, we want to analyze the influence of center vortices on these Green's functions. Since we use mainly $SU(2)$ Yang-Mills theory in quenched approximation, we concentrate our interest on gluon and ghost propagators and postpone the investigation of the impact of center vortices on the quark propagator to future work. The form factors are gauge dependent quantities and hence we have to choose a particular gauge. Our choice of Landau gauge stems from the fact that this gauge is usually used in the DSE approach for calculating the form factors and we want to compare our measurement data with the results of the coupled ghost-gluon Dyson equation of the DSE approach [vSHA98], [vSAH97], [AB98a]. But note that, from the LGT point of view there is nothing special or unique in the choice of Landau gauge, we can use e.g. Coulomb gauge as well.

The motivation of a non-perturbative treatment of calculating propagators is based on the fact that the predictions of perturbation theory are in fact in good accordance with experimental data, if the effective quark-gluon coupling $\alpha(p^2)$ is small, i.e. at high momentum transfers. But on the other hand, if the coupling becomes large at small momentum transfers, perturbation theory fails. Since this behavior of the running coupling $\alpha(p^2)$ in the infra-red prevents a perturbative treatment of the theory, non perturbative approaches are needed, e.g. LGT or DSE.

Our calculations of the form factors are straight forward with the exception that a novel method is used that allows us to compute the form factors directly leading to an improvement in statistical errors. The form factors are directly

calculated, because they are defined as the deviation of the propagators from the free propagators and hence incorporate all the non-perturbative physics relevant for the color confinement problem. By removing the percolating vortex cluster from the $SU(2)$ Yang-Mills ensemble by hand, we produce a non-confining theory [LSWP99], [B$^+$00]. By comparing the results of the form factors of the confining, pure $SU(2)$ Yang-Mills theory with the results obtained from the non-confining model, it is possible to study the relevance of center vortices on the behavior of the gluon and ghost form factors.

## 5.1 The Gluon Propagator

### 5.1.1 Introduction

The gluon propagator is defined in the continuum by

$$\mathcal{D}_{\mu\nu}^{\mathrm{ab}}(k) = -i \int \mathsf{d}^4 x \, \left\langle 0 | \mathsf{T} \left[ A_\mu^{\mathrm{a}}(x) A_\nu^{\mathrm{b}}(0) \right] \right\rangle \exp\left\{ ikx \right\}, \tag{5.1}$$

where $\mathsf{T}$ is the time ordering operator and $A_\mu^{\mathrm{a}}(x)$ are the gluon fields. We can decompose the propagator into a transverse and a longitudinal part in the following way:

$$\mathcal{D}_{\mu\nu}^{\mathrm{ab}}(k) = -i\delta^{\mathrm{ab}} \left[ \left( \delta_{\mu\nu} - \frac{k_\mu k_\nu}{k^2} \right) d_{\mathrm{t}}(k^2) + \xi \frac{k_\mu k_\nu}{k^2} \frac{d_{\mathrm{l}}(k^2)}{k^2} \right]. \tag{5.2}$$

The scalar function $d_{\mathrm{l}}(k^2)$ of the longitudinal part reduces to a constant for linear covariant gauges. This constant can be absorbed by the gauge fixing parameter $\xi$ which is zero in Landau gauge. In the following, we consider Landau gauge ($\xi = 0$). In this gauge the gluon propagator is diagonal in color and transverse in Lorentz space. The interesting information in the gluon propagator is thus contained in

$$D(k) = N \sum_{a,\mu} \mathcal{D}_{\mu\mu}^{aa}(k^2) =: N \frac{F(k^2)}{k^2}, \tag{5.3}$$

with a normalization constant $N$ and $F(k^2)$ represents the gluon form factor which measures the deviation of the full propagator from the free one. The form factor contains the full physical information.

Perturbative Yang-Mills theory suggests that the deviation of the full propagator from the free propagator is logarithmically small for large momenta and to zeroth order in perturbation theory the free propagator is

$$D_0(k^2) = \frac{1}{k^2}. \tag{5.4}$$

The asymptotic behavior of the gluon propagator for large momenta is given to one-loop level in perturbation theory by [DZ89], [Man79]

$$D_{\mathrm{uv}}(k) = \frac{1}{k^2} \left( \frac{1}{2} \ln\left( \frac{k^2}{\Lambda^2} \right) \right)^{-d_D}, \tag{5.5}$$

with the exponent $d_D = 13/44$ in Landau gauge for quenched QCD and the momentum cut-off $\Lambda$.

Concerning the color confinement problem, the infra-red region of the momentum is of great importance. In this region one expects a measurable deviation of the gluon propagator from the free one. Various lattice simulations have shown that the propagator falls off quite differently than in perturbation theory. This led to a couple of interpretations for the functional form of the gluon propagator. The lattice data in [MMST93] was interpreted in terms of an anomalous dimension $\gamma$ being consistent with $\gamma \approx 1$, or in other works [MO87], [G$^+$87] the data of the gluon propagator in Landau gauge was consistent with a massive particle propagator. The existence of an effective mass of the gluon is additionally supported by phenomenological considerations [CF94]. On the other hand, a vanishing gluon propagator at zero momentum was also suggested in [Gri78] and is motivated by various works [Sti86], [CR91], [vSAH97], [vSHA98].

We are interested in the non-perturbative information contained in the gluon propagator in the infra-red limit and measure directly the gluon form factor $F(k^2)$. Since there exist different ways to extract the gluon fields, i.e. the gauge fields $A_\mu^{\mathrm{a}}(x)$, from the link variables $U_\mu(x)$, we discuss our definition of the gluonic degrees of freedom which is motivated by continuum Yang-Mills theory.

### 5.1.2   Gluon Fields From Lattice Link Variables

The gluon propagator is directly defined as a two point Green's function of the gauge fields $A_\mu^{\mathrm{a}}(x)$, but the degrees of freedom of $SU(2)$ Yang-Mills LGT are the link variables $U_\mu(x) \in SU(2)$ being complex $(2 \times 2)$-matrices. Hence, we have to extract the gluon fields corresponding to the link variables. A frequently used definition of the gluon fields is given by

$$A_\mu^{\mathrm{a}}(x) = \frac{1}{4i}\mathsf{Tr}\left[\left(U_\mu(x) - U_\mu^\dagger(x)\right)\tau^{\mathrm{a}}\right] + \mathcal{O}(a^3), \tag{5.6}$$

where lattice gauge fields $A_\mu^{\mathrm{a}}(x)$ approach the conventional continuous vector potentials $\bar{A}_\mu^{\mathrm{a}}(x)$ in the continuum limit. There exist alternative definitions of the gluon fields extracted from the link variables. These definitions are accurate to higher order in $a$, but it was shown [GPP$^+$98], [Cuc99] that the occurring deviations can be absorbed into the multiplicative renormalization constant of the fields.

We want to introduce an additional definition of the lattice gluon fields which respects the behavior of the gluon fields under a gauge transformation of the fundamental matter fields. If we consider the continuum field theory, then the fundamental matter fields, which are defined in the fundamental representation, transform under a gauge transformation as follows

$$\psi(x) \rightarrow \psi'(x) = \Omega(x)\psi(x), \quad \Omega(x) \in SU(2). \tag{5.7}$$

Whereas the gluon fields transform according to the adjoint representation:

$$A_\mu^{a\prime}(x) = O^{ab}(x)A_\mu^b + \frac{1}{2}\varepsilon^{aef}O^{ec}\partial_\mu O^{fc} \tag{5.8}$$

$$O^{ab}(x) := 2\text{tr}\left[\Omega(x)t^a\Omega^\dagger t^b\right], \quad O^{ab}(x) \in SO(3). \tag{5.9}$$

This behavior under gauge transformations is compared with the lattice gauge field theory, where the link variables transform under gauge transformations as

$$U_\mu'(x) = \Omega(x)U_\mu(x)\Omega^\dagger(x+\mu), \quad \Omega(x) \in SU(2). \tag{5.10}$$

In order to allow for comparison with the continuum formulation, the adjoint links are additionally introduced as follows:

$$\tilde{U}_\mu^{ab}(x) := 2\text{tr}\left[U_\mu(x)\hat{t}^a U^\dagger(x)\hat{t}^b\right], \quad \hat{t} = \frac{1}{2}\tau^a \tag{5.11}$$

$$\tilde{U}_\mu'(x) := O(x)\tilde{U}_\mu(x)O^{\text{T}}(x+\mu), \quad O(x) \in SO(3), \tag{5.12}$$

where $O(x)$ is defined as in eq. (5.9) and $\tau^a$ are the Pauli matrices. The gauge fields are extracted from the lattice configurations by analyzing the behavior of the continuum gluon fields under gauge transformations (see eq. (5.7)), whereby the lattice gluon fields $A_\mu^a(x)$ are identified as the algebra valued fields of the adjoint representation:

$$\tilde{U}_\mu^{cd}(x) := \left(\exp\left\{\hat{t}^f A_\mu^f(x)a\right\}\right)^{cd}, \quad \hat{t}_{ac}^f := \varepsilon^{afc}, \tag{5.13}$$

with the total antisymmetric tensor $\varepsilon^{abc}$ being the generator of the $SU(2)$ gauge group in the adjoint representation. The lattice spacing is again denoted by $a$. We obtain the explicit formula for the (lattice) gluon fields $A_\mu^a(x)$ defined in eq. (5.13) in terms of the $SU(2)$ link variables $U_\mu(x)$, if we consider the spinor representation of the link variables

$$u_\mu(x) = u_\mu^0(x) + i\vec{u}_\mu(x)\vec{\tau}, \quad \left(u_\mu^0(x)\right)^2 + \left(\vec{u}_\mu(x)\right)^2 = 1. \tag{5.14}$$

If this representation for the link variables $U_\mu(x)$ is inserted into eq. (5.11), we expand the equations (5.11) and (5.13) in powers of the lattice spacing $a$, where

$$\vec{u}_\mu(x) = O(a) \text{ and } \left(u_\mu^0\right)^2(x) = 1 - O\left(a^2\right)$$

were used. Subsequently, if we compare to order $O(a)$, we finally receive for the gluonic fields the following identity

$$A_\mu^b(x)a + O(a^2) = 2u_\mu^0(x)u_\mu^b(x), \tag{5.15}$$

without summation over the space-time index $\mu$. An important point is that this gauge field $A_\mu^a(x)$ has been defined by the adjoint link (5.11). As a consequence,

the representation of the gluon field (5.15) is invariant under a non-trivial $\mathbb{Z}_2$ center transformation:

$$U_\mu(x) \rightarrow -U_\mu(x). \tag{5.16}$$

To contrast the definition (5.15) of the lattice gluonic fields with the previous definition of the gauge field from the fundamental link, i.e.

$$U_\mu(x) = \exp\left\{ia\bar{A}_\mu^{\mathrm{b}}t^{\mathrm{b}}\right\}, \quad a\bar{A}_\mu^{\mathrm{b}} = 2u_\mu^{\mathrm{b}}(x) + O(a^2), \tag{5.17}$$

where one must assume that the link field $U_\mu(x)$ is close to the unit element, i.e. $u_\mu^0(x) = 1 - O(a^2)$. Indeed, the gluon field $\bar{A}_\mu(x)$ changes the sign under a non-trivial center transformation. The previous definition of the gauge field $\bar{A}_\mu(x)$ therefore contains information on center elements and the coset fields as well. Here, we propose to disentangle the information carried by the center elements and the coset fields $A_\mu(x)$ and to study their correlation separately. We will present the correlation function of the coset "gluon" fields $A_\mu^{\mathrm{b}}(x)$.

### 5.1.3   The Lattice Approach to the Gluon Propagator

As pointed out before, the gluon propagator is defined as the two point Green's function of the gluon fields. The lattice version thereof is given by

$$D_{\mu\nu}^{\mathrm{ab}}(x - y) = \langle A_\mu^{\mathrm{a}}(x)\, A_\nu^{\mathrm{b}}(y)\rangle_{\mathrm{MC}}, \tag{5.18}$$

where $A_\mu^{\mathrm{a}}(x)$ is defined in terms of the coset part of the link variables (see eq. (5.15)). The subscript MC denotes the Monte-Carlo average which is taken over a sufficiently large number of properly thermalized gauge configurations.

The Fourier transform of the gluon propagator on the lattice is given by

$$D_{\mu\nu}^{\mathrm{ab}}(\hat{p}) = a^4 \sum_x D_{\mu\nu}^{\mathrm{ab}} \exp\left\{i\hat{p}x\right\}, \quad \hat{p}_k = \frac{2\pi}{N_k a(\beta)} n_k, \tag{5.19}$$

where $n_k$ labels the Matsubara mode in $k$-direction and where $N_k$ is the number of lattice points in this direction. The lattice momentum on the lattice is given by

$$p_k = \frac{2}{a(\beta)} \sin\left(\frac{\pi}{N_k} n_k\right). \tag{5.20}$$

This coincides with the Matsubara momentum $\hat{p}_k$ in (5.19) for the limit of $n_k \ll N_k$. The advantage of this definition is that the free lattice propagator takes the familiar form $1/p_k^2$. Since the extension of the lattice in a single direction is $L_k = N_k\, a(\beta)$, with $N_k$ the number of lattice points in the $k$-direction, the momentum range covered in the actual simulation induces an $UV$-cutoff at $\Lambda = \pi/a(\beta)$. The dependence of the lattice spacing $a(\beta)$ on the simulation parameter $\beta$ is given by renormalization, see eq. (2.69).

The propagator (5.18) is a rapidly decreasing function in coordinate space implying that the physical information at large distances $|x - y|$ is washed out by statistical noise. From this it follows that the information on the low momentum behavior is lost. The solution that was proposed in [Zwa91], [Cuc99] is to measure the propagator directly in momentum space. For this we Fourier transform the gluon fields

$$\tilde{A}(k) := \sum_x A(x) \exp\{ikx\} = \sum_x A(x) \left(\cos(kx) + i \sin(kx)\right). \qquad (5.21)$$

The Fourier transformed gluon fields are inserted into the momentum-space gluon propagator being defined by

$$\tilde{D}(k) := \frac{1}{N^2} \sum_{a,\mu} \left\langle \tilde{A}(k)\tilde{A}(-k) \right\rangle_{\text{MC}}. \qquad (5.22)$$

This yields the propagator in momentum space

$$\tilde{D}(k) = \frac{1}{N^2} \sum_{a,\mu} \left\langle \left(\sum_x A_\mu^a(x) \cos(kx)\right)^2 + \left(\sum_y A_\mu^a(y) \sin(ky)\right)^2 \right\rangle_{\text{MC}}, \qquad (5.23)$$

where $N$ is the number of lattice points.

If translation invariance of the gluon propagator is used, i.e.

$$\left\langle A_\mu^a(x) A_\nu^b(y) \right\rangle_{\text{MC}} \propto f(x - y), \qquad (5.24)$$

one finds from (5.23) that the gluon propagator contains the trivial factor $1/k^2$ which is also present in the free theory. Finally, one obtains for the following gluon propagator

$$\tilde{D}(k) = \sum_{a,\mu} \sum_x \left\langle A_\mu^a(x) A_\mu^a(0) \right\rangle_{\text{MC}} \cos(kx). \qquad (5.25)$$

If we directly measure the deviation of the gluon propagator from the free one, namely the form factor $F(k^2)$ implicitly defined in eq. (5.3), we expect a further increase of numerical accuracy. Without any loss of generality, we choose the momentum transfer to be in the fourth direction, $k = (0, 0, 0, k_4)$, and define

$$\Delta_t \phi_\mu^a(x) := A_\mu^a(x + a\hat{e}_4) - A_\mu^a(x), \qquad (5.26)$$

with $\hat{e}_4$ the unit vector in time direction. A computation, which is given in detail in Appendix (C.1), yields

$$F(k_4^2) = \frac{1}{N} \sum_{a,\mu} \left\langle \left(\sum_x \Delta_t \phi_\mu^a(x) \cos(\hat{k}x)\right)^2 + \left(\sum_y \Delta_t \phi_\mu^a(y) \cos(\hat{k}y)\right)^2 \right\rangle_{\text{MC}}, \qquad (5.27)$$

where $k_4$ is the lattice momentum (5.20) in time direction. The free part $1/k^2$ of the propagator $D(k)$ is precisely canceled by using the difference operator $\Delta_t$ and we are thus capable to calculate directly the gluon form factor $F(k^2)$. The Monte-Carlo average (5.27) defined in this way allows for a high precision measurement of the gluon form factor.

## 5.2   The Numerical Simulation

In this section we want to outline our procedure for calculating the gluon form factor. Properly thermalized configurations are produced by the usual heat bath algorithm. Afterwards the Landau gauge is implemented by maximizing the following gauge fixing functional[1]

$$F_U\left[g(x)\right] = \sum_{x,\mu} \frac{1}{2} \mathsf{Re\, Tr}\left[g(x)U_\mu(x)g^\dagger(x+\mu)\right]. \qquad (5.28)$$

We use two different numerical procedures for fixing the Landau gauge iteration: 1) the iterated over-relaxation algorithm (IO) which averages over Gribov copies and 2) the simulated annealing algorithm (SA) which tries to locate the global maximum of the gauge functional (5.28). The algorithms used are explained in detail in the appendix B. The effect of the gauge fixing ambiguities, i.e. Gribov copies, on the form factors is discussed in chapter 6 where we further discuss gauge fixing on the lattice. We will refer to the gauge fixed by the IO-algorithm as IO-gauge, since we will compare this gluonic form factor with one obtained of configurations which were gauge fixed to the Landau gauge condition (5.28) by using the simulated annealing algorithm (SA-gauge).

Then the gluon form factor (5.27) is evaluated from the gauge fixed configurations as the mean expectation value of 200 configurations of a $L_\mathbf{x} \times L_t = 16^3 \times 32$ lattice, where 1000 thermalization steps were used to thermalize the configurations and 10 thermalization steps were used between two different measurements of the form factor to cancel autocorrelations between those two configurations. A flow chart of the simulation is given in figure (5.1).

The gluon propagator and ghost propagator are both functions with respect to momentum $p$. Physical units are obtained with the use of the scaling function eq. (2.69) and the definition of the lattice momentum (5.20). Calculations with different $\beta$-values and fixed numbers of lattice points correspond to simulations with a different UV-cutoff $\Lambda$ and of different physical volume of the lattice respectively.

The effect of center vortices on both form factors is disentangled by first performing the MCG and center projection which produces the center vortex

---

[1]Here the Landau gauge is given for the gauge group $SU(2)$, an extension to $SU(N)$ gauge group can be done easily.
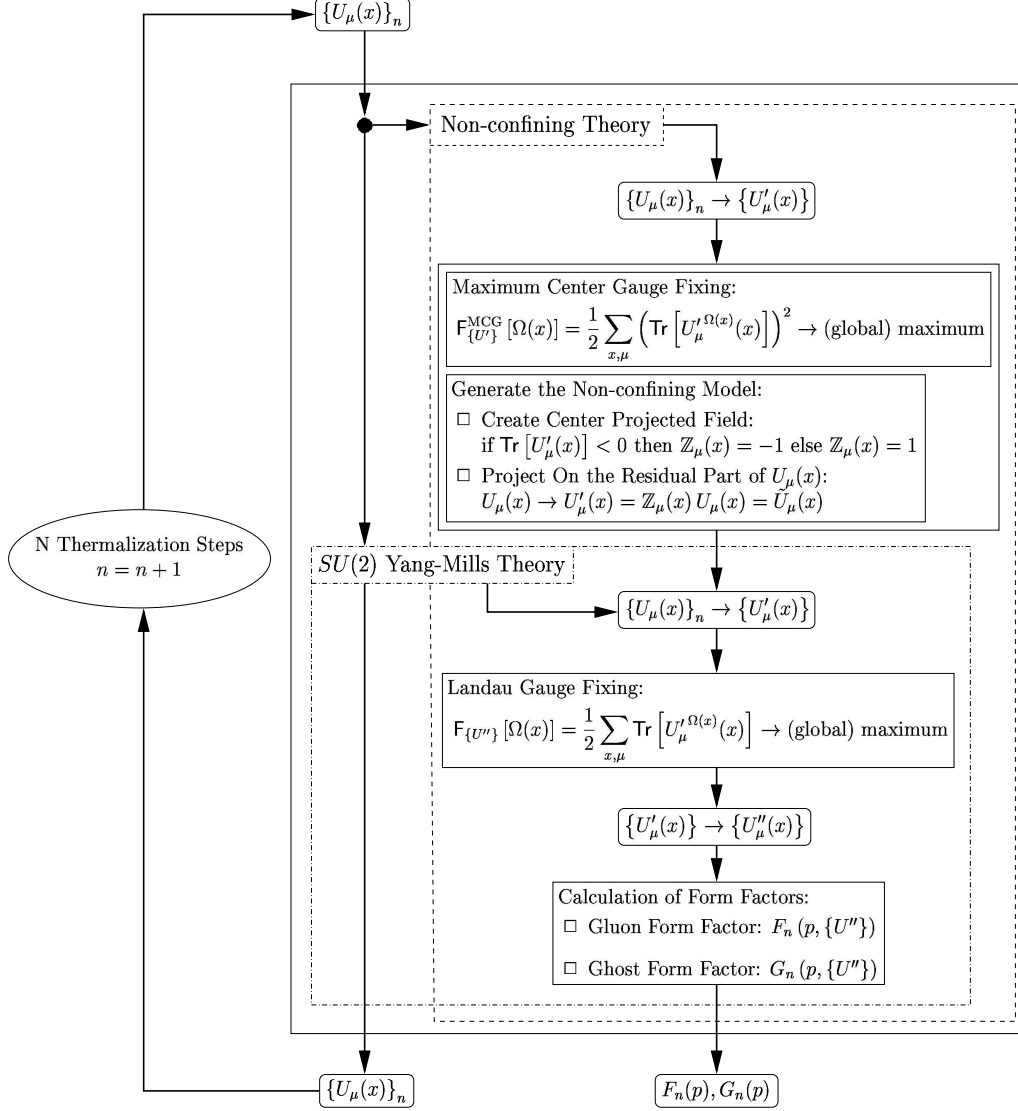
Figure 5.1: The flow chart for the measurement of the gluon and ghost form factors for the pure $SU(2)$ Yang-Mills theory and for the non-confining model. For the full, confining theory, the links ensembles are gauge fixed to Landau gauge and the form factors are subsequently calculated. For the non-confining model, the maximal center gauge fixing, the center projection and the elimination of the center vortex content of the link ensembles are performed before the gauge fixing procedure.

ensemble $\{\mathbb{Z}_\mu(x)\}$. Afterwards, the center vortex content is removed from the link configurations $\{U_\mu(x)\}$ by multiplying every link variable $U_\mu(x)$ with its center content $\mathbb{Z}_\mu(x)$ which extracts the coset content $\tilde{U}_\mu(x)$ of the link variable that finally defines the ensemble $\{\tilde{U}_\mu(x)\}$ of the non-confining model. Subsequently, the center vortex free ensemble $\tilde{U}$ is gauge fixed to Landau gauge and the gluon and ghost form factors are calculated from the non-confining ensemble. The differences between the form factors of full Yang-Mills theory and those of the non-confining model are interpreted as the effect of center vortices.

## 5.3   Numerical Results: Gluon Form Factor

Our measurement results of the form factor $F_B(p^2)$ are generally an unrenormalized function of the momentum in physical units. The renormalized form factor $F_R(p^2)$ is obtained via multiplicative renormalization

$$F_R(p^2) = Z_3^{-1}(\Lambda)\, F_B(p^2), \qquad (5.29)$$

with the gluonic wave function renormalization $Z_3(\Lambda)$ being chosen to get a finite value for the renormalized form factor $F_R$ at a fixed momentum transfer which defines the renormalization point. The subscripts will be dropped in the following and $F(p^2)$ always refers to the renormalized form factor. In fig.(5.2) we present our measurement results of the gluon form factor in the IO-Landau gauge [LRG02]. The range for the different values of the $\beta$-parameter was set to $\beta \in [2.1, 2.6]$ and the reference scale was fixed by setting the string tension to $\sigma = (440\text{MeV})^2$ which assigns physical units to momenta. In order for our measured data of the gluon form factor at different values of $\beta$ to give a single smooth function of the lattice momentum, we have to exploit the property of full Yang-Mills theory to be multiplicatively renormalizable (see Appendix (D) for the model independent maximum likelihood method used here). The data of the gluonic form factor $F(p^2)$ obtained with different $\beta$-values nicely agree within numerical accuracy signaling independence of the UV-cutoff and of the lattice volumes.

In the high momentum region, our data nicely agree with the behavior expected from perturbation theory,

$$F(p^2) \propto \left(\ln \frac{p^2}{\Lambda^2}\right)^{-\frac{13}{22}}, \text{ for } p^2 \approx \Lambda^2 \gg (1\,\text{GeV})^2. \qquad (5.30)$$

The fit represented in fig.(5.2) has the functional form

$$F_{\text{fit}}(p^2) = N\, \frac{p^2}{p^2 + m_1^2} \left(\frac{1}{p^4 + m_2^4} + \frac{s}{(\ln(m_L^2 + p^2))^{13/22}}\right), \qquad (5.31)$$

which is called the coarse grained mass fit with the fit parameters $(N, m_1, m_2, s)$. Momentum $p$ and all mass scales are in units of GeV. The normalization $N$ is

the sole parameter affected by the multiplicative renormalization, the remaining parameters are renormalization group invariants. The following values of the parameters gives a fit function which accords with the data within the statistical error bars:

$$N = 8.1133, \quad m_1 = 0.64 \text{ GeV}, \quad m_2 = 1.31 \text{ GeV},$$
$$s = 0.32, \quad m_L = 1.23 \text{ GeV}.$$

## 5.3.1 Comparison with Dyson-Schwinger Equations solutions

As a next topic we want to compare our results with those achieved by the second non-perturbative treatment of QCD: the Dyson-Schwinger equations (DSE). In this approach, the coupled set of continuum DSEs of the gluon and ghost propagators has been addressed in [vSAH97], [vSHA98] and newer treatments are given in [AB98a], [Blo01]. It was first pointed out in [vSAH97], [vSHA98] that the gluon and ghost form factors satisfy scaling laws in the infra-red for a specific truncation scheme of the infinite tower of coupled Dyson-Schwinger equations:

$$F(p^2) \propto \left(p^2\right)^{2\kappa}, \quad p^2 \ll \Lambda_{\text{QCD}}^2. \tag{5.32}$$

The concrete values of $\kappa$ depend on the truncation of the Dyson-Schwinger series and whether an angular approximation of the momentum loop integral is used. The given values of $\kappa$ in the literature have a range of $\kappa \in [0.77, \dots, 1]$. Our lattice data are consistent with $\kappa = 0.5$ corresponding to an infra-red screening by a gluonic mass (see fig.(5.2)).

A further interesting topic is the infra-red behavior of the ghost-gluon-vertex form factor which corresponds to the running coupling strength in four space-time dimensions. The functional form can by written in terms of the gluon and ghost form factors in the following way:

$$\alpha(p^2) = \alpha(\mu^2)F(p^2)G^2(p^2), \tag{5.33}$$

where $G(p^2)$ is the ghost form factor that will be addressed in the following sections. This function approaches a constant in the limit $p^2 \to 0$ that is independent of the approximations and truncation schemes used [vSAH97], [vSHA98], [AB98a], [WA01]. At this point, the running coupling is mentioned, since it was used in the DSEs as an input at a certain renormalization point:

$$\alpha(\mu = 6 \text{ GeV}) = \frac{3}{22} \frac{4\pi}{\ln\left(\frac{\mu^2}{\Lambda_{\text{QCD}}^2}\right)} \approx 0.449. \tag{5.34}$$

Furthermore, the truncation of [vSAH97], [vSHA98] was solved in [FAR02] for the case of the $SU(2)$ gauge group which yields the DSE result shown in fig.(5.2).
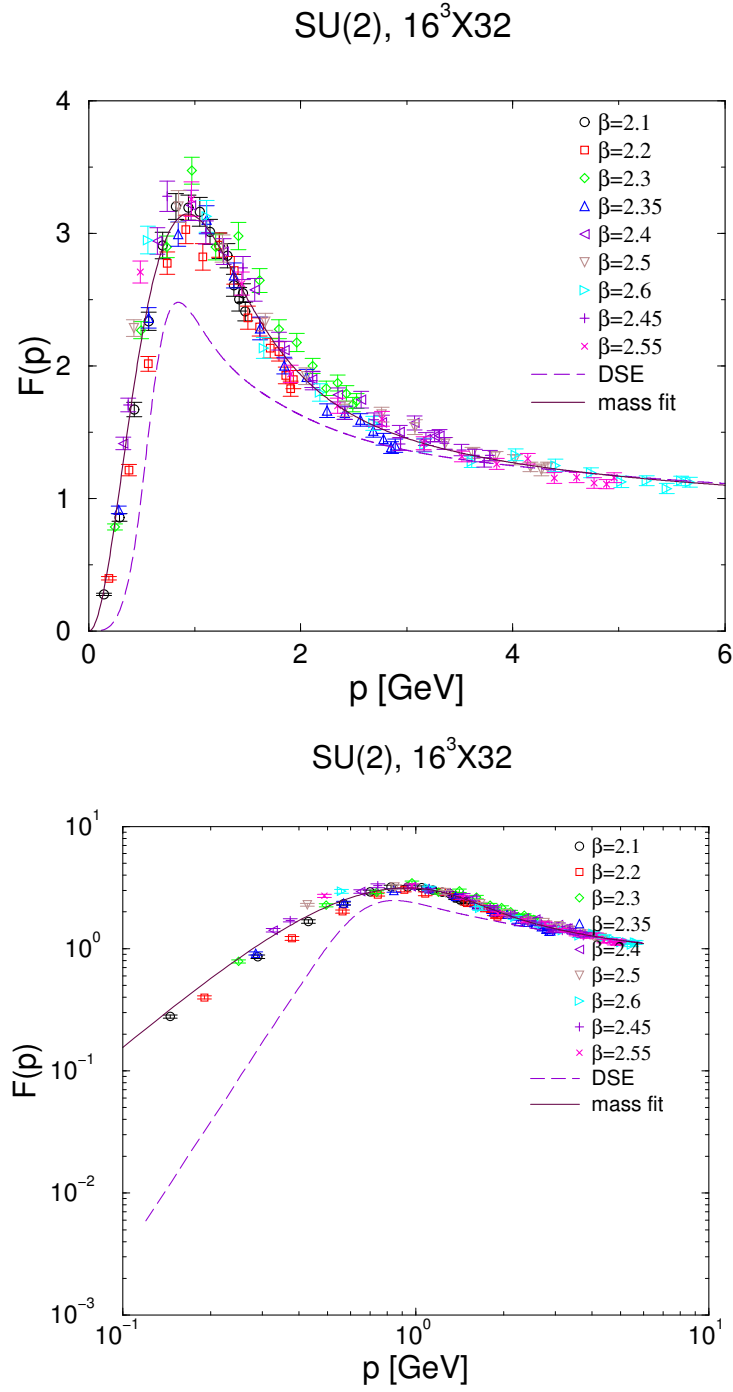
Figure 5.2: The gluon form factor $F(p^2)$ of the lattice data and the DSE solution from ([FAR02]) as a function of the momentum transfer (top panel: linear scale; bottom panel: log-log-scale). Remarkable is the good agreement of the DSE solution and the lattice data on a qualitative level.

On a qualitative level, we find an agreement of the DSE solution with our lattice result. Since there exist a variety of values of $\kappa$ depending on the truncation of the DSEs, we do not expect a detailed agreement of both gluon form factors close to vanishing momentum. We want to emphasize that the peak of the form factor at the intermediate momentum range is also observed in the DSE approach, although there are quantitative deviations concerning its steepness.

## 5.3.2 Signatures of Confinement in the Gluon Propagator

In the preceding chapter 3 we introduced the concept of center vortices as a possible candidate for the mechanism of color confinement. To investigate the effect of the center vortices on the gluon form factor, we implement first the maximal center gauge. In this gauge, the coset part of the links which corresponds to the gluons in the infra-red physics, is de-emphasized and the center vortices appear as physical degrees of freedom in the continuum limit [LRT98]. If the full Yang-Mills theory is reduced to the vortex content alone, the full string tension is still obtained [DDFGO97a], [DDFG⁺98] and the $q\bar{q}$-potential is still linearly rising. On the other hand, if we remove the center vortex content from the full theory, i.e. we project on the residual part of the link variables, a vanishing string tension is measured [DDFGO97a], [DDFG⁺98], [dFD99] and only the Coulomb part of the $q\bar{q}$-potential is recovered. Hence, removing the center vortex content from the link configurations yields a non-confining model[2]. See also fig.(5.4) for both $q\bar{q}$-potentials in the confining (full) Yang-Mills theory and the non-confining model. In order to extract the information of quark confinement encoded in the gluon form factor in Landau gauge, we remove the center vortex content from the link variables which results in the non-confining theory mentioned before. Afterwards, we perform the Landau gauge and compare the form factor of the modified theory with the result of the full $SU(2)$ Yang-Mills theory. The numerical procedure is outlined in the preceding section (5.2).

Our measurement results of the non-confining ensemble are shown in figure (5.3). The striking feature is that the strength of the form factor in the intermediate momentum range is strongly reduced.

## 5.3.3 The Gluon Form Factor in MCG-Gauge

If the maximal center gauge is implemented, important parts of the non-trivial information of the links is shuffled into the center vortex degrees of freedom. A study of the maximal center gauge in the continuum limit ([ER00a]) has shown, that the gauge condition (5.28) in the continuum limit corresponds to a background gauge

$$\left[\partial_\mu + iA_\mu^{\mathrm{B}}(x), A_\mu(x)\right] = 0, \tag{5.35}$$

---

[2]This must not be confused with the deconfinement phase of the full Yang-Mills theory, where still center vortices are present and we have still a (spatial) string tension.

SU(2) 16³x32 Landau gauge



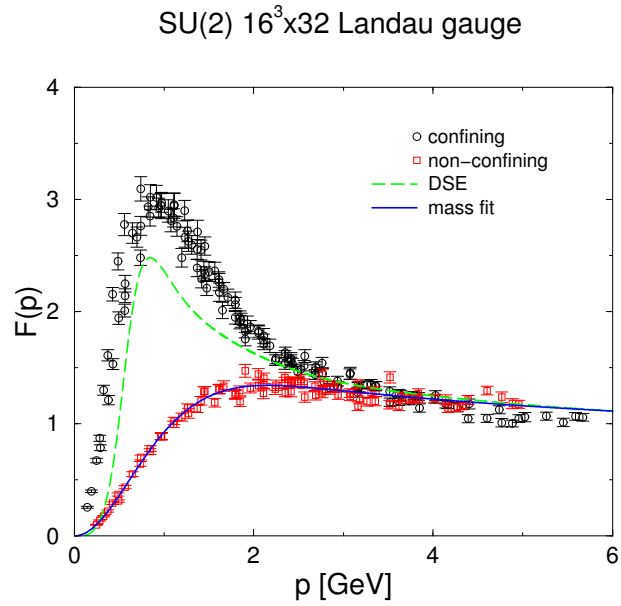Figure 5.3: The gluon form factors $F(p^2)$ of the full $SU(2)$ Yang Mills ensemble and of the modified, non-confining theory. The loss of strength of the gluon form factor of the modified theory compared to the gluon form factor of the full theory in the region at 1 GeV is clear visible.

SU(2), 12⁴
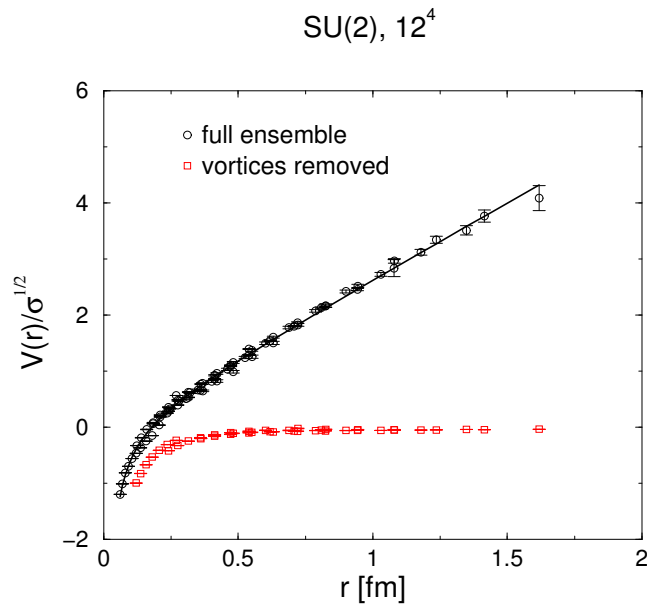


Figure 5.4: The static $q\bar{q}$-potential for full Yang-Mills theory and for the non-confining model.

where the back ground gauge field $A_\mu^{\mathrm{B}}(x)$ marks a specific (thin) center vortex field. The back ground gauge (5.35) complies with the Landau gauge, if center vortices are absent in the gauge fields $A_\mu(x)$.

The procedure of calculating the gluon form factor in maximal center gauge is the same as for the Landau gauge with the sole exception that the center gauge is implemented and not the Landau gauge. If we use the definition (5.15) for the adjoint representation of the gluon fields, then the MCG corresponds to the adjoint Landau gauge and the gluon fields satisfies the Landau condition $\partial_\mu A_\mu^{\mathrm{a}}(x) = 0$. The gauge condition (5.35) does not imply that the gluon propagator $D_{\mu\nu}^{\mathrm{ab}}(k)$
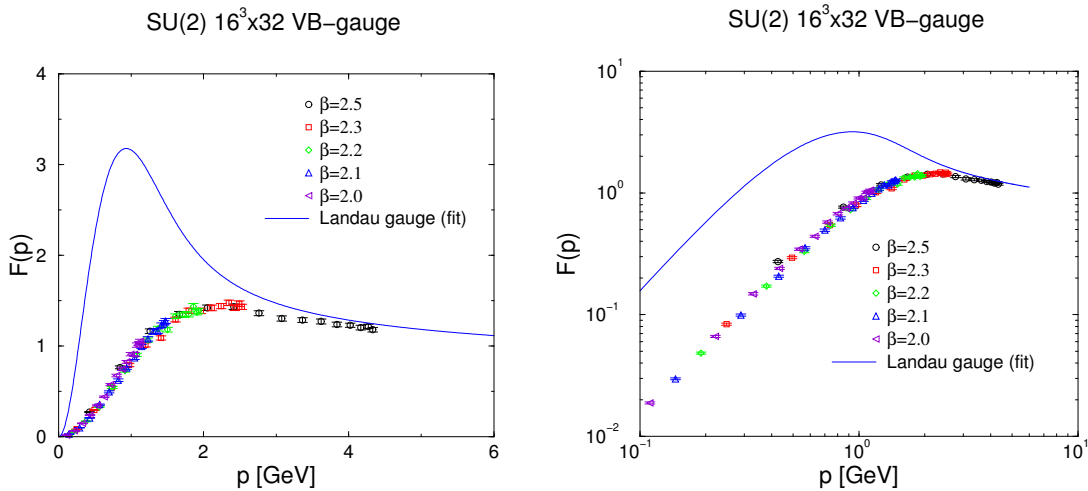


Figure 5.5: The gluon form factor $F(p^2)$ in MCG-gauge as a function of the momentum transfer compared with the fit function of the gluon form factor in Landau gauge (left panel: linear scale; right panel: log-log-scale).

is transversal. Hence the result of the gluon form factor shown in figure (5.5) incorporates only parts of the information contained in the gluon propagator of the maximal center gauge. The gluon form factor of maximal center gauge is presented only as a comparison with the Landau gauge result.

It is apparent that the form factors of Landau and maximal center gauge differ in the intermediate region. In the maximal center gauge, the non-perturbative content of information of the degrees of freedom is shuffled into the center part of the links, whereas the gluon form factor is calculated from the residual (coset) part of the link variables. On the other side, most of the information is contained in the residual part of the link variables in Landau gauge. This explains why the gluon form factor of maximal center gauge represents the behavior of the form factor of the non-confining model. Our findings support the fact that the center vortices are the relevant degrees of freedom for the infra-red physics.

## 5.4   The Ghost Propagator

In this section we will investigate the relevance of the center vortices on the ghost form factor $G(p^2)$. The ghost fields emerge in a continuum field theory because of the need of gauge fixing which is required to be able to calculate a well defined gluon propagator. The continuum field theory is usually gauge fixed in its functional description with the the Faddeev-Popov method. In this method, the gauge-fixing condition $\mathsf{G}[A^\Omega] \equiv \frac{\delta}{\delta\Omega}\mathsf{F}[A^\Omega] = 0$, see e.g. eq. (5.28), is implemented by inserting into the functional integral of the pure Yang-Mills theory

$$\mathcal{Z}\left[U_\mu(x)\right] = \int \left[\mathsf{D}U_\mu(x)\right] \exp\left\{-\beta\mathcal{S}_{\mathrm{YM}}\left[U_\mu(x)\right]\right\} \tag{5.36}$$

the quantity[3]

$$\int \left[\mathsf{D}\Omega(x)\right] \delta\left(\mathsf{G}\left(A^\Omega\right)\right) \det\left[\frac{\delta\mathsf{G}\left(A^\Omega\right)}{\delta\Omega(x)}\right], \tag{5.37}$$

where $\Omega$ denotes the gauge transformation used to fulfill the gauge fixing condition $\mathsf{G}[\Omega] \equiv \mathsf{G}(A^\Omega)$. In contrast to QED, where the Faddeev-Popov determinant is independent of the gauge fields $A_\mu^\mathrm{a}(x)$, the gauge fields contribute to the Faddeev-Popov determinant of Yang-Mills theories. The Faddeev-Popov determinant is given in components by

$$\det\left[(\mathbb{M})_{xy}^{\mathrm{ab}}\right] := \det\left[\frac{\delta G\left(A_\mu^{\mathrm{a},\Omega}(y)\right)}{\delta\omega^\mathrm{b}(x)}\right], \tag{5.38}$$

with the components $\omega^\mathrm{b}(x)$ of the gauge transformation $\Omega(x)$. This determinant can be represented as a functional integral over a new set of anti-commuting fields (Grassmann numbers) belonging to the adjoint representation:

$$\det\left[(\mathbb{M})_{xy}^{\mathrm{ab}}\right] = \int \left[\mathsf{D}c\right]\left[\mathsf{D}\bar{c}\right] \exp\left\{i\int \mathsf{d}^4x\, \bar{c}^\mathrm{a}(y)\left(-(\mathbb{M})_{xy}^{\mathrm{ab}}\right) c^\mathrm{b}(x)\right\}, \tag{5.39}$$

with the (anti-) ghost fields $(\bar{c}^\mathrm{a}(y))\, c^\mathrm{b}(x)$. The following matrix $(\mathbb{M})_{xy}^{\mathrm{ab}}$ defines the Faddeev-Popov operator $\mathbb{M}$ for the Landau gauge condition $\partial_\mu A_\mu = 0$:

$$(\mathbb{M})_{xy}^{\mathrm{ab}} = \left(\partial^2 - f^{\mathrm{abc}}A_\mu^\mathrm{c}(x)\partial_\mu\right)\delta^4(x-y), \tag{5.40}$$

where $\mathrm{a},\mathrm{b}$ are the color indices and $x,y$ are the space-time coordinates. The ghost propagator $G(x-y)$ in Landau gauge is then given in terms of the inverse of the Faddeev-Popov operator $\mathbb{M}$

$$G(x,y) := \delta^{\mathrm{ab}}\left\langle\left((\mathbb{M})_{xy}^{\mathrm{ab}}\right)^{-1}\right\rangle_{\mathrm{MC}}, \tag{5.41}$$

---

[3]Strictly speaking, the absolute value of the Faddeev-Popov determinant has to be used, but this requirement is usually dropped corresponding to a insertion of a zero instead of unity [BRS96], [BS98], [Sch99]. More about this ambiguity follows in chapter (6), see also eq. (6.1).

where the subscript MC indicates again the Monte-Carlo average over the field configurations. The ghost propagator in momentum space is given by

$$G(k) = \sum_{x,y} \left( \cos\left(\frac{2\pi}{N}x\right) (\mathbb{M}^{-1})^{ab}_{xy} \cos\left(\frac{2\pi}{N}y\right) + \right. \tag{5.42}$$
$$\left. + \sin\left(\frac{2\pi}{N}x\right) (\mathbb{M}^{-1})^{ab}_{xy} \sin\left(\frac{2\pi}{N}y\right) \right),$$

with $N$ the number of lattice points in time (fourth) direction. The lattice ghost propagator was first calculated in [SS96] for pure $SU(2)$ and $SU(3)$ Yang-Mills theory. The operator for the direct measurement of the ghost form factor is given in the next section.

### 5.4.1 The Ghost Form Factor

To improve our numerical statistics, we want again to evaluate directly the deviation of the ghost propagator from the free propagator, namely the ghost form factor $\bar{G}(k) = k^2 G(k)$. The ghost form factor is defined by an improved Faddeev-Popov operator $\bar{M}$:

$$\bar{G}(x,y) = \left\langle (\bar{\mathbb{M}}^{-1})^{ab}_{xy} \right\rangle_{MC}$$
$$= \left\langle (\mathbb{M}^{-1})^{ab}_{x+1\,y} - 2(\mathbb{M}^{-1})^{ab}_{x\,y} + (\mathbb{M}^{-1})^{ab}_{x\,y+1} \right\rangle_{MC}, \tag{5.43}$$

which cancels exactly the contribution of the free ghost propagator. From this it follows the ghost form factor in momentum space:

$$\bar{G}(k) = \sum_{x,y} \left( \cos\left(\frac{2\pi}{N}x\right) (\bar{\mathbb{M}}^{-1})^{ab}_{xy} \cos\left(\frac{2\pi}{N}y\right) + \right. \tag{5.44}$$
$$\left. + \sin\left(\frac{2\pi}{N}x\right) (\bar{\mathbb{M}}^{-1})^{ab}_{xy} \sin\left(\frac{2\pi}{N}y\right) \right),$$

A detailed derivation of the ghost form factor and of the action of the Faddeev-Popov operator on an arbitrary element $\omega(x) = \omega^a(x)\tau^a$ in the algebra of the gauge group $SU(2)$ is given in the appendix (C).

## 5.5 Numerical Results: Ghost Form Factor

The numerical simulation of the ghost form factor is identically to the description given for the gluon propagator (see sec.(5.2)). The lattice volume was $\mathrm{vol}[\mathbf{\Lambda}] = 16^3 \times 32$ sites and 100 Monte-Carlo configurations were used to calculate the averages.

For the evaluation of the ghost form factor, we used a Gauss-Seidel pre-conditioned Conjugate-Gradient method. This new algorithm gives a benefit of time roughly about a factor of two (see app.(C)).

In the high momentum region, our data nicely agree with the behavior expected from perturbation theory

$$G(p^2) \propto \left( \log \frac{p^2}{\Lambda^2} \right)^{-\frac{9}{44}}, \text{ for } p^2 \approx \Lambda_{\mathrm{UV}}^2 \gg (1\mathrm{GeV})^2. \tag{5.45}$$

We use the high momentum region ($p > 1.8$ GeV) of the ghost form factor and the left hand site of eq. (5.45) multiplied by an irrelevant normalization constant to fix our "momentum cutoff"

$$\Lambda_{\mathrm{UV}} = 1.09(78), \text{ for } p \gg 1.0 GeV. \tag{5.46}$$

With $\Lambda_{\mathrm{UV}}$ set, we use the following functional form as a fit function

$$R^G(p) = N_{\mathrm{g}} \frac{c_1 + p^{2\kappa}}{p^{2\kappa}} \left( \frac{4\pi}{\beta_0} \left( \frac{1}{\ln \frac{p^2}{\Lambda_{\mathrm{UV}}^2}} - \frac{1}{\frac{p^2}{\Lambda_{\mathrm{UV}}^2} - 1} \right) \right)^{\frac{9}{44}}, \tag{5.47}$$

where $N_{\mathrm{g}}$ is an irrelevant normalization factor and $\beta_0 = 22/3$ for the $SU(2)$ gauge group. The functional form of the fit function was chosen in such a way, that a scaling behavior in the infrared limit might be extracted. It was shown by investigating the coupled set of Dyson-Schwinger equations [vSAH97], [vSHA98], [AB98b] that the ghost propagator behaves as $G(p) \propto p^{-2-2\kappa}$ at small momenta. The ghost form factor shows a scaling behavior in the infrared limit. We obtain for our fit parameters[4]

$$\kappa = 0.471(821), \qquad N_{\mathrm{g}} = 0.849(296). \tag{5.48}$$

As mentioned before, the values of $\kappa$ have a range of $\kappa \in [0.5, 1.0]$ which depends on the truncation scheme of the DSE. Our lattice data supports an infra-red diverging form factor with $\kappa = 0.5$. Our fit function does not represent our lattice data in the high momenta region which is no surprise, since the functional form was chosen to be simple and at the same time to give a good agreement in the infrared region.

---

[4]The fit parameters were calculated by only considering the statistical errors. For a better estimate of the values of the fit parameters, one has to include the systematical errors. Since a unique estimation of the systematical errors was not possible up to now, only the result for for the statistical errors is show. First attempts with systematical errors have shown that $\kappa$ increases.
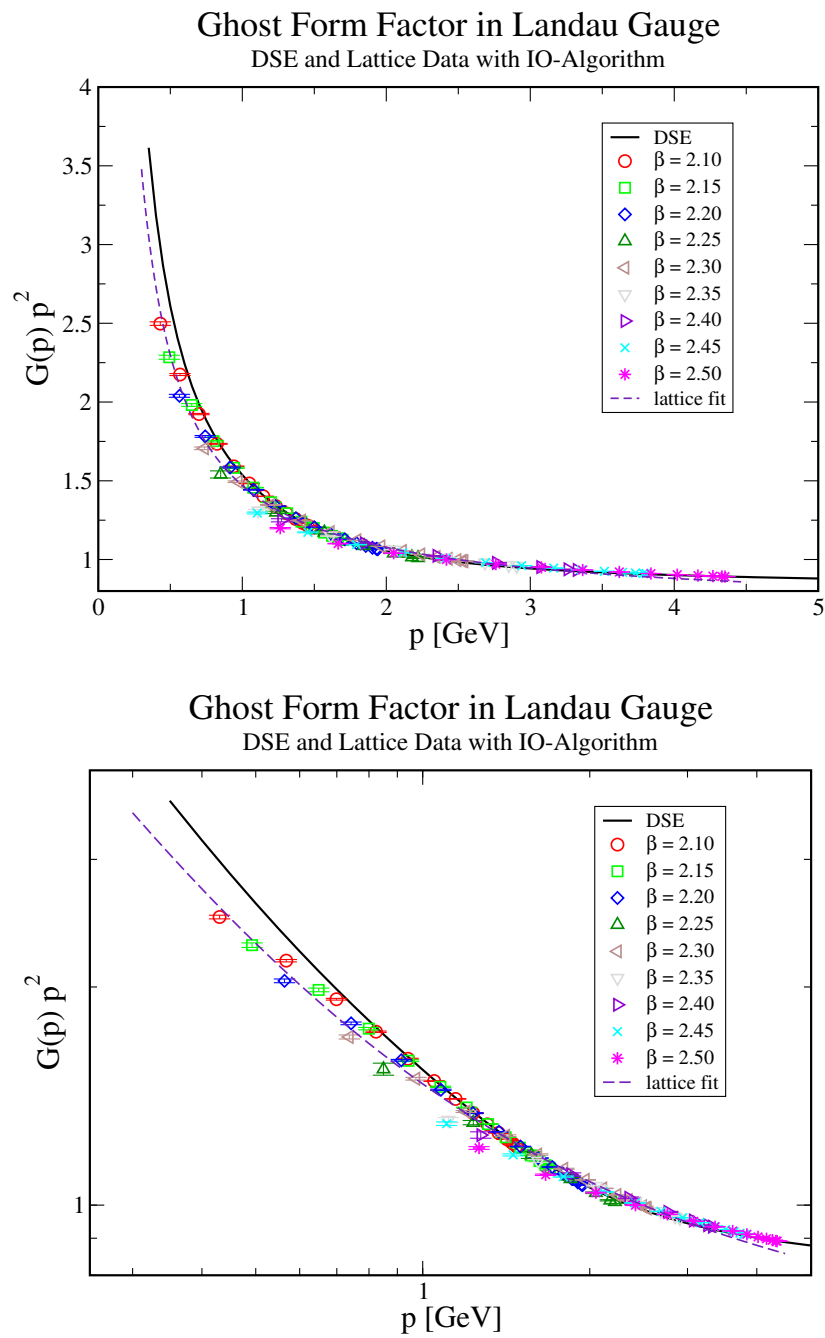
Figure 5.6: The ghost form factor $G(p^2)$ as function of the momentum transfer, the DSE result stems from (top panel: linear scale; bottom panel: log-log-scale).

## 5.5.1   Comparison with the Dyson-Schwinger Equation Solution

We used again the possibility of multiplicative renormalization of the lattice ghost form factor to compare the results obtained by the Dyson-Schwinger equations with the data obtained from our lattice calculations. It is remarkable that the agreement between the ghost form factor of the DSE approach[5] [FA02] and the ghost form factor obtained from the lattice with different $\beta$-values is so good. Even in the region around the maximum of the gluon form factor, both results are in good agreement. The slight difference between the lattice data and the DSE result in the infra-red compared to the result published in [L$^+$02] stems from the fact that we used here a model independent method for the multiplicative renormalization of the lattice data which uses the maximum likelihood method (see app. D).

## 5.5.2   Signature of Confinement in the Ghost Form Factor

The impact of the center vortices on the ghost form factor is investigated in the following. A divergent ghost form factor indicates color confinement by virtue of the confinement criterion of Gribov [Gri78]. This criterion states that the behavior of the ghost form factor in the infra-red limit is important for confinement [Zwa92]. In the case of Landau gauge, the ghost form factor diverges in the infra-red limit showing confinement. If the ghost form factor ceases to diverge, we have a non-confining setting.

To single out the effect of the center vortices we again transform the confining $SU(2)$ Yang-Mills theory to a model without confinement. After projecting out the center vortices from the theory, we perform the Landau gauge via the IO-Algorithm, see appendix B.2.1, and calculate the ghost form factor. Afterwards we compare the ghost form factor of the modified theory with the previous results of the full $SU(2)$ Yang-Mills theory. Our measurement data are shown in fig.(5.7).

It is in evidence that the ghost form factor looses drastically its strength in the low momentum region and it ceases to diverge in the low momentum regime [GLR04].

Consequently, we can conclude that the divergence of the ghost form factor in the infrared limit is caused by the presence of center vortices. By removing the center vortices from the full field configurations, the ghost form factor ceases to diverge in the low momentum region and thus the confinement criterion of Gribov is violated. This fact is in agreement with the behavior of the non-confining $q\bar{q}$-potential of the modified theory which does not rise linearly with distance both indicate the lack of color confinement. On the other hand, if the center vortices are present, i.e. full Yang-Mills configurations are considered, the ghost form

---

[5]We want to thank Ch. Fischer for sharing his DSE results and for the illuminating discussions
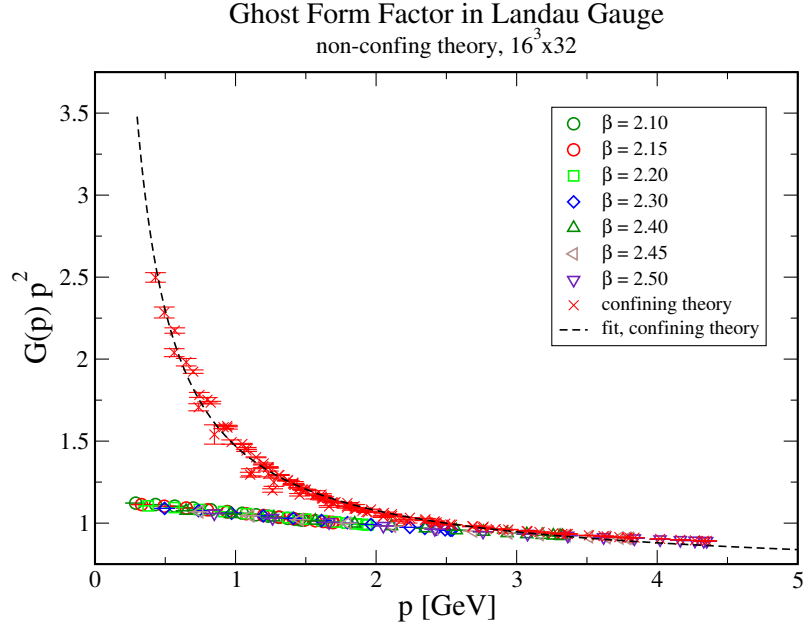
Figure 5.7: The ghost form factor $G(p^2)$ of the confining and of the non-confining theory. The loss of strength in the infrared limit is clear visible.

factor diverges in the infrared limit and the potential rises linearly with distance. Both indicate color confinement.

## 5.6  The Running Coupling $\alpha_\mathrm{s}(p^2)$ of the Strong Interaction

The next quantity we want to consider is the running coupling $\alpha_\mathrm{s}(p^2)$ of the strong interaction. In Landau gauge, this quantity can be directly obtained from the ghost-gluon vertex which incorporates only the ghost and gluon form factors. For this, we consider the ghost-gluon vertex in Landau gauge which contributes an additional term to the pure Yang-Mills Lagrangian

$$\mathcal{L}_{\bar{c}Ac} = gf^{\mathrm{abc}}k^\mu \bar{c}^{\mathrm{c}} A_\mu^{\mathrm{a}} c^{\mathrm{b}}, \tag{5.49}$$

where $g$ denotes the coupling parameter and $\bar{c}, c$ denote the anti-ghost and ghost fields respectively. Due to multiplicative renormalizability, all Green's functions can be rendered finite by renormalizing the fields and parameters of the Lagrangian. This is done without changing the functional form of the Lagrangian. The relations between the bare quantities, in the following labeled by 0 in the subscript, and the corresponding renormalized ones are given by the multiplicative

renormalization constants $Z_3$, $\tilde{Z}_3$ and $Z_g$

$$A^{\mathrm{a}}_{\mu,0} \;\rightarrow\; \sqrt{Z_3}\, A^{\mathrm{a}}_{\mu} \tag{5.50}$$

$$\bar{c}^{\mathrm{c}}_{0} \;\rightarrow\; \sqrt{\tilde{Z}_3}\, \bar{c}^{\mathrm{c}} \tag{5.51}$$

$$c^{\mathrm{b}}_{0} \;\rightarrow\; \sqrt{\tilde{Z}_3}\, c^{\mathrm{b}} \tag{5.52}$$

$$g_0 \;\rightarrow\; Z_g\, g. \tag{5.53}$$

From the definition of the ghost-gluon vertex renormalization constant $\tilde{Z}_1$ and from $\Gamma^{\mathrm{abc}}_{\mu,0} \rightarrow \tilde{Z}_1 \Gamma^{\mathrm{abc}}_{\mu}$ follows the relation between the renormalization constants of the constituents and of the vertex function and its renormalization constant

$$\tilde{Z}_1 = Z_g \tilde{Z}_3 Z_3^{\frac{1}{2}}. \tag{5.54}$$

This leads to the renormalized contribution of the ghost-gluon vertex to the Lagrangian

$$\mathcal{L}^{\mathrm{ren.}}_{\bar{c}Ac} = \tilde{Z}_1 g f^{\mathrm{abc}} k^{\mu} \bar{c}^{\mathrm{c}} A^{\mathrm{a}}_{\mu} c^{\mathrm{b}}. \tag{5.55}$$

The running coupling constant is finally defined by

$$\alpha := \frac{g^2}{4\pi}. \tag{5.56}$$

We can transform this into the following relation

$$\alpha(\Lambda^2) = \frac{\alpha(\mu^2)}{\tilde{Z}_3^2(\mu^2,\Lambda^2)\, Z_3(\mu^2,\Lambda^2)}, \tag{5.57}$$

where we used the renormalization eq. (5.53) and eq. (5.54) with the identity $\tilde{Z}_1 \equiv 1$ in Landau gauge [Tay71]. The behavior of the renormalization constant $\tilde{Z}_1$ and of the running coupling $\alpha(\Lambda^2)$ was also numerically investigated in [BCLM04].

From the multiplicative renormalization scheme of the fields follows the renormalized ghost and gluon form factors

$$G(p^2,\Lambda^2) = \tilde{Z}_3(\mu^2,\Lambda^2)\, G(p^2,\mu^2) \tag{5.58}$$

$$F(p^2,\Lambda^2) = Z_3(p^2,\Lambda^2)\, F(p^2,\mu^2). \tag{5.59}$$

Note that the choice of the renormalization point $\mu$ is arbitrary. By substituting this into Eq. (5.57) and renormalizing once at renormalization point $\mu$ and once at a specific value of momentum $p$, we achieve

$$\alpha(\Lambda^2)G^2(p^2,\Lambda^2)F(p^2,\Lambda^2) = \alpha(\mu^2)G^2(p^2,\mu^2)F(p^2,\mu^2) = \alpha(p^2)G^2(p^2,p^2)F(p^2,p^2). \tag{5.60}$$

Imposing the renormalization condition

$$G^2(p^2,p^2)F(p^2,p^2) = G^2(\mu^2,\mu^2)F(\mu^2,\mu^2) = 1 \tag{5.61}$$

on Eq. (5.60) yields for the running coupling

$$\alpha(p^2) = \alpha(\mu^2)G^2(p^2, \mu^2)F(p^2, \mu^2). \tag{5.62}$$

This defines the non-perturbative running coupling $\alpha(p^2)$ of the strong interaction in Landau gauge QCD [vSAH97], [vSHA98], [AB98b], [AB98a]. The running coupling $\alpha(p^2)$ defined in such a way does not depend on the renormalization point $\mu$, i.e. the defining relation of the coupling constant is a renormalization group invariant [Man79].

In the following, we show the non-perturbative running coupling constant $\alpha_{\mathrm{lat.}}(p^2)$ for the confined theory and for the non-confining model, which are deduced from out lattice form factors. We choose $\mu = 3\,\mathrm{GeV}$ as our renormalization point and set

$$G(p^2, \mu^2) = F(p^2, \mu^2) = \alpha(\mu^2) = 1, \text{ for } \mu = 3\,\mathrm{GeV}. \tag{5.63}$$

Our choice of the renormalization point and the value of the form factors and the running coupling at this point are arbitrarily. Since we are concerned with pure $SU(2)$ Yang-Mills theory, there exists no measurement data from experiments. If someone wants to related his data with our results, he is free to use the possibility of multiplicative renormalization to match our data to his results.

In the following figure, fig. 5.8, we show our lattice running coupling $\alpha_{\mathrm{lat.}}(p^2)$ of the confining theory and the non-confining model, i.e with and without center vortices respectively. The huge difference in the infra-red momentum region is quite evident: For the confining theory, the running coupling rises strongly in the infra-red and seems to converge to a value well above six in the limit of vanishing momentum. Our assumption of an existence of a fixed point at $p = 0$ stems from a comparison of results from Dyson-Schwinger equations with lattice data (see [BCLM03], [L$^+$02]). In contrast, the running coupling of the non-confining model fails to rise, even vanishes, in the infra-red limit. A vanishing running coupling shows clearly the fact that a theory without center vortices ceases to confine and gives further evidence to the importance of center vortices for confinement.

Figure 5.8: The lattice running coupling $\alpha_{\text{lat.}}(p^2)$ of the confining theory and the non-confining model. The wide difference between the two couplings is quite evident. The loss of strength in the infrared regime of the coupling constant without center vortices seems to have the limit zero at vanishing momentum showing non-confinement.
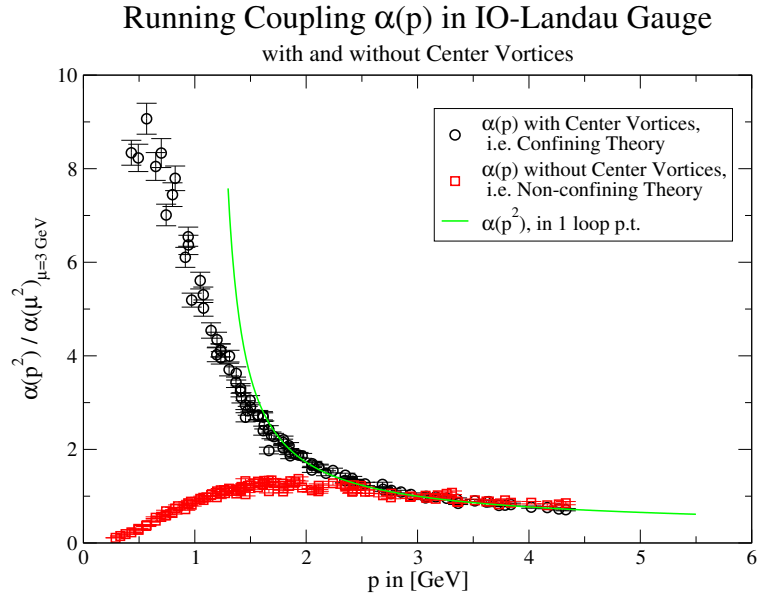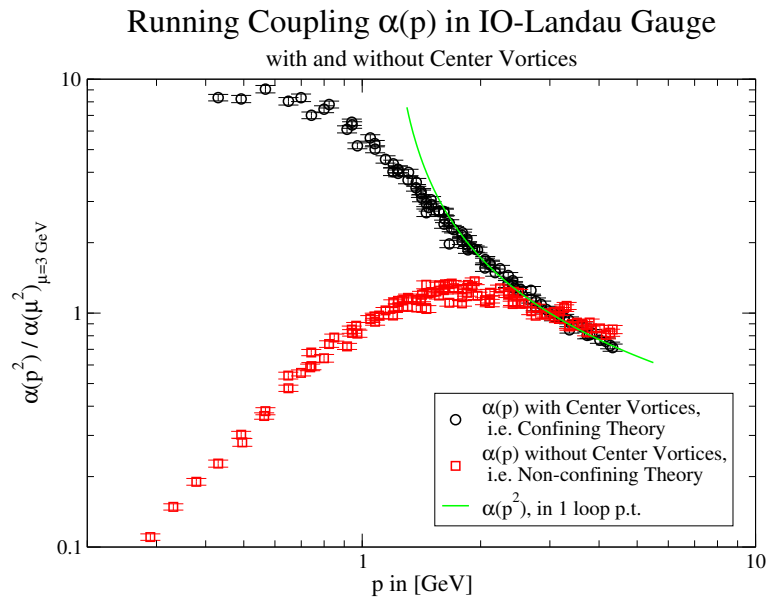


Figure 5.9: The logarithmic plot of the lattice running coupling $\alpha_{\text{lat.}}(p^2)$ of the confining theory and the non-confining model.

## 5.7   The Green's Functions at Finite Temperature

Finally, we want to address the gluon and ghost form factors at finite temperatures. It was mentioned in chapter (4) that the dimensional reduced pure $SU(2)$ Yang-Mills theory can be regarded as the high temperature limit of the usual four-dimensional theory. Furthermore, it was shown that the theory is in the $SU(2)$ symmetric phase, i.e. in the confining phase. This follows from the fact that a non-vanishing string tension is measured in the spacial hypercube indicating a linearly rising $q\bar{q}$-potential. Additionally, a percolation of center vortices is still extracted from the spatial cube of the space-time lattice. This indicates a non-vanishing string tension too, since the Wilson loop are randomly pierced by those center vortices which leads to an area law for the potential.

The gluon and ghost form factors are calculated directly with the algorithm introduced in the preceding chapter. In doing so, we only consider the spatial link variables $U_{\mu=i}(x)$ with $i \in 1, 2, 3$ and hence we concentrate on the purely spatial part of our space-time lattice,

$$D(\vec{x} - \vec{y}) = \langle A_i(\vec{x}) A_i(\vec{y}) \rangle_{\mathrm{MC}}. \tag{5.64}$$

This corresponds to the usual finite temperature propagators without summing over the Matsubara frequencies

$$\omega_n = \frac{2\pi n}{\beta} = 2\pi n T. \tag{5.65}$$

Hence, the only contribution to the form factors arises from the part with a vanishing Matsubara frequency $\omega_{n=0} = 2\pi n/\beta = 0$. This is valid in the limit of high temperatures, since the correction term to the next leading order of the Matsubara frequencies ($\omega_1$) is of the order $\mathcal{O}(1/T^2)$, e.g. with a fixed temperature of $T = 420$ MeV (or $T \propto \infty$ for the dimensional reduced theory) we have a correction term of the order $\mathcal{O}(1/(420\,\mathrm{MeV})^2) \approx 1/(1.7 \cdot 10^5 (\mathrm{MeV})^2)$. For a detailed introduction to finite-temperature field theory see e.g. [Kap], [LB96].

Monte-Carlo simulations at finite temperatures are obtained, if one dimension of the space-time lattice is compactified, $\mathbf{\Lambda} = S^1 \times \mathbb{R}^3$. Practically, this adds up to shorten the length of one dimension drastically compared to the remaining extensions. The temperature is then given by the relation

$$T := \frac{1}{N_t\, a(\beta)}, \tag{5.66}$$

with $N_t$ the number of sites in the reduced lattice dimension and $a(\beta)$ the $\beta$-dependent lattice constant.

First, we consider the form factors at high, finite temperatures. We choose a temperature of $T = 420$ MeV which is well above the critical temperature of the

confinement-deconfinement phase transition. The values for $\beta$ to the different lattice extensions $N_t$ are given in table (5.1), so that the fixed temperature is obtained. The gluon and ghost form factors are invariably calculated in the spatial domain of the lattice volume and are shown in fig.(5.10) and fig.(5.11) respectively.

| $N_t$ | 2 | 3 | 4 | 5 | 6 | 7 |
|---|---|---|---|---|---|---|
| $\beta$ | 2.146(38) | 2.297(01) | 2.403(89) | 2.486(79) | 2.554(52) | 2.611(79) |

Table 5.1: The numbers of lattice points and the corresponding values of $\beta$ are given so that a temperature of $T = 420$ MeV is achieved.

For the form factors of the dimensionally reduced theory, we disregard the Higgs field as a simplification. We have seen that the Higgs field incorporates a correction on the level of 10% to our measurement results in our investigation of the reduced Yang-Mills field theory. Since we are only interested in the qualitative behavior of the gluon and ghost form factors this additional correction factor is left for subsequent investigations.

Note additionally, that the three dimensional running coupling $g_3$ has a dimension of mass, i.e. $\beta = 4/(a\, g_3^2)$. We consider a scaling function for the lattice constant $a(\beta)$ for three dimensions which was introduced first in [Tep99],

$$\beta_I\, a\, \sqrt{\sigma} = c_0 + \frac{c_1}{\beta_I}, \quad \text{with } \beta_I = \beta \times \langle \frac{1}{N_c} \mathsf{Tr}\,[\mathsf{P}_{\mu\nu}(x)]\rangle_{\mathrm{MC}}, \qquad (5.67)$$

where the color index $N_c$ is set to two for $SU(2)$. The $\beta$-dependent expectation values of trace of the plaquette $\frac{1}{2}\mathsf{Tr}[\mathsf{P}_{\mu\nu}(x)]$ are given in the following table:

| $\beta$ | 4.0 | 5.0 | 6.0 | 7.0 | 8.0 |
|---|---|---|---|---|---|
| $\langle\frac{1}{2}\mathsf{Tr}[\mathsf{P}]\rangle$ | 0.727(46) | 0.786(68) | 0.824(56) | 0.851(23) | 0.870(45) |

Table 5.2: The expectation values of the trace of the plaquettes are given for different $\beta$-values.

The constants $c_0$ and $c_1$ are read of table 18 in [Tep99] and are thus set to

$$c_0 = 1.341, \quad \text{and } c_1 = -0.421.$$

Again, the measurement data are calculated with the same numerical procedures as explained in the preceding sections and in the appendices. Our measurement results for the gluon and ghost form factors support our previous picture of the spatial sub-domain of our space-time lattice at finite temperature and of the pure three dimensional lattice. Both gluon form factors are still enhanced in the low
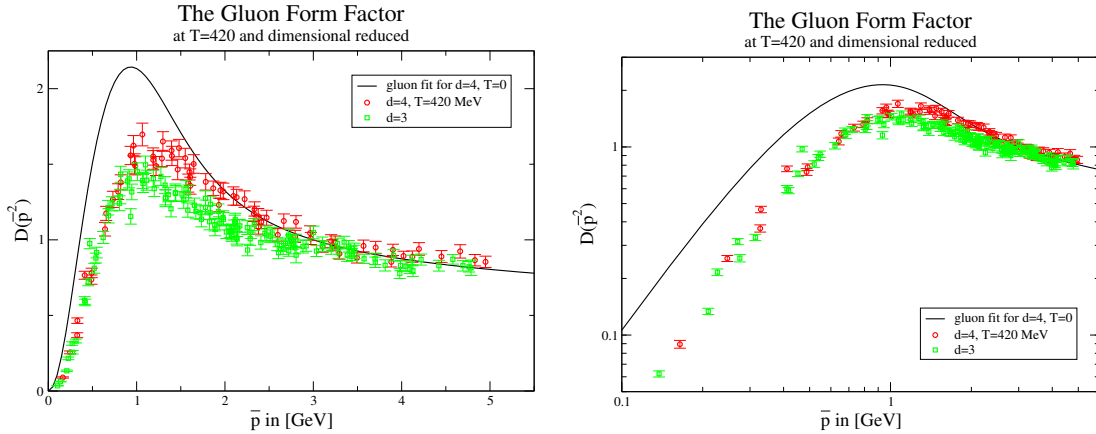
Figure 5.10: The gluon form factors for T=420 MeV and at asymptotic temperatures, i.e. dimensional reduced theory ($N_t = 0$). The left panel represents the measurement data in linear scale, the right one in logarithmic scale. Here $\bar{p}$ denotes the absolute value of the spatial momentum $\vec{p}$ at vanishing Matsubara frequency, $\omega_0 = 0$.
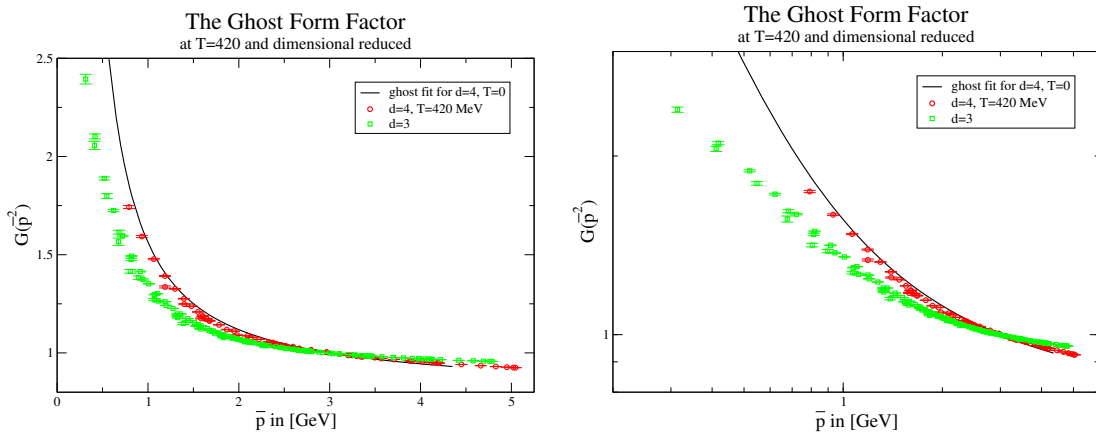


Figure 5.11: The ghost form factors for T=420 MeV and at asymptotic temperatures, i.e. dimensional reduced theory. The left panel represents the measurement data in linear scale, the right one in logarithmic scale.

momenta range and both ghost form factors are divergent in the infrared limit. Our findings are in agreement with the fact that the three dimensional theory is in the confining phase and that the center vortices are still percolating in three dimensions. Further, the Gribov picture of confinement is also supported. The same arguments are valid for the spatial domain for the field theory at finite temperatures.
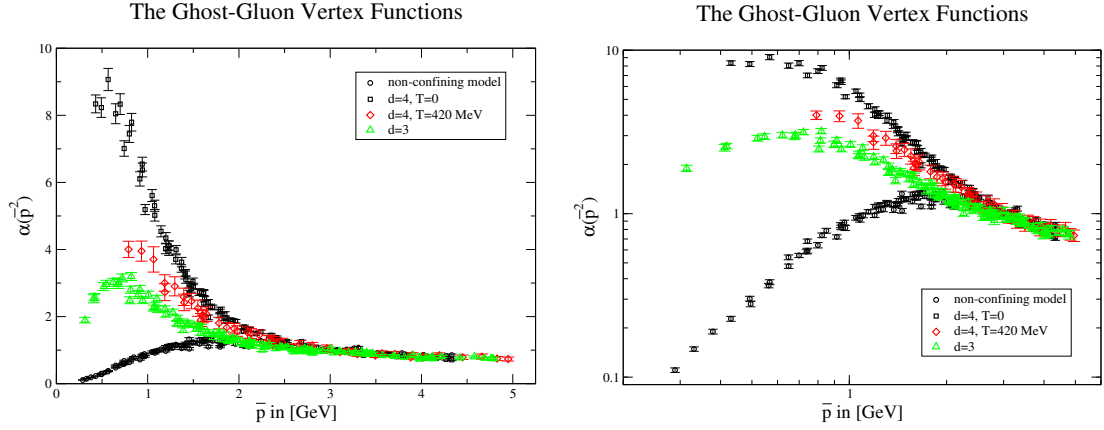
Figure 5.12: The ghost-gluon vertex functions for T=420 MeV and at asymptotic temperatures. The left panel represents the measurement data in a linear scale, the right one in a logarithmic scale.

Finally, we address the gluon-ghost vertex function which corresponds directly to the running coupling constant in four dimensions, see eq. (5.62). In both cases, we see an increase in the low momentum range and the vertex functions are well above the vertex function of the non-confining theory. With the exception of the non-confining model, the other three settings are in the confining phase. Motivated from our measurement data we suppose that the limit value of the running coupling constant may be not the relevant quantity for confinement, but rather the functional behavior of the running couplings in the low momentum range may be of importance, i.e. the enhancement of the running coupling in the low momentum range.

# Chapter 6

# Gauge Fixing and Gribov Noise

In general, we do not have to choose a particular gauge of Yang-Mills theory to perform lattice simulations. Lattice gauge theory is a non-perturbative approach to non-Abelian field theories and we can construct lattice operators which are gauge invariant observables, e.g. the Wilson loop operator. With gauge invariant operators, one has access to fundamental phenomenological quantities, e.g. the string tension, gauge-invariant correlation functions, e.g. correlation functions of two Polyakov loops, or of arbitrary (polynomial) functions of Wilson loops, e.g. the Creutz ratios.

On the other hand, non-perturbative lattice gauge fixing is needed if we want to analyze quantities being gauge dependent, such as propagators of the fundamental fields of a gauge field theory. Propagators are only well defined in certain gauges. For example, the expectation value of the gluon propagator would be zero without gauge fixing, since the sum over all field configurations contain negative and positive contributions to the path integral which cancel each other in the average. In particular, the ghost propagator is not defined without a gauge, since the ghost propagator is given by the inverse of the Faddeev-Popov operator which can only be defined by the use of a gauge fixing condition. Our motivation in calculating the gauge-dependent quantities is that we want to compare our lattice predictions with results stemming from perturbation theory and/or from the Dyson-Schwinger-Equations approach to QCD. In the infrared region where perturbation theory ceases to be valid, a comparison of propagators calculated by the DSE approach with propagators measured on the lattice is of particular interest.

The problem of gauge fixing is that gauge fixing procedures do not produce generally a unique gauge field configuration but a number of copies exists fulfilling the gauge condition: Gribov copies. As mentioned before, Gribov copies play a minor role in the perturbative regime of the theory but may be relevant for the non-perturbative dynamics of the theory.

87

# 6.1   Gauge Fixing and Gribov Copies in the Continuum

The gauge fixing procedure is commonly performed both in the continuum theory and in the DSE by the non-perturbative Faddeev-Popov method [FP67]. The gauge fixing procedure is done by inserting the quantity

$$\int [\mathrm{D}\Omega(x)]\,\delta\left(\mathsf{G}\left[A^{\Omega}\right]\right)\det\left[\frac{\delta\mathsf{G}\left[A^{\Omega}\right]}{\delta\Omega(x)}\right] \tag{6.1}$$

into the generating functional of the theory

$$\mathcal{Z}\left[U_{\mu}(x)\right]=\int\left[\mathrm{D}U_{\mu}(x)\right]\exp\left\{-\beta\mathcal{S}_{\mathrm{YM}}\left[U_{\mu}(x)\right]\right\}, \tag{6.2}$$

where the gauge fixing functional $\mathsf{G}$ is defined as a set of conditions

$$\mathsf{G}[\Omega]=\mathsf{G}\left[A_{\mu}^{\mathrm{a},\Omega}\right]\equiv 0. \tag{6.3}$$

If ghost fields being Grassmann variables are introduced, the Faddeev-Popov determinant can be incorporated into the Lagrangian of the theory by the identity

$$\det\left[\frac{\delta\mathsf{G}\left[A_{\mu}^{\mathrm{a},\Omega}(y)\right]}{\delta\omega^{b}(x)}\right] = \det\left[(\mathbb{M})_{xy}^{\mathrm{ab}}\right]\propto$$
$$\propto\int[\mathrm{D}\bar{c}]\,[\mathrm{D}c]\exp\left\{-i\int d^{4}y\,d^{4}x\bar{c}^{\mathrm{a}}(x)(\mathbb{M})_{xy}^{\mathrm{ab}}c^{\mathrm{b}}(y)\right\}. \tag{6.4}$$

The partition function $\mathcal{Z}$ can be multiplied by an arbitrary factor, since only normalized partition functions are of physical relevance. This may be used to incorporate a gauge fixing condition into the Lagrangian. Then, the Lagrangian obtains the form

$$\mathcal{L}_{\mathrm{eff.}}=\mathcal{L}+\mathcal{L}_{\mathrm{gf.}}+\mathcal{L}_{\mathrm{FP}}, \tag{6.5}$$

where $\mathcal{L}_{\mathrm{gf.}}$ is the gauge fixing term and $\mathcal{L}_{\mathrm{FP}}$ is the Faddeev-Popov ghost term eq. (6.4). This is then the starting point for perturbation theory in a particular gauge and of the derivation of the Feynman rules for QED or QCD.

As mentioned before, the Faddeev-Popov method cannot produce a unique solution of a field configuration in a particular gauge. Rather, it suffers from Gribov copies [Gri78]. This means that there exists multiple solutions of the gauge fixing functional $\mathsf{G}[A_{\mu}^{\mathrm{a},\Omega}]=0$ for a given ensemble of field variables $A_{\mu}^{\mathrm{a}}$. The quantity eq. (6.1) being inserted into the generating functional does not have a single value anymore, but causes that the functional integral sums over all Gribov copies, i.e. over all configurations fulfilling the root equation of the gauge fixing condition. A summation over all zeros of an equation corresponds basically

to summing over all maxima and minima of the primitive $\mathsf{F}[A_\mu^a]$ of the gauge fixing functional. This leads to an alternating sign of the Faddeev-Popov determinant which results in rather inserting a zero than inserting a one into the partition function [Sch99]. Taking the absolute value of the Faddeev-Popov determinant is not a complete solution, since a summation over maxima and minima of the gauge fixing functional still occurs. The partition function is in fact well defined and Gribov copies may be irrelevant as far as perturbative expansions are concerned. But the Gribov copies may be relevant for non-perturbative dynamics, because the distance in function space between the copies is large [Smi].

The problem of Gribov copies can be circumvented, if one restricts oneself to the fundamental domain [Zwa94] in which only the global minima of the primitive of the gauge fixing functional lies. We do not want to investigate the problem of Gribov copies in detail, for an introduction see [vB00] and the references in there.

## 6.2   LGT: Gauge Fixing and Gribov Copies

The numerical gauge fixing procedure on the lattice [Cre77] is obtained by using the gauge invariance of the Lagrangian and by using the right invariance of the Haar measure in the partition function.

The link variables $U_\mu(x)$ are gauge rotated by gauge transformations $\Omega(x)$ as long as the primitive $\mathsf{F}[U_\mu^\Omega]$ of the gauge condition $\mathsf{G}[U_\mu^\Omega]$ reaches an extremal. The gauge fixing condition is not incorporated into the Lagrangian but enters the lattice simulation as an additional constraint on the ensemble of the link variables $\{\mathbf{U}\}$,

$$
\begin{aligned}
\mathcal{Z}[U] &= \int [\mathsf{D}(\Omega U)] \exp\{-\mathcal{S}_{\mathrm{YM}}[(\Omega U)]\} \\
&= \int [\mathsf{D}U] \exp\{-\mathcal{S}_{\mathrm{YM}}[U]\},
\end{aligned}
\tag{6.6}
$$

with the constraint

$$
\mathsf{F}[U_\mu^\Omega] \to \text{ (global) extremal .}
\tag{6.7}
$$

From this we can deduce the prescription for the numerical algorithm for gauge fixing on the lattice:

- thermalize the ensemble of link variables $\{\mathbf{U}\}$ according to the gauge invariant Gibbs factor $\exp\{-\mathcal{S}[U]\}$;

- the gauge transformations $\Omega(x)$ are computed by an algorithm prescribed by a particular gauge;

- the link variables of the ensemble are rotated until the gauge fixing condition is fulfilled within certain accuracy $\{\mathbf{U}\} \to \{\mathbf{U}^\Omega\}_{\mathrm{gf}}$;

- the expectation value of an observable is given then by the average of the values of the operator evaluated of the gauge fixed ensemble of a set of configurations.

Note, that this prescription of gauge fixing introduces neither a Faddeev-Popov determinant nor terms involving Faddeev-Popov ghosts into the Lagrangian.

Generally, one may fix the link variables by gauge transformation to arbitrary prescribed values and the expectation values of gauge invariant observables $O_{\mathrm{gi}}$ are unchanged,

$$
\begin{aligned}
\langle O[U] \rangle &= \mathcal{Z}^{-1} \int [\mathsf{D}U^{\Omega}] \, O_{\mathrm{gi}}[U^{\Omega}] \, \exp \left\{ -\mathcal{S}[U^{\Omega}] \right\} \\
&= \mathcal{Z}^{-1} \int [\mathsf{D}U] \, O_{\mathrm{gi}}[U] \, \exp \left\{ -\mathcal{S}[U] \right\}.
\end{aligned}
\tag{6.8}
$$

On the other hand, for gauge dependent observables, the expectation values are certainly changed by gauge fixing and they depend on the particular choice of gauge. Since the Haar measure and the Gibbs factor are both gauge invariant, different expectation values of a gauge dependent quantity in different gauges stems from the operator itself and neither from the gauge transformation of the Haar measure nor from the gauge transformation of the Gibbs factor.

So far, we were only concerned with gauge fixing on the lattice, but we did not consider the Gribov problem. In lattice gauge simulations, the gauge fixing procedures reduce to find numerical the (global) extremum of a functional $\mathsf{F}[U^{\Omega}]$. The problem of Gribov copies in the continuum theory transforms into the impossibility of finding the global extremum of $\mathsf{F}[U^{\Omega}]$ in finite time, since many different extrema of the functional may exist. A numerical gauge fixing procedure finds in most cases a local extremum. To succeed in reaching the absolute extremum is nearly impossible. The different extrema are called lattice Gribov copies.

The mean value of a gauge invariant observable is not changed by the presence of Gribov copies. It was shown in [Sha84] that Gribov copies do not affect normalized functional integrals in general, if only gauge invariant observables $O_{\mathrm{gi}}[U]$ are considered. The effect of Gribov copies is that the mean value of an observable is multiplied by the number of Gribov copies, because the observable has the same value for each Gribov copy. This factor is then canceled by the normalization, since the delta-function of the gauge condition is also inserted which gives the additional factor of the number of Gribov copies to the normalization constant. In a lattice formulation of a gauge field theory, the expectation value

of an gauge invariant observable is given by

$$
\begin{aligned}
\langle O_{\mathrm{gi}}[U] \rangle &= \frac{\int [\mathsf{D}\Omega\, U] O[U^\Omega] \delta[\mathsf{G}[\Omega]] \exp\{-\mathcal{S}[U^\Omega]\}}{\int [\mathsf{D}\Omega\, U] \delta[\mathsf{G}[\Omega]] \exp\{-\mathcal{S}[U^\Omega]\}} \\
&= \frac{\int [\mathsf{D}U] \overbrace{\left( O_{\mathrm{gi}}[U^{\Omega_1}] + \cdots + O_{\mathrm{gi}}[U^{\Omega_{n(U)}}] \right)}^{n(U)\, O[U]} \exp\{-\mathcal{S}[U]\}}{n(U) \int [\mathsf{D}U] \exp\{-\mathcal{S}[U]\}} \qquad (6.9) \\
&= \frac{n(U)}{n(U)} \langle O_{\mathrm{gi}}[U] \rangle, \qquad\qquad\qquad (6.10)
\end{aligned}
$$

where $n(U)$ is the number of Gribov copies which depends on the ensemble $\{U\}$. We want to point out that the cancellation of the number of Gribov copies is only possible, since the observable is gauge invariant. If we measure a gauge dependent quantity, the quantity in the integral of the second equation above is not just the quantity multiplied by the number of Gribov copies, but a quantity which may depend on each Gribov copy. This means that a cancellation of $n(U)$ in the numerator and denominator is not possible in general. Consequently, a comparison of our lattice measurement results with the results stemming from analytical calculations or Dyson-Schwinger Equations is not complete without considering the influence of Gribov copies on our measurement results, since the latter approaches can restrict themselves to the fundamental domain, i.e. can consider only the global extremum of a gauge fixing condition by construction.

## 6.2.1 The Gribov Noise of the Form Factors in Landau Gauge

To investigate the effect of Gribov copies on the form factors, we consider two methods for Landau gauge fixing. The iterated over-relaxation algorithm (IO-algorithm), which locates the nearest maximum of the Landau gauge fixing functional in most cases. The mean value of the form factors are calculated from ensembles residing in an arbitrary local maximum of the Landau gauge fixing functional. The second method is the simulated annealing algorithm, which finds the global maximum of $\mathsf{F}[U^\Omega]$ with a higher probability than the IO-algorithm. The numerical expense of finding the global minima with the SA-algorithm is huge. With our setting, the SA-algorithm needed roughly thirty times as long as the IO-algorithm to reach the (global) maximum of the functional $\mathsf{F}[U^\Omega]$. (The IO-algorithm requires approximately a quarter of an hour to reach a (local) minima, the SA-algorithm seven hours for a $16^3 \times 32$ lattice for $\beta = 2.3$.)

We deduce from the fig.(6.1) and fig.(6.2) that the qualitative behavior is not changed by summing over the set of ensembles considering all possible Gribov copies or by summing over the reduced set of ensembles which considering only global Gribov copies with a high probability. There may by a deviation in the

exponents of fit functions to the form factors, but within our statistical and systematical errors we cannot predict any clear difference.

  If we consider the statistical relative error of the form factors, the relative errors of both form factors are of the same magnitude and quality. The error made by the IO-algorithm is hidden in the statistical error of our measured quantities.



Figure 6.1: The gluon form factors in Landau gauge for IO-algorithm and SA-algorithm. The top panel represents the measurement data in linear scale, the bottom panel in logarithmic scale.
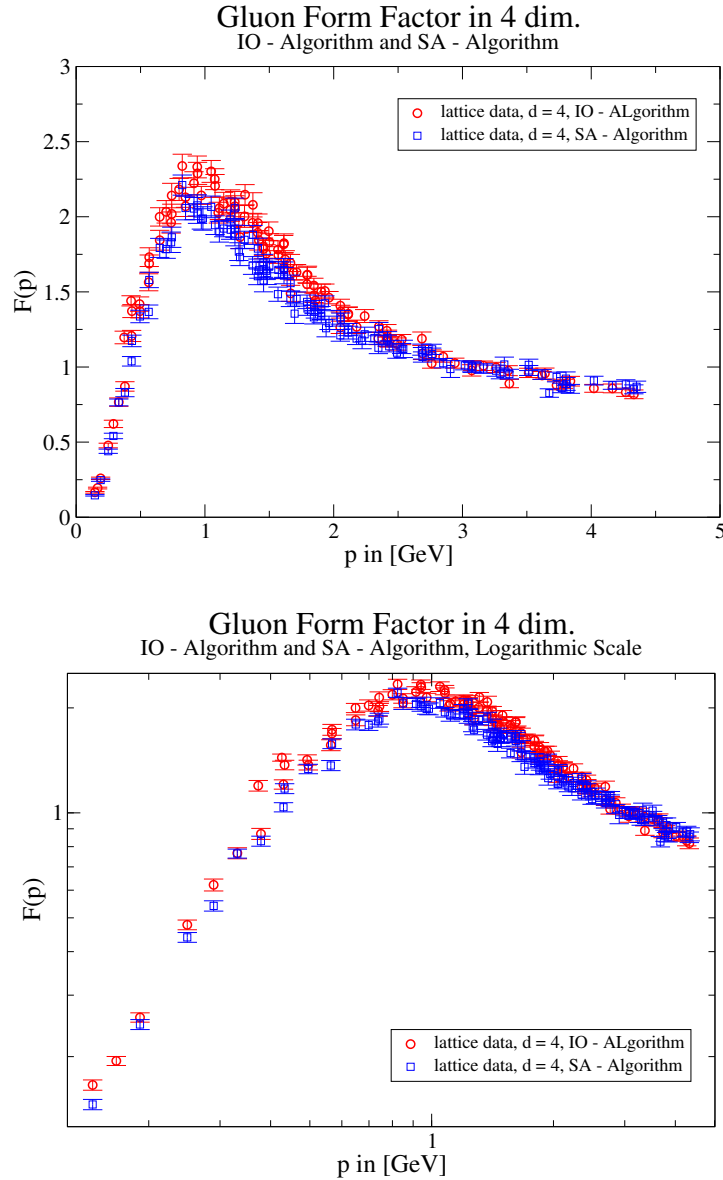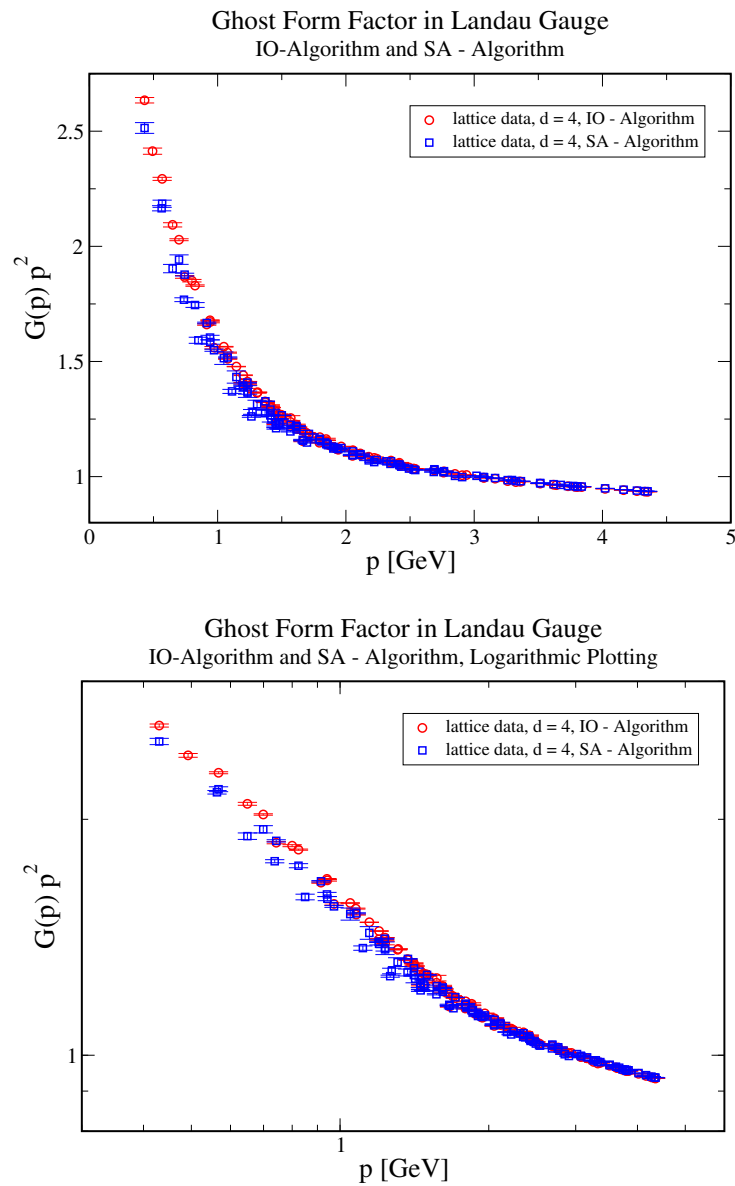
Figure 6.2: The ghost form factors in Landau gauge for IO-algorithm and SA-algorithm. The top panel represents the measurement data in linear scale, the bottom one in logarithmic scale.
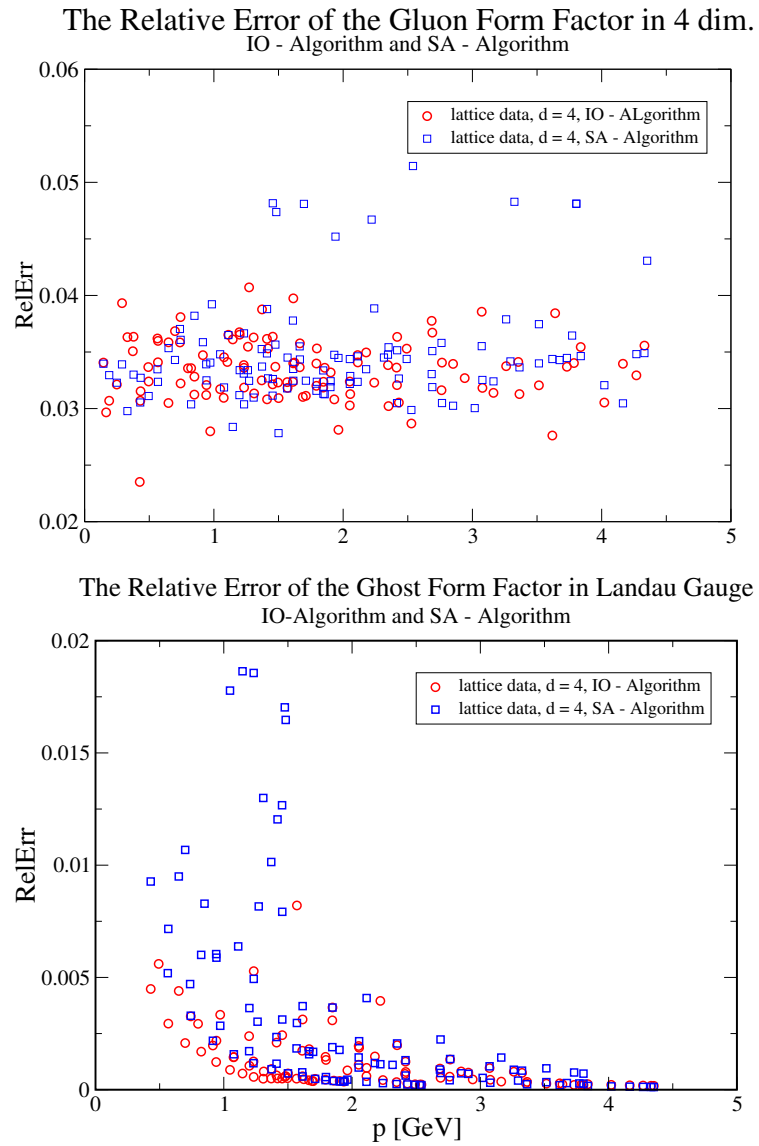
Figure 6.3: The relative errors of the gluon and the ghost form factors in Landau gauge for IO-algorithm and SA-algorithm.

# Chapter 7

# Conclusions

On the basis of the assumption that center vortices are the relevant residual degrees of freedom for color confinement in pure $SU(3)$ Yang-Mills gauge theory, we investigated their significance for the infra-red physics of the theory via Monte Carlo simulations of $SU(2)$ lattice gauge field theory.

First of all, we compared the spatial string tension of three dimensional pure Yang-Mills theory as well as three dimensional pure Yang-Mills theory coupled to adjoint Higgs fields with the value obtained from the pure center vortex content. The latter theory is the dimensionally reduced theory which describes the high temperature phase of four dimensional pure Yang-Mills theory. The vortex ensemble generates the spatial string tension of the full theories within a numerical accuracy of 10%. We argued that the error mainly results from the gauge fixing procedure and is largely produced by the average over Gribov copies.

In the limit of high temperature, we find further evidence that the vortex area density extrapolates to the continuum limit of vanishing lattice spacing. Only a small difference was found between the vortex densities of the pure Yang-Mills theory and of the theory with the adjoint Higgs fields. Therefore, a vortex area density is estimated which is in accordance with the spatial vortex area density of the four dimensional theory.

Consequently, our findings support the center vortex picture of the high temperature phase of four dimensional Yang-Mills theory. In the spatial part of the hypercube, the vortices still percolate whereas the center vortices are aligned along the direction of the time axis. Further, our results of dimensionally reduced theory based on the center vortex picture are in accordance with the findings of dimensional reduction of the four dimensional theory.

In the main part of this thesis, we investigated the relevance of center vortices for the behavior of Green's functions in the infra-red region. In doing so, we concentrated our investigations on the gluon and ghost form factors in Landau gauge.

Firstly, we studied the gluon form factor $F(p^2)$ both in Landau gauge and in maximal center gauge. By using a novel numerical operator, we were capable to

measure directly the gluon form factor giving the deviation of the gluon propaga-tor from the free one. Close to zero momentum transfer, the gluon form factor is consistent with an effective mass. The mass would be $m = 650 \pm 20$ MeV where a string tension of $\sqrt{\sigma} = 440$ MeV was used to fix the scale. The uncertainty is due to statistical errors as well as to Gribov copies. A rather pronounced peak is found in the medium momentum range while at high momenta our numerical data nicely reproduce the result obtained by perturbative Yang-Mills theory. Our data are well fitted over the whole momentum range by a coarse grained mass fit which might be useful for further phenomenological oriented investigations.

The information on quark confinement encoded in the gluon propagator in Landau gauge was a major topic of our research. By removing the confining vortices from the ensemble by hand, we are left with an ensemble of link variables which does not confine quarks. After the implementation of Landau gauge, a good part of strength of the gluon form factor is removed in the medium momentum range. Consequently, we established a relation between the infra-red strength of the gluon form factor in Landau gauge and color confinement.

Afterwards, we investigated the behavior of the ghost form factor in Landau gauge. The importance of the ghost form factor lies in fact that it might be related to quark confinement: This was firstly supposed by Gribov and worked out subsequently by Zwanziger. Especially, the relevant information for confinement in Landau gauge is encoded in the infra-red properties of Green's functions. The gauge configurations being relevant in the thermodynamic limit are concentrated on the Gribov horizon. In this case, the ghost form factor in Landau gauge would diverge at zero momentum transfer showing that the above horizon condition is satisfied. Using lattice simulations, Suman and Schilling obtained first indications that the ghost propagator of $SU(2)$ Yang-Mills theory in Landau gauge is indeed more singular in the infra-red than the free ghost propagator.

For the direct calculation of the ghost form factor in Landau gauge of the full Yang-Mills theory, we used a novel operator which is based on the operator used by the calculations of the gluon form factor. Our results show clearly a divergent ghost form factor in the infra-red limit. This is in accordance with the findings of Suman and Schilling and with the Gribov-Zwanziger criterion for confinement.

It was hypothesized that the center vortex picture and the Gribov-Zwanziger picture are compatible if the center vortex configurations lie on the Gribov hori-zon. Using the same procedure for our investigations of the gluon form factor, we demonstrated that the center vortex picture and the Gribov-Zwanziger picture are indeed compatible: By removing the center vortex content from the link con-figurations, the signals of confinement in the ghost form factor are eliminated; the singularity of the ghost form factor in the infra-red limit disappears. While the ghost form factor of full $SU(2)$ gauge theory diverges in the infra-red limit, our results suggest that it approaches a constant slightly above one in the infra-red limit for the non-confining theory.

We compared our results of gluon and ghost form factors with those results

obtained by solving Dyson-Schwinger equations in continuum Yang-Mills theory. The results of both approaches are qualitatively in good agreement but do not coincide at the quantitative level, except in the high momentum, perturbative regime. The power law behavior of the gluon form factors in the vanishing momentum limit are different. The peak in the medium momentum range of the DSE solution of the gluon form factor is less pronounced provided that both gluon form factors give same results in perturbative momentum regime. Remarkable is the good agreement of both ghost form factors. We want to emphasize that both methods used for the calculations are completely different: Lattice gauge field theory breaks explicitly the Lorentz invariance, because of the discrete space-time lattice. But the gauge invariance is preserved. On the other hand, the Dyson-Schwinger approach explicitly breaks gauge invariance, because of the truncation of the infinite tower of the Dyson-Schwinger equations, but Lorentz invariance is conserved. The nearly complete accordance of the form factors is astonishing.

Using the fact that the running coupling constant can be obtained directly from the gluon and ghost form factors, we demonstrated the relevance of center vortices for the behavior of the running coupling constant in the infra-red limit. The behavior of both, the full $SU(2)$ theory and the one with the center vortices removed, is the same in the region where the perturbation theory holds and nicely reproduce the perturbative behavior. Since the ghost form factor approaches a constant in the vortex removed case and the gluon form factor is suppressed in the infra-red region compared with the free one, it is no surprise that the running coupling seems to vanish in the infra-red limit. The running coupling constant is largely suppressed in the infra-red region when the center vortices are removed. The finding of the behavior of the ghost form factor are in accordance with the results of the gluon form factor after the elimination of center vortices. These results underline the importance of center vortices in the infra-red regime as the effective degrees of freedom for color confinement.

In conclusion, pure $SU(2)$ Yang-Mills theory looses its capability to confine quarks when the confining vortices were removed. At the same time, the divergence of the ghost form factor at vanishing momentum disappears. Our findings therefore establish a connection between the vortex picture of confinement and the Gribov-Zwanziger confinement criterion. Furthermore, the running coupling constant is drastically reduced in the intermediate momentum region. This also indicates a tight relation between the vortex picture and the spontaneous chiral symmetry breaking. Spontaneous chiral symmetry breaking occurs only, if the integrated strength at intermediate momenta exceeds a critical value.

The form factors were also investigated in the spatial subspace of the lattice volume at finite temperatures and in three dimensions which is the high temperature limit of the four dimensional theory. We found that the strength of the gluon form factor is enhanced in the medium momentum range and that the ghost form factor still diverges. Consequently, the running coupling constant is enhanced in the infra-red limit. All our findings are in consensus with the facts

that the center vortices are still percolating in the pure spatial part of the four dimensional theory at finite temperature and that a non-vanishing spatial string tension is measured.

# Appendix A

# Notation

## A.1 Conventions

We choose natural units,

$$c = \hbar = k_\mathrm{B} = 1, \tag{A.1}$$

which gives us the relation

$$197.327 \,\mathrm{fm}\,\mathrm{MeV} = 1, \tag{A.2}$$

where we used

$$c\hbar = 3.1615 \cdot 10^{-26} \,\mathrm{Jm} = 197.327 \,\mathrm{fm}\,\mathrm{MeV}. \tag{A.3}$$

### A.1.1 Minkowski Space

We use the standard metric of the Minkowskian notation

$$\eta_{\mu\nu} = \eta^{\mu\nu} = \mathsf{diag}[1, -1, -1, -1] \tag{A.4}$$

The contra-variant 4-vectors like the coordinate $x$, momentum $p$ or current density $j$ are given in components by:

$$x = (x^0, \ldots, x^4) = (t, \mathbf{x}), \quad p = (E, \mathbf{p}), \quad j = (j^0, \mathbf{j}). \tag{A.5}$$

For the covariant vectors like the derivative operator $(\partial_\mu := \partial/\partial x^\mu)$ and the vector potential $A_\mu$ we use the convention

$$\partial = (\partial_0, \partial), \quad A = (A_0, \mathbf{A}). \tag{A.6}$$

The scalar product is given in this notation by

$$x \cdot y = \langle x, y \rangle = \eta_{\mu\nu} x^\nu y^\mu = x^0 y^0 - \mathbf{x} \cdot \mathbf{y}. \tag{A.7}$$

## A.1.2   Euclidean Space

The time is Wick rotated from real to imaginary time $t \to -i\tau$ with $\tau \in \mathbb{R}$. The Euclidean metric is then given by

$$x^2 = -(\tau^2 + \mathbf{x}^2), \tag{A.8}$$

In momentum space the corresponding operation is $k^0 \to -ik_4$.

## A.1.3   Lattice Operators

The lattice forward derivative is defined by the finite difference operator

$$\Delta_\mu^f \phi(x) := \frac{1}{a} \left( \phi(x + a\hat{\mu}) - \phi(x) \right), \tag{A.9}$$

with $\hat{\mu}$ the unit vector in $\mu$-direction. The backward finite difference operator is given by

$$\Delta_\mu^b \phi(x) := \frac{1}{a} \left( \phi(x) - \phi(x - a\hat{\mu}) \right), \tag{A.10}$$

where the following relation holds

$$\Delta_\mu^b = -(\Delta_\mu^f)^\dagger. \tag{A.11}$$

The Laplace and d'Alembert lattice operators are given by

$$\Delta \phi(x) := -\Box \phi(x) := \Delta_\mu^f \Delta_\mu^b \phi(x) = \Delta_\mu^b \Delta_\mu^f \phi(x) = \tag{A.12}$$
$$\sum_\mu (\phi(x + \mu) - 2\phi(x) + \phi(x - \mu)).$$

## A.1.4   The Spin Pauli Matrices

The Spin Pauli matrices are defined as usual

$$\sigma_1 = \begin{pmatrix} 0 & 1 \\ 1 & 0 \end{pmatrix}, \quad \sigma_2 = \begin{pmatrix} 0 & -i \\ i & 0 \end{pmatrix}, \quad \sigma_3 = \begin{pmatrix} 1 & 0 \\ 0 & -1 \end{pmatrix}, \tag{A.13}$$

and the multiplication is given by

$$\sigma_i \sigma_j = \delta_{ij} + i\varepsilon_{ijk}\sigma_k \tag{A.14}$$

where $\varepsilon_{ijk}$ is the total antisymmetric tensor.

### A.1.5  The Generators of the $SU(2)$ Gauge Group

The generators of the $SU(2)$ gauge group are given with help of the Pauli matrices

$$\tau_i = i\,\sigma_i \tag{A.15}$$

with the multiplication

$$\tau_i\tau_j = -\delta_{ij} - \varepsilon_{ijk}\tau_k. \tag{A.16}$$

The $SU(2)$ matrix (link variable) is then parameterized as follows

$$U_\mu(x) = u_\mu^0(x)\mathbb{1}_{2\times2} + \vec{u}_\mu(x)\cdot\vec{\tau}. \tag{A.17}$$

## A.2  The Haar Measure

The path integration over the link variables $U_\mu(x)$ involves the Haar measure $[\mathsf{d}U]$. We need to evaluate the Haar measure since the Haar measure is needed as a part of the probability measure for the heat bath algorithm.

First, we consider the parameters (coordinates) of a group multiplication with $V,\Omega,U \in SU(2)$:

$$V(v) = \Omega(\omega)U(u), \quad \det\left[V(v)\right] = 1, \quad V(v) = v_0\mathbb{1} + \vec{v}\vec{\tau}, \tag{A.18}$$

where the variables in the brackets are the parameters of the gauge transformations and not the space-time index. The multiplication table for the parameters $v$ are given by

$$
\begin{aligned}
m_v(\omega,u) &= m_v(v_0; v_1; v_2; v_3) \\
&= m_v(\omega_0 u_0 - \omega_1 u_1 - \omega_2 u_2 - \omega_3 u_3; \omega_0 u_1 + \omega_1 u_0 + \omega_2 u_3 - \omega_3 u_2; \\
&\qquad \omega_0 u_2 + \omega_2 u_0 - \omega_1 u_3 + \omega_3 u_1; \omega_0 u_3 + \omega_3 u_0 + \omega_1 u_2 - \omega_2 u_1).
\end{aligned}
\tag{A.19}
$$

The multiplication table is used to evaluate the Haar measure which is defined for compact Lie groups as follows

$$\mathsf{d}v^1 \wedge \mathsf{d}v^2 \wedge \cdots \wedge \mathsf{d}v^r = \det\left[\frac{\partial m_v^j(\omega,u)}{\partial u^i}\right]\mathsf{d}u^1 \wedge \cdots \wedge \mathsf{d}u^r. \tag{A.20}$$

For $U(u) = \mathbb{1}$, eq.(A.20) reduces to

$$\mathsf{d}^r v = \det\left[\frac{\partial m_v^j(\omega,u)}{\partial u^i}\right]\Bigg|_{U(u)=\mathbb{1}}\mathsf{d}^r u \tag{A.21}$$

and the determinant yields

$$\det\left[\frac{\partial m_v^j(\omega,u)}{\partial u^i}\right] = \omega_0^2 + \omega_1^2 + \omega_2^2 + \omega_3^2 = 1. \tag{A.22}$$

The non-normalized Haar measure for $SU(2)$ is then given by

$$\delta(1 - v^2)\,\mathsf{d}^4 v = \delta(1 - \omega^2)\mathsf{d}^4\omega, \tag{A.23}$$

where we took into account the condition $\mathsf{det}[\Omega(\omega)] = 1$. As next step we have to normalize the integration over the group parameters. The $SU(2)$ group is isomorph to the $SO(3)$ group and we can parameterize the coordinates $v$ by spherical coordinates of four dimensions

$$
\begin{aligned}
\delta(1 - v^2)\,\mathsf{d}^4 v &= \delta(1 - r^2)\mathsf{det}\left[\frac{\partial[v^j(r,\vartheta,\phi,\varphi)]}{\partial[r,\vartheta,\phi,\varphi]}\right]\mathsf{d}r\mathsf{d}\vartheta\mathsf{d}\phi\mathsf{d}\varphi \\
&= \delta(1 - r^2)\,r^3\sin^2\vartheta\,\sin\phi\,\mathsf{d}r\mathsf{d}\vartheta\mathsf{d}\phi\mathsf{d}\varphi.
\end{aligned}
\tag{A.24}
$$

With an integration over the volume with $\vartheta \in [0,\pi]$, $\phi \in [0, 2\pi]$, $\varphi \in [0, 2\pi]$ and $r \in [0, \infty)$, we obtain the normalization factor for the Haar measure of the $SU(2)$ group

$$\mathsf{Vol}_{SU(2)} = 2\pi^2. \tag{A.25}$$

Finally, we obtain the Boltzmann factor by integrating over $|\vec{u}|$ parameterized with spherical coordinates in three dimensions which leads to the appropriate weighting

$$
\begin{aligned}
\mathsf{d}U &= \frac{1}{2\pi^2}r^2\,\delta(1 - u_0^2 + r^2)\,\mathsf{d}r\mathsf{d}u_0\mathsf{d}\Omega \\
&= \frac{1}{4\pi^2}\delta(1 - u_0^2 + r')\,\sqrt{r'}\,\mathsf{d}r'\mathsf{d}u_0\mathsf{d}\Omega, \quad \text{with } r' = r^2 \\
&= \frac{1}{4\pi^2}\sqrt{1 - u_0^2}\,\mathsf{d}u_0\mathsf{d}\Omega.
\end{aligned}
\tag{A.26}
$$

# Appendix B

# Lattice Gauge Fixing

## B.1    The Maximal Center Gauge (MCG)

Maximal center gauge (MCG) is defined by the requirement to choose link variables on the lattice as close as possible to the center elements of the gauge group as the gauge freedom will allow. The (direct) maximal center gauge is defined in the lattice formulation of Yang-Mills theory by the maximum of the functional:

$$\mathsf{F}^{\mathrm{mcg}}_U[\Omega] = \sum_{x,\mu} \left( \frac{1}{2}\mathsf{Tr}\left[ U_\mu(x)^{\Omega(x)} \right] \right)^2 \tag{B.1}$$

with respect to local gauge transformations $\Omega(x)$. This fixes the gauge up to gauge transformations of center elements $z \in \mathbb{Z}_2$ of the gauge group $SU(2)$

$$U_\mu(x) \to U^{\mathbb{Z}}_\mu(x), \quad \mathsf{F}^{\mathrm{mcg}}_U[\Omega] = \max. \tag{B.2}$$

The plaquettes $\mathsf{P}^{\mathbb{Z}}_{\mu\nu}(x)$ constructed from center projected links

$$U^{\mathbb{Z}}_\mu(x) \to z_\mu(x) = \mathsf{sign}\left[ \mathsf{Tr}\left[ U^{\mathbb{Z}}_\mu(x) \right] \right] = \pm 1 \tag{B.3}$$

have values of $\pm 1$

$$\mathsf{P}^{\mathbb{Z}}_{\mu\nu}(x) = \pm 1. \tag{B.4}$$

The center projected vortices (being closed surfaces in four dimensional space with periodic boundary conditions) are made from the plaquettes being dual to plaquettes with $\mathsf{P}^{\mathbb{Z}}_{\mu\nu}(x) = -1$.

The maximum center gauge moves ,as much as possible, information of the link variables which may be relevant for confinement near the center elements of the gauge group. Subsequently, the link variables are projected onto the centers of the group. If the expectation value of an observable calculated only from the center elements reproduces the expectation value of the observable calculated from the full link variables (within a certain accuracy), then the observable is

called center dominant and the center vortices are the relevant collective degrees of freedom.

Any link variable $U_\mu(x)$ can be formally decomposed into its center part $z_\mu(x) \in \mathbb{Z}_2$ and its coset part $\tilde{U}_\mu(x)$:

$$U_\mu(x) = z_\mu(x)\tilde{U}_\mu(x), \quad z_\mu(x) = \text{sign}\left[\text{Tr}\left[U_\mu(x)\right]\right] = \pm 1. \qquad (B.5)$$

Using maximal center gauge and subsequently projecting on the center elements, the center content of a link variable can be removed

$$U_\mu(x) \to z_\mu(x)U_\mu(x) = \tilde{U}_\mu(x) := \overbrace{z_\mu(x)z_\mu(x)}^{1}\tilde{U}_\mu(x). \qquad (B.6)$$

This produces our non-confining model.

## B.1.1   The Numerical Implementation of MCG

Our derivation of MCG-algorithm follows the outline given in [DDFG$^+$98]. To implement the MCG-algorithm we have to maximize the following local functional at the lattice site $x$

$$\mathsf{F}_x^{\text{mcg}}[\Omega(x)] = \frac{1}{4}\left(\sum_\mu \text{Tr}\left[\Omega(x)U_\mu(x)\right]^2 + \sum_\mu \text{Tr}\left[U_\mu(x-\hat{\mu})\Omega^\dagger(x)\right]^2\right), \qquad (B.7)$$

with respect to the local gauge transformation $\Omega(x)$. We consider infinitesimal gauge transformations at a fixed space-time point $x$:

$$\Omega(x) = \omega_4\mathbb{1} - \vec{\omega}\vec{\tau} \qquad (B.8)$$
$$U_\mu(x) = u_4(l = \mu)\mathbb{1} + \vec{u}(l = \mu)\vec{\tau} \qquad (B.9)$$
$$U_\mu(x-\hat{\mu}) = u_4(l = \mu+4)\mathbb{1} + \vec{u}(l = \mu+4)\vec{\tau}, \qquad (B.10)$$

where the sign before the imaginary parts are for convenience, the index $l = 1, 2, \ldots, 8$ is introduced which labels the eight link variables connected to the site $x$. After some calculations (see app. B.1.2) we obtain

$$\mathsf{F}_x^{\text{mcg}}[\Omega(x)] = \frac{1}{2}\sum_{l=1}^{8}\left(\sum_{k=1}^{4}\omega_k u_k(l)\right)^2, \qquad (B.11)$$

which has to be maximized under the constraint that $\Omega(x)$ is unitary. For this reason we introduce a Lagrange multiplier

$$\tilde{\mathsf{F}}[\Omega(x)] = \mathsf{F}_x^{\text{mcg}}[\Omega(x)] + \frac{\lambda}{2}\left(1 - \sum_{k=1}^{4}\omega_k^2\right). \qquad (B.12)$$

Hence, one gets the following condition for a maximum of the functional (B.7):

$$\sum_{j=1}^{4}\sum_{l=1}^{8} u_i(l)u_j(l)\omega_j = \lambda\omega_i, \tag{B.13}$$

$$\sum_{k=1}^{4}\omega_k^2 = 1. \tag{B.14}$$

The procedure for the maximum center gauge is know reduced to an eigenvalue problem of the form:

$$\mathbb{D}\vec{\omega} = \lambda\vec{\omega}, \quad (\mathbb{D})_{ij} = \sum_{l=1}^{8} u_i(l)u_j(l).$$

The unitarian condition changes to the norm condition $\vec{\omega}\vec{\omega} = 1$. Now, finding the gauge transformation $\Omega(x)$ maximizing the functional condition is reduced to an eigenvalue problem of a $(4 \times 4)$-matrix. This eigenvalue problem can be solved by standard procedures. The eigenvector with the highest eigenvalue corresponds to the gauge transformation maximizing the gauge functional at the space-time point $x$.

## B.1.2 MCG: Auxiliary Calculation

$$
\begin{aligned}
\mathsf{F}_x^{\mathrm{mcg}}[\Omega(x)] &= \frac{1}{4}\Bigg\{\sum_{l=1}^{4} \mathsf{Tr}\left[(\omega_4\mathbb{1} - \vec{\omega}\vec{\tau})\,(u_4(l)\mathbb{1} + \vec{u}(l)\vec{\tau})\right]^2 + \\
&\quad + \sum_{l=5}^{8} \mathsf{Tr}\left[(u_4(l)\mathbb{1} - \vec{u}(l)\vec{\tau})\,(\omega_4\mathbf{1} + \vec{\omega}\vec{\tau})\right]^2\Bigg\} \\
&= \frac{1}{4}\Bigg\{\sum_{l=1}^{4} \mathsf{Tr}\left[\omega_4 u_4(l)\mathbb{1} - \omega_i u_j(l)\tau_i\tau_j + (\omega_4 u_k(l)\tau_k - u_4\omega_n\tau_n)\right]^2 + \\
&\quad + \sum_{l=5}^{8} \mathsf{Tr}\left[\omega_4 u_4(l)\mathbb{1} - \omega_i u_j(l)\tau_i\tau_j + (\omega_4 u_n(l)\tau_n - u_4\omega_k\tau_k)\right]^2\Bigg\} \\
&= \frac{1}{4}\Bigg\{\sum_{l=1}^{4}(2\omega_4 u_4(l) + 2\omega_i u_i(l))^2 + \sum_{l=5}^{8}(2\omega_4 u_4(l) + 2\omega_i u_i(l))^2\Bigg\} \\
&= \sum_{l=1}^{8}\left(\sum_{k=1}^{4}\omega_k u_k(l)\right)^2.
\end{aligned}
$$

From step two to three we used the relation eq. (A.16) and $\mathsf{Tr}[\tau_i] = 0$.

## B.2    The Minimal Landau Gauge

In our lattice simulations, we use the Landau gauge for calculating the gluon and
ghost form factors. We want to calculate form factors for two reasons: 1) to inves-
tigate of the impact of center vortices onto the form factors, 2) to get in contact
with results of perturbation theory and of the Dyson-Schwinger Equations.

### B.2.1    The Iterated Overrelaxated Algorithm

On the lattice the (minimal) Landau gauge is achieved by finding gauge trans-
formations $\Omega(x)$ which maximize the following functional $\mathsf{F}_U^{\mathrm{mlg}}[\Omega(x)]$:

$$\mathsf{F}_U^{\mathrm{mlg}}[\Omega(x)] \equiv \sum_{x,\mu} \frac{1}{2}\mathsf{Re}\,\mathsf{Tr}\left[\Omega(x)U_\mu(x)\Omega^\dagger(x+\mu)\right]. \tag{B.15}$$

With the usual continuum definition of the gauge transformation $\Omega(x)$ and its
linearization thereof

$$\Omega(x) = \exp\left\{\omega^a(x)\tau^a\right\} \simeq \mathbb{1} + \omega(x) + \mathcal{O}(\omega^2(x)), \quad \omega(x) = \omega^a(x)\tau^a. \tag{B.16}$$

One can evaluate the condition for the minimal Landau gauge if one considers the
maximum of $\mathsf{F}_U^{\mathrm{mlg}}[g(x)]$. The first variation of $\mathsf{F}_U$ has to be zero for the maximum

$$\frac{\delta\mathsf{F}_U^{\mathrm{mlg}}[\Omega]}{\delta\Omega} = 0. \tag{B.17}$$

Hence, one obtains

$$\begin{aligned}
\frac{\delta}{\delta\Omega}\mathsf{F}_U^{\mathrm{mlg}}[\Omega] &= \frac{1}{2}\sum_{x,\mu}\mathsf{Tr}\left[U_\mu^\Omega(x) - U_\mu(x)\right]\\
&= \frac{1}{2}\sum_{x,\mu}\mathsf{Tr}\left[(\mathbb{1}+\omega(x))\,U_\mu(x)\,(\mathbb{1}-\omega(x+\mu)) - U_\mu(x)\right] + \mathcal{O}\left(\omega^2\right)\\
&= \frac{1}{2}\sum_{x,\mu}\mathsf{Tr}\left[(\omega(x)-\omega(x+\mu))\,U_\mu(x)\right]\\
&= \frac{1}{2}\sum_{x,\mu}\mathsf{Tr}\left[(\omega(x)-\omega(x+\mu))^a\,\tau^a U_\mu(x)\right].
\end{aligned}$$

For next steps we insert the parameterization (A.17) of the $SU(2)$ matrices:

$$\begin{aligned}
(\omega(x)-\omega(x-\mu))^a\,\tau^a\left(u^0\mathbb{1}+u^i(x)\tau^i\right) &=\\
&= (\omega(x)-\omega(x+\mu))^a\left(u^0(x)\tau^a + u^i(x)\tau^a\tau^i\right)\\
&= (\omega(x)-\omega(x+\mu))^a\left(u^0(x)\tau^a + u^i(x)(-\delta^{ai}-\varepsilon^{aik}\tau^k)\right)\\
&= (\omega(x)-\omega(x+\mu))^a\left(u^0(x)\tau^a - u^a(x)\mathbb{1} - u^i(x)\varepsilon^{aik}\tau^k\right)\\
&= -(\omega(x)-\omega(x+\mu))^a\left(u^a(x)\mathbb{1} + u^i(x)\varepsilon^{aik}\tau^k - u^0(x)\tau^a\right).
\end{aligned}$$

The terms containing the $\tau$ matrices are zero with respect to the trace operation. We obtain

$$\frac{1}{2}\mathsf{Tr}\left[(\omega(x) - \omega(x+\mu))^a \, \tau^a U_\mu(x)\right] = (\omega(x+\mu) - \omega(x))^a \, u^a(x). \qquad (B.18)$$

The condition for the minimal Landau gauge reads

$$\frac{\delta}{\delta\Omega}\mathsf{F}_U^{\mathrm{mlg\cdot}}\left[\Omega(x)\right] = \sum_{x,\mu} \left(\omega(x+\mu) - \omega(x)\right)^{\mathrm{a}} u_\mu(x). \qquad (B.19)$$

For a local gauge transformation update step, only the dependency on $\omega(x)$ is needed:

$$
\begin{aligned}
\frac{\delta}{\delta\Omega(x)}\mathsf{F}_U^{\mathrm{mlg}}[\Omega(x)] &= \sum_{x,\mu} \left(\omega(x+\mu) - \omega(x)\right)^{\mathrm{a}} u_\mu^{\mathrm{a}}(x) \\
&= \frac{1}{2}\sum_{x,\mu}\left(\left(\omega(x+\mu) - \omega(x)\right)^{\mathrm{a}} u_\mu^{\mathrm{a}}(x) + \right. \\
&\qquad \left. + \left(\omega(x) - \omega(x-\mu)\right)^{\mathrm{a}} u_\mu^{\mathrm{a}}(x-\mu)\right) \\
&= \sum_{x,\mu}\omega^{\mathrm{a}}(x)\left(u_\mu^{\mathrm{a}}(x-\mu) - u_\mu^{\mathrm{a}}(x)\right) \\
&= \sum_{x}\omega^{\mathrm{a}}(x)\sum_{\mu}\left(u_\mu^{\mathrm{a}}(x-\mu) - u_\mu^{\mathrm{a}}(x)\right),
\end{aligned}
$$

and finally the condition for the minimal Landau gauge is achieved

$$0 \equiv \frac{\delta}{\delta\Omega(x)}\mathsf{F}_U^{\mathrm{mlg\cdot}}[\Omega(x)] = \sum_{x}\omega^{\mathrm{a}}(x)\sum_{\mu}\left(u_\mu^{\mathrm{a}}(x-\mu) - u_\mu^{\mathrm{a}}(x)\right). \qquad (B.20)$$

From this conditions follows the equation for the gauge transformation $\Omega(x)$ for the iterated overrelaxation algorithm:

$$\Omega(x) = \mathsf{det}\left[\Omega'(x)\right]^{-\frac{1}{2}}\Omega'(x), \qquad (B.21)$$

with

$$\Omega'(x) = \left(\left(\sum_{\mu}u_\mu^0(x-\mu) + u_\mu^0(x)\right)\mathbb{1} + \left(\sum_{\mu}u_\mu^{\mathrm{i}}(x-\mu) - u_\mu^{\mathrm{i}}(x)\right)\tau^{\mathrm{i}}\right). \quad (B.22)$$

## B.2.2 The Simulated Annealing Algorithm

The accomplishment of minimal Landau gauge fixing needs the maximization of a multidimensional functional. The IO-algorithm searches for the nearest (local) maximum and not for the global one. But we need to search for the global one,

since we want to communicate and compare our results to people performing their calculations analytically. In the analytical modus operandi, the Landau gauge is fixed a priori and resides in the global maximum of the Landau gauge fixing functional leading to a prevention of Gribov copies.

A further numerical method to find the global extremum of a multivariate function is the simulated annealing algorithm. The name of the method derives from the physical process of heating and then slowly cooling a substance to obtain a crystalline structure containing very few defects. The temperature is slowly lowered step by step so that the system freezes and no further changes occur. At each step of the simulation, the system must reach a steady equilibrium. The system is thermalized and the time required for thermalization is the decorrelation time, i.e. correlated micro-states are eliminated.

We want to summarize briefly the annealing schedule for a general functional $\mathsf{F}[\mathbf{\Omega}]$ to be minimized. We start the algorithm with a temperature of $T = a_0$ and wait a sufficiently long time for the Markov chain $\{\mathbf{\Omega}_n\}$ to get close to its stationary state. A possible probability of acceptance of the new state $\mathbf{\Omega}_{n+1}$ is given by $p_\mathrm{a} = \mathsf{min}\left[1, \exp\{(\mathsf{F}[\mathbf{\Omega}_n] - \mathsf{F}[\mathbf{\Omega}_{n+1}])/T\}\right]$. This is the Metropolis step (explained in section (1.6)) and the fundamental procedure of simulated annealing. The metropolis step allows a chance to accept a state which produces an increase of $\mathsf{F}[\mathbf{\Omega}]$. In our implementation of the SA-algorithm it is efficient to use the heat bath algorithm as a supplement for the Metropolis step.

The temperature is then successively lowered step by step, whereby at each step until the steady state has to be reached. This is sometimes called the cooling schedule. After the $k$-th change of the temperature $T$, the Markov chain will be close to the stationary regime and therefore for $k \to +\infty$, one expects for large enough $n$ that the global minimum of $\mathsf{F}$ is reached with a high probability, i.e. $\delta\mathsf{F}[\mathbf{\Omega}]/\delta\Omega \to 0$.

The ensemble $\{\mathbf{U}\}$ of link variables is a back ground field, the degrees of freedom are the gauge transformations $\Omega(x)$. We initialize the ensemble $\{\mathbf{\Omega}\}$ with

$$\bar{\Omega}(x) = \sum_{\mu=0}^{3} -U_\mu^\dagger(x) + U_\mu(x-\mu) \tag{B.23}$$

$$\Omega(x) = \left(\mathsf{det}\left[\bar{\Omega}(x)\right]\right)^{-\frac{1}{2}} \bar{\Omega}(x).$$

The same heat bath algorithm of the updating scheme of the link variables is used, see sec.(2.4.2), with the exception that for the contribution of a gauge

transformation $\Omega(x)$ to the action of the gauge fixing procedure we use now:

$$\bar{V}(x) \quad := \quad \sum_{\mu=0}^{3} \left( U_\mu^\dagger(x-\mu)\Omega^\dagger(x-\mu) + U_\mu(x)\Omega^\dagger(x+\mu) \right) \qquad \text{(B.24)}$$

$$V(x) \quad = \quad \left( \det\left[\bar{V}(x)\right] \right)^{-\frac{1}{2}} \bar{V}(x) \qquad \text{(B.25)}$$

$$\tilde{\mathcal{S}}_{\text{mlg}}[\Omega(x)] \quad = \quad -\frac{1}{2}\text{Tr}\left[\Omega(x)V(x)\right]. \qquad \text{(B.26)}$$

The action $\mathcal{S}_{\text{mlg}}[\Omega]$ of Landau gauge is given by

$$\mathcal{S}_{\text{mlg}}[\Omega] := \beta_{\text{fix}} \sum_{x} \left( 1 - \frac{1}{2}\text{Tr}\left[\Omega(x)V(x)\right] \right), \qquad \text{(B.27)}$$

where $\beta_{\text{fix}} = 1/T$ is the inverse cooling temperature. If the temperature is low enough, one hopes to have the ensemble of gauge transformation $\{\mathbf{\Omega}\}$ which transforms the link ensemble $\{\mathbf{U}\}$ to an ensemble of link variables being near the global maximum of the Landau gauge condition with a higher probability than the IO-algorithm.

Subsequently, the IO-algorithm is used so that the near maximum is reached to a high accuracy.

# Appendix C

# Concerning Form Factors

## C.1   The Gluon Form Factor

### C.1.1   Warm up: The Propagator of the Klein Gordon Field

To see that the Gluon form factor can be directly calculated without the need of a Fourier transformation and the multiplication with $p^2$, we perform firstly some easy calculations. Consider the lattice action of the Klein Gordon field with the action

$$
\begin{aligned}
\mathcal{S}_0[\phi, a] &= \frac{1}{2} \left( \phi, \left( \Box + m^2 \right) \phi \right) \\
&= \frac{1}{2} \sum_{x,y} a^8 \phi(x) \left( \Box + m^2 \right)_{xy} \phi(y),
\end{aligned}
\tag{C.1}
$$

with the d'Alembert operator eq.(A.12). We start with the ansatz

$$
\sum_y a^4 (\Box + m^2)_{xy} G(y, z; a) = a^{-4} \delta_{xz}
\tag{C.2}
$$

and perform a Fourier transformation

$$
G(x, y; a) = \int_{-\frac{\pi}{a}}^{\frac{\pi}{4}} \frac{d^4 p}{(2\pi)^4} \exp\left\{ ip(x - y) \right\} \tilde{G}(p; a)
\tag{C.3}
$$

111

with the integration boundary chosen in such a way, so that the periodic boundary conditions are fulfilled. Inserting this into Eq.(C.2) one obtains

$$\sum_y a^4 (\Box + m^2)_{xy} \int_{-\frac{\pi}{4}}^{\frac{\pi}{4}} \frac{d^4p}{(2\pi)^4} \exp\{ip(y-z)\} \tilde{G}(p;a) = a^{-4}\delta_{xz}$$

$$\int_{-\frac{\pi}{4}}^{\frac{\pi}{4}} \frac{d^4p}{(2\pi)^4} a^4 \sum_y (\Box + m^2)_{xy} \exp\{ip(y-z)\} \tilde{G}(p;a) = a^{-4}\delta_{xz}$$

$$\int_{-\frac{\pi}{4}}^{\frac{\pi}{4}} \frac{d^4p}{(2\pi)^4} a^2 e^{ip(x-z)} \left( \sum_\mu (2 - e^{ip(a\mu)} - e^{-ipa\mu} + m^2) \right) \tilde{G}(p;a) = a^{-4}\delta_{x,z}$$

$$\int_{-\frac{\pi}{4}}^{\frac{\pi}{4}} \frac{d^4p}{(2\pi)^4} e^{ip(x-z)} \left( \frac{2}{a^2} \sum_\mu (1 - \cos(p_\mu a)) + m^2 \right) \tilde{G}(p;a) = \int_{-\frac{\pi}{4}}^{\frac{\pi}{4}} \frac{d^4p}{(2\pi)^4} e^{ip(x-z)} \mathbb{1}.$$

Finally, the propagator for the Klein Gordon field is given by

$$\tilde{G}(p;a) = \frac{1}{\frac{2}{a^2} \sum_\mu \left( \sin^2 \frac{ap_\mu}{2} \right) + m^2}. \tag{C.4}$$

## C.1.2   The Gluon Propagator and the Gluon Form Factor

Form perturbation theory one knows that renormalized gluon propagator in the continuum is given to one-loop level for large momenta $p^2$ [Man79], [DZ89] by

$$D_{\text{pt}}(p^2) \sim \frac{1}{p^2} \ln \left( \frac{p^2}{\Lambda_{\text{QCD}}} \right)^{-13/22}. \tag{C.5}$$

For the lattice version we use the form

$$D(\hat{p}^2) = \frac{F(\hat{p}^2)}{\hat{p}^2}, \tag{C.6}$$

where $F(\hat{p}^2)$ is the gluon form factor being looked for. On the lattice, the sites are numbered from 0 to $N-1$, with $N$ the number of lattice points in one direction. There are a number of $N-1$ different momenta which depend on the lattice constant $a$. Now consider the lattice version of the $\delta$-function:

$$\sum_{x=0}^{N-1} \exp \left\{ i\frac{2\pi}{N} x(k-q) \right\} = N\delta_{kq}, \tag{C.7}$$

which is proved with the help of the geometric series

$$\frac{1 - e^{i2\pi(k-q)}}{1 - e^{i\frac{2\pi}{N}(k-q)}} = 0, \text{ for } k \neq q; \quad k, q \neq \nu N \tag{C.8}$$

because $(k - q) \in \mathbb{Z}$ and $\exp\{i2\pi n\} = 1$ for $n \in \mathbb{Z}/\{0\}$. This leads to the lattice version of the Fourier transform of the field:

$$\phi(x) = \sum_{k=0}^{N-1} \exp\left\{i\frac{2\pi}{N}kx\right\} \tilde\varphi(k), \tag{C.9}$$

which is periodic $\phi(x + N) = \phi(x)$.

The lattice propagator is now (for simplicity, we consider only one space-time dimension) given by

$$\begin{aligned}
\Box\phi(x) &= \phi(x+1) - 2\phi(x) + \phi(x-1) \\
&= \sum_{k=0}^{N-1} e^{i\frac{2\pi}{N}kx} \left(e^{i\frac{2\pi}{N}k} - 2 + e^{-i\frac{2\pi}{N}k}\right) \tilde\varphi(k) \\
&= \sum_{k=0}^{N-1} e^{i\frac{2\pi}{N}k} \left(-4\sin^2\frac{\pi}{N}k\right) \tilde\varphi(k).
\end{aligned} \tag{C.10}$$

The Measurement of the gluon propagator is usually performed on a space-time lattice

$$D(x - y) = \langle\phi(x)\phi(y)\rangle, \tag{C.11}$$

but one is generally interested of the gluon form factor in the momentum space

$$\begin{aligned}
D(k) &= \langle\tilde\varphi(k)\tilde\varphi(k)\rangle \\
&= \left(\sum_x \phi(x)\cos\left(\frac{2\pi}{N}kx\right)\right)^2 + \left(\sum_x \phi(x)\sin\left(\frac{2\pi}{N}kx\right)\right)^2 \\
&= \sum_{x,y} \phi(x)\phi(y)\left(\cos\left(\frac{2\pi}{N}kx\right)\cos\left(\frac{2\pi}{N}ky\right) + \sin\left(\frac{2\pi}{N}kx\right)\sin\left(\frac{2\pi}{N}ky\right)\right) \\
&= \sum_{x,y} \phi(x)\phi(y)\cos\left(\frac{2\pi}{N}k(x-y)\right).
\end{aligned} \tag{C.12}$$

Our goal is, to evaluate the gluon form factor directly, since we are interested in the deviation of the non-perturbative gluon propagator from the free one in the one infra-red limit. To obtain an algorithm for a direct measurement of the gluon form factor we make the ansatz

$$F(x, y) = \langle(\phi(x+1) - \phi(x))(\phi(y+1) - \phi(y))\rangle. \tag{C.13}$$

With the lattice Fourier transform of the fields $\phi(x)$, we obtain

$$(\phi(x+1) - \phi(x)) = \sum_{k=0}^{N-1} e^{i\frac{2\pi}{N}kx} \left(e^{i\frac{2\pi}{N}k} - 1\right) \tilde{\varphi}(k) \tag{C.14}$$

and

$$(\phi(x+1) - \phi(x))(\phi(y+1) - \phi(y)) =$$
$$= \sum_{k,q=0}^{N-1} e^{i\frac{2\pi}{N}kx} e^{i\frac{2\pi}{N}qy} \left(e^{i\frac{2\pi}{N}k} - 1\right)\left(e^{i\frac{2\pi}{N}q} - 1\right) \tilde{\varphi}(k)\tilde{\varphi}(q) \tag{C.15}$$

If we use the relation

$$\langle \tilde{\varphi}(k)\tilde{\varphi}(q) \rangle = f(q)\delta_{k,-q}, \tag{C.16}$$

because translation invariance holds, we obtain the proof that our ansatz Eq.(C.13) indeed calculates the gluon form factor

$$\begin{aligned} F(x,y) &= \sum_{k=0}^{N-1} e^{i\frac{2\pi}{N}k(x-y)} \left(1 - e^{i\frac{2\pi}{N}(-k)} - e^{i\frac{2\pi}{N}k} + 1\right) \tilde{\varphi}(k)\tilde{\varphi}(-k) \\ &= \sum_{k=0}^{N-1} e^{i\frac{2\pi}{N}k(x-y)} 2\left(1 - \frac{e^{i\frac{2\pi}{N}k} + e^{-i\frac{2\pi}{N}k}}{2}\tilde{\varphi}(k)\tilde{\varphi}(-k)\right) \\ &= 2\sum_{k=0}^{N-1} e^{i\frac{2\pi}{N}k(x-y)} \sin^2\left(\frac{\pi}{N}k\right)\tilde{\varphi}(k)\tilde{\varphi}(-k) \\ &= \sum_{k=0}^{N-1} e^{i\frac{2\pi}{N}k(x-y)} p^2 D(k). \end{aligned} \tag{C.17}$$

## C.2 The Ghost Propagator for LGT

### C.2.1 The Ghost Propagator in Continuum Gauge Field Theory

In the functional approach of continuum gauge field theory, the gauge is usually fixed by the Faddeev-Popov procedure. In this method, the gauge-fixing condition

$$\mathsf{G}[A^\Omega] \equiv \frac{\delta}{\delta\Omega}\mathsf{F}[A^\Omega] = 0 \tag{C.18}$$

is implemented by inserting the "*identity*"

$$1 = \int [\mathsf{D}\Omega(x)]\, \delta\left(\mathsf{G}\left(A^\Omega\right)\right) \det\left[\frac{\delta\mathsf{G}\left(A^\Omega\right)}{\delta\Omega(x)}\right] \tag{C.19}$$

into the functional integral of pure Yang-Mills theory, where $A^\Omega$ represent the gauge transformed gauge fields $A$

$$A^\Omega = \Omega\,A\,\Omega^\dagger - i(\partial U)U^\dagger, \quad \Omega = e^{i\omega^{\mathrm{a}}(x)\hat{t}^{\mathrm{a}}}, \tag{C.20}$$

where $\hat{t}$ are the generators of the gauge group and all space-time indices were ignored. The infinitesimal form of eq.(C.20) is given by

$$A^{\mathrm{a}} = A^{\mathrm{a}} + f^{\mathrm{abc}}A^{\mathrm{b}}\omega^{\mathrm{c}} + \partial\omega^{\mathrm{a}}, \tag{C.21}$$

with the structure constants $f^{\mathrm{abc}}$ of the gauge group under consideration.

In QED, the determinant in Eq.(C.19) is independent of the gauge fields $A$ and can hence be covered up to a normalization factor. Whereas in QCD, this determinant depends on the gauge fields and thus contributes new terms to the Lagrangian. The Faddeev-Popov determinant can be represented as a functional integral over a new set of anti-commuting fields belonging to the adjoint representation:

$$\mathsf{det}\left[i(\mathbb{M})^{\mathrm{a,b}}_{x,y}\right] = \int [\mathrm{D}c]\,[\mathrm{D}\bar{c}]\exp\left\{-i\int d^4x\,\bar{c}(y)\left((M)^{\mathrm{a,b}}_{x,y}\right)c(x)\right\}, \tag{C.22}$$

where $c$, $\bar{c}$ are the ghost and anti-ghost fields respectively. The Faddeev-Popov matrix $(\mathbb{M})^{\mathrm{a,b}}_{x,y}$ for the Landau gauge is given by

$$(\mathbb{M})^{\mathrm{a,b}}_{x,y} = \left(\partial^2 - f^{\mathrm{abc}}A^{\mathrm{c}}_\mu(x)\partial_\mu\right)\delta^4(x-y). \tag{C.23}$$

This explicit expression of the Faddeev-Popov matrix follows from the Landau gauge fixing condition

$$\mathsf{G}\left[A^\Omega\right] = \partial A^\Omega = 0 \tag{C.24}$$

and the explicit definition of the Faddeev-Popov matrix

$$\begin{aligned}(\mathbb{M})^{\mathrm{a,b}}_{x,y} &= \left.\frac{\delta\mathsf{F}\left[A^{\mathrm{a}\,\Omega}_\mu(x)\right]}{\delta\omega^{\mathrm{b}}(y)}\right|_{\omega^{\mathrm{b}}(y)=0} \\ &= \left.\frac{\delta\mathsf{F}\left[A^{\mathrm{a}\,\Omega}_\mu(x)\right]}{\delta A^{\mathrm{c}\,\Omega}_\nu(z)}\frac{\delta A^{\mathrm{c}\,\Omega}_\nu(z)}{\delta\omega^{\mathrm{b}}(y)}\right|_{\omega^{\mathrm{b}}(y)=0},\end{aligned} \tag{C.25}$$

where the identity Eq.(C.18) was used and a summation over $\mu$ is implied. The Faddeev-Popov matrix exhibits a diagonal structure in the algebra space.

The corresponding ghost propagator is defined by the inverse of the Faddeev-Popov operator[1]

$$G(x-y)\,\delta^{\mathrm{ab}} := \left\langle\bar{c}^{\mathrm{a}}(x)c^{\mathrm{b}}(y)\right\rangle = \left\langle\left(\mathbb{M}^{-1}\right)^{\mathrm{a,b}}_{x,y}\delta^{\mathrm{ab}}\right\rangle. \tag{C.26}$$

---

[1]It is seen from the path integral quantization that propagators are generally given by the inverse of the operator appearing in the quadratic term in the Lagrangian.

### C.2.2   The Faddeev-Popov Determinant in LGT

Before we can give the lattice definition of the ghost form factor, the lattice
version of the Faddeev-Popov determinant has to be worked out in detail. For
this, we investigate the infinitesimal variation of a gauge transformed gauge field
from the link variables $U_\mu(x)$, see also [Zwa94], [SS96]. We use the following
definition for the extraction of the gauge fields $A_\mu^{\mathrm{a}}(x)$ from the link variables
$U_\mu(x)$,

$$A_\mu^{\mathrm{a}}(x) := -\frac{\mathsf{tr}\left[\tau^{\mathrm{a}}U_\mu(x)\right]}{2}.$$

From this it follows the variation of the gauge fields under a finite gauge trans-
formation, whereby we concentrate on the $SU(2)$ gauge group for simplicity:

$$
\begin{aligned}
\delta A_\mu^{\mathrm{a}\,\Omega}(x) &= -\frac{1}{2}\mathsf{tr}\left[\tau^{\mathrm{a}}\left(U_\mu^\Omega(x) - U_\mu(x)\right)\right] \\
&= -\frac{1}{2}\mathsf{tr}\left[\tau^{\mathrm{a}}\left(\Omega(x)U_\mu(x)\Omega_\mu^\dagger(x+\mu) - U_\mu(x)\right)\right] \\
&= -\frac{1}{2}\mathsf{tr}\left[\tau^{\mathrm{a}}\left(\left(\mathbb{1}+\omega(x)\right)U_\mu(x)\left(\mathbb{1}-\omega(x+\mu)\right) - U_\mu(x)\right)\right] \\
&= -\frac{1}{2}\mathsf{tr}\left[\tau^{\mathrm{a}}\left(\omega(x)U_\mu(x) - U_\mu(x)\omega(x+\mu) + \mathcal{O}(\omega^2)\right)\right] \\
&= -\frac{1}{2}\mathsf{tr}\left[\tau^{\mathrm{a}}\left(\omega^{\mathrm{b}}\tau^{\mathrm{b}}\left(u_\mu^0(x)\mathbb{1} + u_\mu^{\mathrm{c}}(x)\tau^{\mathrm{c}}\right) - \left(u_\mu^0(x)\mathbb{1} + u_\mu^{\mathrm{c}}(x)\tau^{\mathrm{c}}\right)\omega^{\mathrm{b}}(x+\mu)\tau^{\mathrm{b}}\right)\right] \\
&= -\frac{1}{2}\mathsf{tr}\Big[\omega^{\mathrm{b}}(x)u_\mu^0(x)\left(-\delta^{\mathrm{a,b}} - \varepsilon^{\mathrm{abc}}\tau^{\mathrm{c}}\right) + \omega^{\mathrm{b}}(x)u_\mu^{\mathrm{c}}\tau^{\mathrm{a}}\tau^{\mathrm{b}}\tau^{\mathrm{c}} \\
&\qquad\quad -\omega^{\mathrm{b}}(x+\mu)u_\mu^0(x)\left(-\delta^{\mathrm{a,b}} - \varepsilon^{\mathrm{abc}}\tau^{\mathrm{c}}\right) - \omega^{\mathrm{b}}(x+\mu)u_\mu^{\mathrm{c}}(x)\underbrace{\tau^{\mathrm{a}}\tau^{\mathrm{c}}\tau^{\mathrm{b}}}_{\mathsf{tr}[\tau^{\mathrm{a}}\tau^{\mathrm{c}}\tau^{\mathrm{b}}]=-\mathsf{tr}[\tau^{\mathrm{a}}\tau^{\mathrm{b}}\tau^{\mathrm{c}}]}\Big] \\
&= -\frac{1}{2}\mathsf{tr}\left[\left(-\omega^{\mathrm{a}}(x) + \omega^{\mathrm{a}}(x+\mu)\right)u_\mu^0(x)\right] \\
&\quad -\frac{1}{2}\mathsf{tr}\left[\omega^{\mathrm{b}}(x)u_\mu^{\mathrm{c}}(x)\left(-\delta^{\mathrm{a,b}} - \varepsilon^{\mathrm{abd}}\tau^{\mathrm{d}}\right)\tau^{\mathrm{c}} + \omega^{\mathrm{b}}(x+\mu)\left(-\delta^{\mathrm{ab}} - \varepsilon^{\mathrm{abd}}\tau^{\mathrm{d}}\right)\tau^{\mathrm{c}}\right] \\
&= -\frac{1}{2}\mathsf{tr}\left[\left(-\omega^{\mathrm{a}}(x) + \omega^{\mathrm{a}}(x+\mu)\right)u_\mu^0(x)\right] \\
&\quad -\frac{1}{2}\mathsf{tr}\left[\left(\omega^{\mathrm{b}}(x) + \omega^{\mathrm{b}}(x+\mu)\right)u_\mu^{\mathrm{c}}(x)\left(-\varepsilon^{\mathrm{abd}}\left(-\delta^{\mathrm{cd}} - \varepsilon^{\mathrm{dcf}}\tau^{\mathrm{f}}\right)\right)\right] \\
&= -\frac{1}{2}\mathsf{tr}\left[\left(-\omega^{\mathrm{a}}(x) + \omega^{\mathrm{a}}(x+\mu)\right)u_\mu^0(x)\right] \\
&\quad -\frac{1}{2}\mathsf{tr}\left[\varepsilon^{\mathrm{abc}}\left(\omega^{\mathrm{b}}(x) + \omega^{\mathrm{b}}(x+\mu)\right)u_\mu^{\mathrm{c}}(x)\right].
\end{aligned}
$$

Finally, one achieves for the variation of the $SU(2)$ gauge field

$$\delta A_\mu^{\mathrm{a}\,\Omega}(x) = u_\mu^0(x)\left(\omega^{\mathrm{a}}(x) - \omega^{\mathrm{a}}(x+\mu)\right) - \varepsilon^{\mathrm{abc}}u_\mu^{\mathrm{c}}(x)\left(\omega^{\mathrm{b}}(x) + \omega^{\mathrm{b}}(x+\mu)\right). \quad \text{(C.27)}$$

Now, inserting Eq.(C.27) in the definition of the Faddeev-Popov matrix Eq.(C.25) and using the lattice description of the Landau gauge fixing condition

$$\mathsf{F}\left[A_\mu^{a\,\Omega}(x)\right] = A_\mu^{a\,\Omega}(x-\mu) - A_\mu^{a\,\Omega}(x), \tag{C.28}$$

we obtain the the explicit lattice version of the Faddeev-Popov matrix for Landau gauge:

$$
\begin{aligned}
(\mathbb{M})_{x,y}^{a,b} &= \delta^{ab}\Big(u_\mu^0(y)\delta(x-\mu-y) - \big(u_\mu^0(y)+u_\mu^0(y-\mu)\big)\,\delta(x-y) \\
&\qquad + u_\mu^0(y-\mu)\delta(x+\mu-y)\Big) \\
&\quad - \varepsilon^{abc}\Big(u_\mu^c(y)\delta(x-\mu-y) - u_\mu^c(y-\mu)\delta(x+\mu-y) \\
&\qquad + \underbrace{\big(u_\mu^c(y-\mu) - u_\mu^c(y)\big)}_{=0,\ \text{lgf}}\,\delta(x-y)\Big) \\
&= \delta^{ab}\Big(u_\mu^0(y)\delta(x-\mu-y) - \big(u_\mu^0(y)+u_\mu^0(y-\mu)\big)\,\delta(x-y) \\
&\qquad + u_\mu^0(y-\mu)\delta(x+\mu-y)\Big) \\
&\quad - \varepsilon^{abc}\Big(u_\mu^c(y)\delta(x-\mu-y) - u_\mu^c(y-\mu)\delta(x+\mu-y)\Big).
\end{aligned}
\tag{C.29}
$$

### C.2.3 Numerical Evaluation of the Ghost Propagator

In the preceding subsection, we derived the Faddeev-Popov matrix for Landau gauge. To obtain the ghost propagator, we need the inverse of this matrix. The Faddeev-Popov matrix $\mathbb{M} = (\mathbb{M})_{x,y}^{a,b}$ is a real symmetric matrix acting on the algebra space $\mathcal{A}$ of the gauge group. But $\mathbb{M}$ is a singular matrix in Landau gauge. Therefore, we have to take out the zero modes, $v_0 \in \mathcal{A}_0$, from the algebra space and perform the inversion only on the regular part, $\mathcal{A}_{\text{reg.}} := \mathcal{A}/\mathcal{A}_0$, thereof. Following [SS96], we decompose the algebra space into two disjoint parts,

$$\mathcal{A} = \mathcal{A}_0 \oplus \mathcal{A}_1, \tag{C.30}$$

so that the zero modes are separated from the regular modes,

$$\mathbb{M}\,v_0 = 0,\ \text{for}\ v_0 \in \mathcal{A}_0 \quad \text{and} \quad \mathbb{M}\,v\begin{cases} \neq 0, \ \text{for}\ v \in \mathcal{A}_1 \\ = 0, \ \text{for}\ v = 0. \end{cases} \tag{C.31}$$

For the calculation of the ghost propagator, we have to solve the following linear equation

$$\mathbb{M}\,(\mathbb{M}v) = \mathbb{M}\,c, \tag{C.32}$$

for arbitrary $v$ and a given source term $c$. Note that $\mathbb{M}v$ belongs to the regular part of the algebra space $\mathcal{A}_1$. A usual way to solve the algebraic linear system

is the conjugate gradient method (CG). The algorithm starts from some initial guess $v_0$ and achieves an approximation to the solution by adding $\alpha\, d_k$ to the current value $v_k$ at each iteration step $k$:

$$v_k \rightarrow v_{k+1} = v_k + \alpha\, d_k,$$

where $\alpha$ is defined in the fourth line of the CG-algorithm (C.1):

Set $b = \mathbb{M}c$, thus $b \in \mathcal{A}_1$. Note that $\mathbb{M}$ is real, symmetric and positive definite.

1:  `choose arbitrary` $v^{(0)} \in \mathcal{A}_1$`, i.e.` $x^{(0)} = \mathbb{M}v^{(0)}$
2:  $r^{(0)} = b - \mathbb{M}v^{(0)}$, $d^{(0)} = r^{(0)}$
3:  `for` $k = 0, 1, \dots$ `do`
4:      $\alpha^{(k)} = \frac{||r^{(k)}||_2^2}{\langle d^{(k)}, \mathbb{M}d^{(k)}\rangle}$, `save` $\mathbb{M}d^{(k)}$
5:      $v^{(k+1)} = v^{(k)} + \alpha_k d^{(k)}$
6:      $r^{(k+1)} = r^{(k)} - \alpha_k \mathbb{M}d^{(k)}$
7:      $\beta_k = \frac{||r^{(k+1)}||_2^2}{||r^{(k)}||_2^2}$, `save` $||r^{(k+1)}||_2^2$
8:      $d^{(k+1)} = r^{(k+1)} + \beta_k d^{(k)}$
9:  `if` $\frac{||\mathbb{M}v^{(k+1)} - b||_2^2}{||b||_2^2} < \varepsilon$ `then stop and end for`

**Algorithm C.1**: The algorithm for the conjugate gradient method.

Since $\mathbb{M}(\mathbb{M}v) = \mathbb{M}c$ ensures that both, the starting vector $v_0$ and the source vector $c$ belong to the algebraic subspace $\mathcal{A}_1$, $v_k$ and $\alpha\, d_k$ will be also a member of the regular part $\mathcal{A}_1$ of the algebraic space $\mathcal{A}$. The iteration will therefore converge to a unique solution within $\mathcal{A}_1$.

The vector-matrix multiplication is explicitly given by

$$
\begin{aligned}
v^{\mathrm{a}}(x) \;\; :=\;\; & (\mathbb{M})^{\mathrm{a,b}}_{x,y}\, c^{\mathrm{b}}(y) \\
=\;\; & u^0_\mu(x)\, \delta^{\mathrm{ab}} \left(c^{\mathrm{b}}(x) - c^{\mathrm{b}}(x+\mu)\right) - \\
& -u^0_\mu(x-\mu)\, \delta^{ab} \left(c^{\mathrm{b}}(x-\mu) - c^{\mathrm{b}}(x)\right) - \\
& -\varepsilon^{\mathrm{abc}} \left(u^{\mathrm{b}}_\mu c^{\mathrm{c}}(x+\mu) - u^{\mathrm{b}}_\mu(x-\mu)c^{\mathrm{c}}(x-\mu)\right),
\end{aligned}
\tag{C.33}
$$

where an addition over the direction index $\mu$ and over the color indices is implied. The vector components $c^a(x)$ and $v^a(x)$ live in the algebra of the gauge group, i.e.

$$v := v^{\mathrm{a}}(x)\tau^{\mathrm{a}} \text{ and in the following } \vec{v}(x) := \begin{pmatrix} v^1(x) \\ v^2(x) \\ v^3(x) \end{pmatrix}. \tag{C.34}$$

## C.2.4  CG-Method with symmetric Gauß-Seidel Preconditioning

In the preceding section, the CG-method was introduced as a method for solving the algebraic linear system eq.(C.32). Here, an improvement of the CG-method, the Gauß-Seidel preconditioned CG-method (GSP-CG method), is suggested which can solve linear systems with Hermitian, positive definite matrices $\mathbb{M}$. This algorithm is applicable to solve our linear system, since the Faddeev-Popov matrix is a symmetric, real and positive definite matrix. The symmetric Gauß-Seidel preconditioning leads in many cases to an acceleration of convergence and exhibits no significant additional expenses.

For our purpose we separate the Faddeev-Popov matrix as follows

$$\mathbb{M} := \mathbb{D} - \mathbb{R} - \mathbb{R}^{\star}, \qquad (C.35)$$

where $\mathbb{D}$ labels the diagonal part of $\mathbb{M}$, $\mathbb{R}$ and $\mathbb{R}^{\star}$ label the lower left and upper right part of $\mathbb{M}$ respectively.

With the definition of the source vector Eq.(C.34) the multiplication separates as follows

$$\vec{v}(x) = [-\mathbb{R}]_x^{\mu} \, \vec{c}(x - \mu) + [\mathbb{D}]_x^{\mu} \, \vec{c}(x) + [-\mathbb{R}^{\star}]_x^{\mu} \, \vec{c}(x + \mu), \qquad (C.36)$$

where we again sum over $\mu$. The matrices are parameterized by the space-time index $x$ of the corresponding color vector $\vec{c}(x)$ which multiplies to the diagonal part of the Faddeev-Popov matrix. The diagonal part $\mathbb{D}$ is given by

$$\mathbb{D}_{x'} := - \left( u_{\mu}^{0}(x') + u_{\mu}^{0}(x' - \mu) \right) \, \mathbb{1}_{3\times 3}, \qquad (C.37)$$

whereby an addition over the direction index $\mu$ is again implied. The lower-left matrix $\mathbb{R}$ of the Faddeev-Popov matrix is given by

$$[-\mathbb{R}]_{x'}^{\mu} := \begin{pmatrix} u_{\mu}^{0}(x' - \mu) & -u_{\mu}^{3}(x' - \mu) & u_{\mu}^{2}(x' - \mu) \\ u_{\mu}^{3}(x' - \mu) & u_{\mu}^{0}(x' - \mu) & -u_{\mu}^{1}(x' - \mu) \\ -u_{\mu}^{2}(x' - \mu) & u_{\mu}^{1}(x' - \mu) & u_{\mu}^{0}(x' - \mu) \end{pmatrix} \qquad (C.38)$$

and the upper-right matrix $\mathbb{R}^{\star}$ is given by

$$[-\mathbb{R}^{\star}]_{x'}^{\mu} := \begin{pmatrix} u_{\mu}^{0}(x') & u_{\mu}^{3}(x') & -u_{\mu}^{2}(x') \\ -u_{\mu}^{3}(x') & u_{\mu}^{0}(x') & u_{\mu}^{1}(x') \\ u_{\mu}^{2}(x') & -u_{\mu}^{1}(x') & u_{\mu}^{0}(x') \end{pmatrix}. \qquad (C.39)$$

Note, that the symmetry of the Faddeev-Popov matrix is respected by this decomposition, since $[-\mathbb{R}^{\star}]$ is the transpose of $[-\mathbb{R}]$ and the $\mu$-addition to the space-time index for the next row is canceled in $[-\mathbb{R}]$, see the following abstract

representation of the Faddeev-Popov matrix:

$$x' = x - \mu \quad x' = x \quad x' = x + \mu$$

$$
\begin{array}{lllll}
[-\mathbb{R}]_{x'}^{\mu} & [\mathbb{D}]_{x'}^{\mu} & [-\mathbb{R}^{\star}]_{x'}^{\mu} & & x' = x - \mu \qquad (\text{C.40})\\
 & [-\mathbb{R}]_{x'}^{\mu} & [\mathbb{D}]_{x'}^{\mu} & [-\mathbb{R}^{\star}]_{x'}^{\mu} & x' = x \\
 & & [-\mathbb{R}]_{x'}^{\mu} & [\mathbb{D}]_{x'}^{\mu} & [-\mathbb{R}^{\star}]_{x'}^{\mu} \quad x' = x + \mu,
\end{array}
$$

where in the first row the indices $x'$ label the space-time index of the corresponding column. The indices in the last column label the space-time index of the vector $\vec{c}(x')$, so that a matrix-vector multiplication for the middle row of the matrix above results in $\vec{v}(x)$ of Eq.(C.36).

This decomposition is now used for the symmetric Gauß-Seidel preconditioning for the CG-method. The main difference between the CG-method and the GSP-CG-method lies in the fact, that the matrix-vector multiplication occurring in the CG-method (line 4 in the CG-algorithm) is separated into two parts (line 4 and 5 in the GSP-CG-method), where the multiplication occurs only over the half matrix, i.e over the lower-left part with the diagonal part or over the upper-right part with the diagonal part. Those two linear systems can be now solved by the symmetric Gauß-Seidel method for linear equations. The numerical expense is approximately halved compared to the CG-method, see fig.(C.1).

Set $b := \mathbb{M}c$, thus $b \in \mathcal{A}_1$. Initialize $\mathbb{M} := \mathbb{D} - \mathbb{R} - \mathbb{R}^{\star}$ being real, symmetric and positive definite.

01:  `choose arbitrary` $x^{(0)} \in \mathcal{A}_1$`, i.e.` $x^{(0)} = \mathbb{M}x^{(0)}$
<u>02:</u>  `solve` $(\mathbb{D} - \mathbb{R}^{\star})s^{(0)} = b - \mathbb{M}x^{(0)}$, $w^{(0)} = s^{(0)}$
03:  `for` $k = 0, 1, \ldots$ `do`
<u>04:</u>      `solve` $(\mathbb{D} - \mathbb{R})d^{(k)} = \mathbb{D}w^{(k)}$`, save` $\mathbb{D}w^{(k)}$
<u>05:</u>      `solve` $(\mathbb{D} - \mathbb{R}^{\star})g^{k} = \mathbb{D}w^{(k)} - \mathbb{D}d^{(k)}$
<u>06:</u>      $v^{(k)} = d^{(k)} + g^{(k)}$
<u>07:</u>      $\alpha_k = \dfrac{\langle s^k, \mathbb{D}s^k \rangle}{\langle v^{(k)}, \mathbb{D}w^{(k)} \rangle}$
08:      $x^{(k+1)} = a^{(k)} + \alpha_k d^k$
09:      $s^{(k+1)} = s^{(k)} - \alpha_k v^{(k)}$
<u>10:</u>      $\beta_k = \dfrac{\langle s^{(k+1)}, \mathbb{D}s^{(k+1)} \rangle}{\langle s^{(k)}, \mathbb{D}s^{(k)} \rangle}\rangle$
11:      $w^{(k+1)} = s^{(k+1)} + \beta_k w^{(k)}$
12:  `if` $\dfrac{||\mathbb{M}x^{(k+1)} - b||_2^2}{||b||_2^2} < \varepsilon$ `then stop and end for`

**Algorithm C.2**: The algorithm for the conjugate gradient method with symmetric Gauß-Seidel preconditioning. The underlined numbers indicate new or changed lines in the algorithm with respect to the CG-algorithm.

The GSP-CG-algorithm needs less than the half iterations steps of the CG-algorithm which leads to the half time needed to solve the linear equation. As a
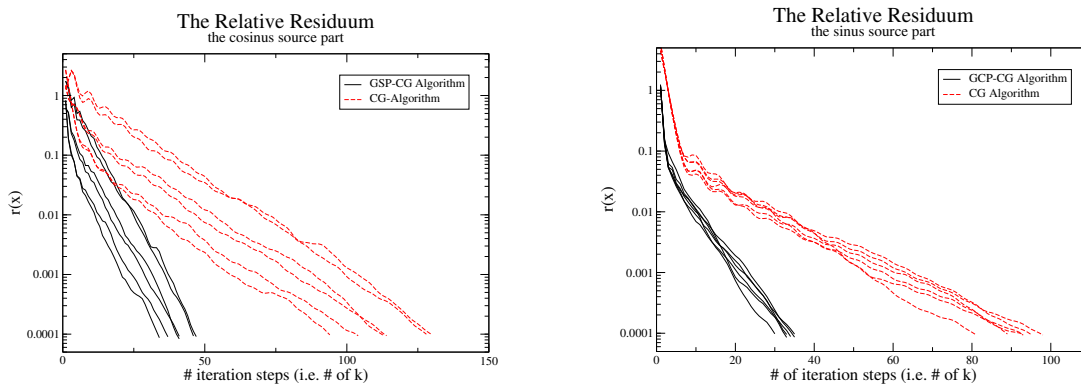
Figure C.1: The relative residue $r$, algorithm (C.1) line 2, is shown for the cosinus and sinus part for the GSP-CG-method and the CG-method. The calculation was done at a $12^4$ lattice at $\beta = 2.3$ which leads to 6 different values for the momentum. Clearly, the GSP-CG-method is at least twice as fast as the CG-method.

byproduct, we see that the cosinus part needs more iteration steps than the sinus part and the momentum dependence of the relative residue of the cosinus part is greater than that of the sinus part.[2]

## C.2.5 The Ghost Form Factor in LGT

Since we are interested in the deviation of a general ghost propagator from the free one, i.e. the ghost form factor, we try again the trick used for the gluon form factor. This means we have to find an operator which gives us directly the expectation value of the ghost form factor.

We make the ansatz

$$G(x,y) = \left\langle \left(\mathbb{M}^{-1}\right)^{a,b}_{x,y} - \left(\mathbb{M}^{-1}\right)^{a,b}_{x+\hat{\mu},y} + \left(\mathbb{M}^{-1}\right)^{a,b}_{x+\hat{\mu},y+\hat{\mu}} - \left(\mathbb{M}^{-1}\right)^{a,b}_{x,y+\hat{\mu}} \right\rangle, \quad \text{(C.41)}$$

to get directly the form factor of the ghost propagator in Landau gauge. Here, $\hat{\mu}$ is the unit vector of the space-time lattice which corresponds in the following to the direction of the momentum.

If we consider the expectation value of the inverse Faddeev-Popov operator $(\mathbb{M}^{-1})^{a,b}_{x,y}$ and we use again the translation invariance of the expectation value, i.e.

$$\left\langle \tilde{\mathbb{M}}_{k,q} \right\rangle = f(q)\delta_{k,-q},$$

---

[2]This calculation was done for the ghost form factor directly and not for the ghost propagator, see the following subsection.

we obtain

$$
\begin{aligned}
\left\langle \left(\mathbb{M}^{-1}\right)_{x,y}^{a,b} \right\rangle &= \sum_{k,q} \exp\left\{ i\frac{2\pi}{N}kx \right\} \left(\tilde{\mathbb{M}}^{-1}\right)_{k,q}^{a,b} \exp\left\{ i\frac{2\pi}{N}qy \right\} \\
&= \sum_{k} \exp\left\{ i\frac{2\pi}{N}kx \right\} \left(\tilde{\mathbb{M}}^{-1}\right)_{k,-k}^{a,b} \exp\left\{ -i\frac{2\pi}{N}ky \right\}.
\end{aligned}
$$

This defines the ghost propagator in Landau gauge, since we are interested in the ghost form factor, we start with the Fourier transform of our ansatz (C.41) and show that the ghost form factor is given by

$$
F(k^2) = k^2\, G(k^2) := \mathsf{FT}\left[G(x,y)\right]. \tag{C.42}
$$

For a better survey of our ansatz (C.41) , we separate it into two parts

$$
\begin{aligned}
\left\langle \left(\mathbb{M}^{-1}\right)_{x,y}^{a,b} - \left(\mathbb{M}^{-1}\right)_{x+1,y}^{a,b} \right\rangle &= \sum_{k} \left[ e^{i\frac{2\pi}{N}k(x+1)}\, e^{-i\frac{2\pi}{N}ky} - e^{i\frac{2\pi}{N}kx}\, e^{-i\frac{2\pi}{N}ky} \right] \left(\tilde{\mathbb{M}}^{-1}\right)_{k,-k}^{a,b} \\
&= \sum_{k} \left[ e^{i\frac{2\pi}{N}kx}\, e^{-i\frac{2\pi}{N}ky} \left(1 - e^{i\frac{2\pi}{N}k}\right) \right] \left(\tilde{\mathbb{M}}^{-1}\right)_{k,-k}^{a,b}
\end{aligned}
$$

and with the same procedure for the second part

$$
\begin{aligned}
\left\langle \left(\mathbb{M}^{-1}\right)_{x+1,y+1}^{a,b} - \left(\mathbb{M}^{-1}\right)_{x,y+1}^{a,b} \right\rangle &= \sum_{k} \left[ e^{i\frac{2\pi}{N}kx}\, e^{-i\frac{2\pi}{N}ky} \left( e^{i\frac{2\pi}{N}k(1-1)} - e^{-i\frac{2\pi}{N}k}\right) \right] \left(\tilde{\mathbb{M}}^{-1}\right)_{k,-k}^{a\,b} \\
&= \sum_{k} \left[ e^{i\frac{2\pi}{N}kx}\, e^{-i\frac{2\pi}{N}ky} \left(1 - e^{-i\frac{2\pi}{N}k}\right) \right] \left(\tilde{\mathbb{M}}^{-1}\right)_{k,-k}^{a\,b}.
\end{aligned}
$$

Summarizing both parts, we obtain

$$
\begin{aligned}
\left\langle \left( \left(\mathbb{M}^{-1}\right)_{x,y}^{a,b}\right) - \left(\mathbb{M}^{-1}\right)_{x+1,y}^{a,b} + \left(\mathbb{M}^{-1}\right)_{x+1,y+1}^{a,b} - \left(\left(\mathbb{M}^{-1}\right)_{x,y+1}^{a,b}\right) \right\rangle &= \\
= \sum_{k} e^{i\frac{2\pi}{N}kx} e^{-i\frac{2\pi}{N}ky} \left( 2 - e^{i\frac{2\pi}{N}k} - e^{-i\frac{2\pi}{N}k}\right) &\left(\tilde{\mathbb{M}}^{-1}\right)_{k,-k}^{a,b} \\
= \frac{1}{2} \sum_{k} e^{ik(x-y)} \left( 2\sin\left(\frac{\pi}{N_k}k\right)\right)^2 &\left(\tilde{\mathbb{M}}^{-1}\right)_{k,-k}^{a,b}.
\end{aligned}
$$

The sinus term in the equation above corresponds again exactly to the lattice definition of the dimensionless, discrete lattice momentum

$$
k_{\text{lat.}} = 2\sin\left(\frac{\pi}{N_k}k\right). \tag{C.43}
$$

Hence, we obtain directly the Fourier transform of the ghost form factor in momentum space with our ansatz. A back Fourier transformation leads to the ghost

form factor in momentum space, cf. eq.(C.12). With this, we get for our source terms of the ghost and anti-ghost fields

$$c_1^{\mathrm{a}}(x, k) = \bar{c}_1^{\mathrm{a}}(x, k) = \cos\left(\frac{2\pi}{N_k} kx\right) \tag{C.44}$$

and

$$c_2^{\mathrm{a}}(x, k) = \bar{c}_2^{\mathrm{a}}(x, k) = \sin\left(\frac{2\pi}{N_k} kx\right), \tag{C.45}$$

with $N_k$ the number of lattice sites in the $k$-direction. If we combine these source terms in the following way,

$$b_{1,2}^{\mathrm{a}}(x, k) = c_{1,2}^{\mathrm{a}}(x, k) - c_{1,2}^{\mathrm{a}}(x - 1, k), \tag{C.46}$$

the lattice expectation value of the ghost form factor in Landau gauge is given by

$$
\begin{aligned}
\langle G(k)\rangle_{\mathrm{MC}} \quad &:= \quad \left\langle \bar{b}_{1,2}^{\mathrm{a}}(x, k) \left(\mathbb{M}^{-1}\right)_{x,y}^{\mathrm{a,b}} b_{1,2}^{\mathrm{b}}(y, k) \right\rangle_{\mathrm{MC}} \tag{C.47} \\
&= \quad \left\langle \bar{b}_1^{\mathrm{a}}(x, k) \left(\mathbb{M}^{-1}\right)_{x,y}^{\mathrm{a,b}} b_1^{\mathrm{b}}(y, k) + \bar{b}_2^{\mathrm{a}}(x, k) \left(\mathbb{M}^{-1}\right)_{x,y}^{\mathrm{a,b}} b_2^{\mathrm{b}}(y, k) \right\rangle_{\mathrm{MC}},
\end{aligned}
$$

where a summation is implied over the space-time points $x$, $y$ and the color indices a and b.

# Appendix D

# Multiplicative Renormalization of Lattice Measurement Data

In general, the measurement data achieved by lattice gauge simulations depend on the free parameter $\beta$ of the theory. The physical scale is fixed by the dependence of the lattice spacing $a$ with respect on $\beta$, cf. eq.(2.66). But still there is a dependence of the data on $\beta$: the measurement results of different $\beta$-values ceases to fall on an unique graph of the observable under consideration, e.g. the gluon form factor cf. (fig.(D.1)). In this appendix we explain how multiplicative renormalization is used to bring the lattice data of form factors on a unique graph.

From perturbation theory we know, that physical quantities can be extracted form divergent quantities, the bare ones, by the theory of renormalization. A possible way is the method of multiplicative renormalization, where the divergences stemming from loop integrations are countervailed by multiplicative constants being divergent. For simplicity we consider a field $\Phi$ in the following:

$$\Phi_0 = Z_3^{1/2} \, \Phi_{\mathrm{ren}}, \tag{D.1}$$

with the divergent, bare field $\Phi_0$, the divergent renormalization constant $Z_3$ and the renormalized, physical field $\Phi_{\mathrm{ren}}$. The renormalization constant $Z_3$ depends on the momentum transfer $\mu$ and the momentum cutoff $\Lambda$ and we make the ansatz

$$Z_3 = Z_3(\mu^2, \Lambda^2) := Z_3(\mu^2) \, Z_\beta(\Lambda^2). \tag{D.2}$$

Note that lattice simulations with different $\beta$ values correspond to simulations with different UV-cutoff $\Lambda := \pi/a(\beta)$. We use the renormalization constant $Z_\beta(\Lambda^2)$ to bring our lattice data on the same functional graph of the observable and the constant $Z_3(\mu^2)$ to renormalize the total quantity under consideration at a specific renormalization point $\mu'$ so that a finite (given) value of the renormalized quantity is achieved at the renormalization point $\mu'$.

In the next section we are concerned with the numerical procedure for multiplicative renormalization of lattice data with the goal to achieve the collective graph of the data points.

# D.1    Lattice-MR, A Model Independent Approach

The goal is to find the maximum overlap of the lattice data to the functional form of a given observable. Generally, the functional behavior of the observable is not known and one performs a model analysis. Since the lattice data are calculated at some different $\beta$-values, a direct involvement of the model is tempting, but might lead to a false interpretation of the measurement data. For this reason, we purpose a model independent procedure which is based on the simulated annealing algorithm combined with a linear least square fit of the lattice data to a graph of the model independent function $f(p)$. The cost function of the simulated annealing algorithm is the chi-square of the lattice data with respect to $f(p)$.

The chi-square is generally defined as

$$\chi^2 := \sum_{i=1}^{N} \left( \frac{y(x_i) - f(x_i)}{\sigma(y(x_i))} \right)^2 , \tag{D.3}$$

where $y(x_i)$ are the measurement data at points $x_i$, $\sigma^2(y(x_i))$ is the variance of $y(x_i)$, $N$ is the number of measurement data and $f(x_i) := f(x_i; a_1, \ldots, a_m)$ is usually the searched fit function depending on the $m$ parameters $a_1, \ldots, a_m$. The common use of $\chi^2$ is to find the fit function $f$ which minimizes $\chi^2$ with respect to the parameters $a_j$ to the given measurement data $y(x_i)$. The resulting function $f$ exhibits the maximal likelihood that it represents the measurement data.

Since our problem is quite different, we purpose the following procedure: Our goal is, to find the optimal renormalization constants $Z_\beta$ so that the following extended chi-square,

$$\chi^2 = \sum_{\beta=1}^{n_\beta} \sum_{i=1}^{N_\beta} \left( \frac{Z_\beta \, y_\beta(x_i^\beta) - f(x_i^\beta)}{Z_\beta \, \sigma(y_\beta(x_i^\beta))} \right)^2 , \tag{D.4}$$

is minimized by $Z_\beta$. Here, $\beta$ labels the $n_\beta$ sets of measurement data obtained at $n_\beta$ different $\beta$-values, i.e. different momentum cut-offs $\Lambda_\beta = \pi/a(\beta)$. Note that the fit function $f$ is of no interest, $f$ is only used to renormalize the measurement data so that the measurement data results in a (not yet specified) graph with a maximal likelihood.

To get the renormalization constants, we firstly divide the domain of the measurement data into $ng$ intervals. The intervals $ng$ are not equidistant but include the equal number of measurement data, so that every contribution of the

intervals to the chi-square function eq.(D.4) has the same weight cf. fig.(D.1). In every interval, a (dummy) fit function $f_{ng}$ is defined. We choose a polynomial of degree three

$$f(x) = \sum_{ng} f_{ng}(x) = \sum_{ng} \sum_{n=0}^{3} a_{n,ng}\, x^n. \tag{D.5}$$

The main reasons for this choice is that we need a function being stiff enough to scale the data points and we want to incorporate the possibility of a change of the local curvature. All this conditions are fulfilled by polynomials $f_{ng}(x)$ of degree three with a minimum of free parameters $a_{n,ng}$. At the interfaces of the intervals we demand that $f(x)$ is continuous and at least 1-times differentiable,

$$\begin{aligned}
f_{ng-1}(x_i) &= f_{ng}(x_i), \text{ with } x_i \text{ a point at the interface} \tag{D.6}\\
f'_{ng-1}(x_i) &= f'_{ng}(x_i).
\end{aligned}$$

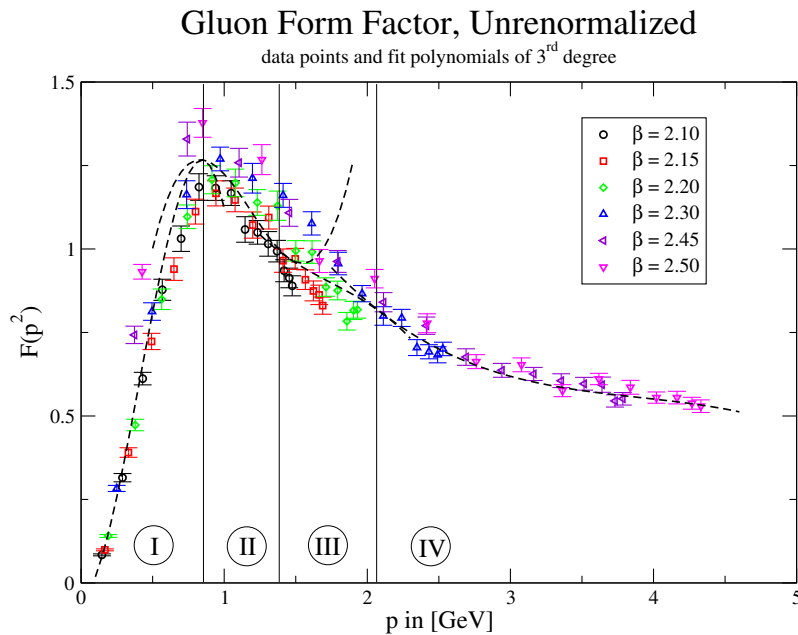This results in a reduction of the number of fit parameters $a_{n,ng}$.



Figure D.1: The un-renormalized data points of the gluon form factor $F(p^2)$ and the four starting fit polynomials are shown.

To find the (global) minimum of $\chi^2$ with respect to the renormalization constants $Z_\beta$, we use a simulated annealing algorithm combined with the downhill simplex method of Nelder and Mead. The result of our method is shown in fig.(D.2). The effect of multiplicative renormalization is clearly visible. Although, not all data points lie on the graph of the fit function $f(x)$ within their statistical error. Their are some systematical errors left from the discretization
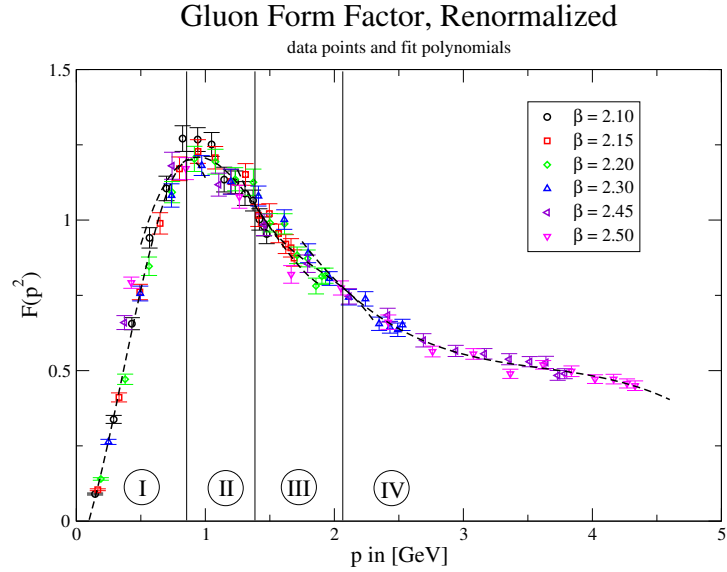
Figure D.2: The renormalized data points of the gluon form factor $F(p^2)$. The four fit polynomials are shown, which yield a minimum of the $\chi^2$.
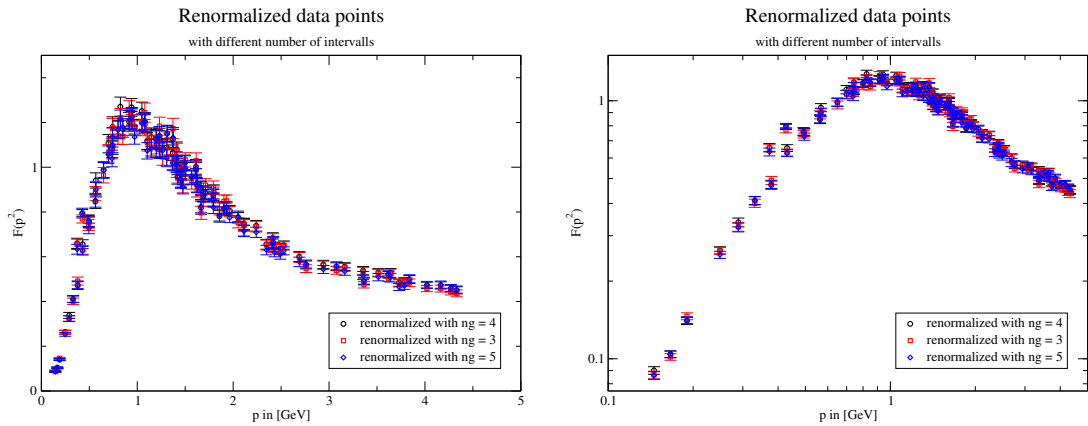


Figure D.3: The renormalized data points of the gluon form factor $F(p^2)$ in dependence of different number of fit polynomials. The data lie all within the statistical errors, so that the independence on the number of fit polynomials is shown.

and the finiteness of our lattice, which have to be incorporated if we want to discuss different models of the form factors.

That our procedure of renormalization is independent of the number of intervals $ng$ is shown in fig.(D.3). It should be clear, that a high enough number of intervals is needed for the renormalization procedure. But the number of intervals should not be to high, since then all data points could be fitted to arbitrary

polynomials. The independence of the chi-square $\chi^2$ of the number of intervals is an indication that the procedure is independent of the number of fit parameters within a certain range.

# Bibliography

[AB98a]      D. Atkinson and J. C. R. Bloch. QCD in the infrared with exact angular integrations. *Mod. Phys. Lett.*, A13:1055–1062, 1998.

[AB98b]      D. Atkinson and J. C. R. Bloch. Running coupling in non-perturbative qcd. i: Bare vertices and y-max approximation. *Phys. Rev.*, D58:094036, 1998.

[AC75]       Thomas Appelquist and J. Carazzone. Infrared singularities and massive fields. *Phys. Rev.*, D11:2856, 1975.

[ACY78]      Y. Aharonov, A. Casher, and S. Yankielowicz. Instantons and confinement. *Nucl. Phys.*, B146:256, 1978.

[Amb79]      Jan Ambjorn. On the decoupling of massive particles in field theory. *Commun. Math. Phys.*, 67:109, 1979.

[AO80]       Jan Ambjorn and P. Olesen. A color magnetic vortex condensate in qcd. *Nucl. Phys.*, B170:265, 1980.

[AP81]       Thomas Appelquist and Robert D. Pisarski. Hot yang-mills theories and three-dimensional qcd. *Phys. Rev.*, D23:2305, 1981.

[AvS01]      Reinhard Alkofer and Lorenz von Smekal. The infrared behavior of qcd green's functions: Confinement, dynamical symmetry breaking, and hadrons as relativistic bound states. *Phys. Rept.*, 353:281, 2001.

[B+00]       D. Becirevic et al. Asymptotic scaling of the gluon propagator on the lattice. *Phys. Rev.*, D61:114508, 2000.

[Bac86]      Constantin Bachas. Convexity of the quarkonium potential. *Phys. Rev.*, D33:2723, 1986.

[Bal00]      Gunnar Singh Bali. Casimir scaling of su(3) static potentials. *Phys. Rev.*, D62:114503, 2000.

[Bar98]      I. M. Barbour. Problems in simulating qcd at finite density on a lattice. *Nucl. Phys.*, A642:251–262, 1998.

[BCLM03]     Jacques C. R. Bloch, Attilio Cucchieri, Kurt Langfeld, and Tereza Mendes. Running coupling constant and propagators in su(2) landau gauge. *Nucl. Phys. Proc. Suppl.*, 119:736–738, 2003.

[BCLM04]     Jacques C. R. Bloch, Attilio Cucchieri, Kurt Langfeld, and Tereza Mendes. Propagators and running coupling from su(2) lattice gauge theory. *Nucl. Phys.*, B687:76–100, 2004.

[BFH+93]     G. S. Bali, J. Fingberg, Urs M. Heller, F. Karsch, and K. Schilling. The spatial string tension in the deconfined phase of the (3+1)-dimensional su(2) gauge theory. *Phys. Rev. Lett.*, 71:3059–3062, 1993.

[Bjo69]      J. D. Bjorken. Asymptotic sum rules at infinite momentum. *Phys. Rev.*, 179:1547–1553, 1969.

[Blo01]      J. C. R. Bloch. Multiplicative renormalizability of gluon and ghost propagators in qcd. *Phys. Rev.*, D64:116011, 2001.

[BMK+98]     Ian M. Barbour, Susan E. Morrison, Elyakum G. Klepfish, John B. Kogut, and Maria-Paola Lombardo. Results on finite density qcd. *Nucl. Phys. Proc. Suppl.*, 60A:220–234, 1998.

[BP69]       J. D. Bjorken and Emmanuel A. Paschos. Inelastic electron proton and gamma proton scattering, and the structure of the nucleon. *Phys. Rev.*, 185:1975–1982, 1969.

[BRS96]      Laurent Baulieu, Alexander Rozenberg, and Martin Schaden. Topological aspects of gauge fixing yang-mills theory on s(4). *Phys. Rev.*, D54:7825–7831, 1996.

[BS98]       Laurent Baulieu and Martin Schaden. Gauge group tqft and improved perturbative yang-mills theory. *Int. J. Mod. Phys.*, A13:985–1012, 1998.

[BSF+93]     G. S. Bali, K. Schilling, J. Fingberg, Urs M. Heller, and F. Karsch. Computation of the spatial string tension in high temperature su(2) gauge theory. *Int. J. Mod. Phys.*, C4:1179–1193, 1993.

[BSS95]      G. S. Bali, K. Schilling, and C. Schlichter. Observing long color flux tubes in su(2) lattice gauge theory. *Phys. Rev.*, D51:5165–5198, 1995.

[BW79]      Lowell S. Brown and William I. Weisberger. Remarks on the static potential in quantum chromodynamics. *Phys. Rev.*, D20:3239, 1979.

[CF94]      M. Consoli and J. H. Field. Effective gluon mass and the determination of alpha-s from j / psi and upsilon branching ratios. *Phys. Rev.*, D49:1293–1301, 1994.

[CJR83]      Michael Creutz, Laurence Jacobs, and Claudio Rebbi. Monte carlo computations in lattice gauge theories. *Phys. Rept.*, 95:201, 1983.

[CK83]      William E. Caswell and A. D. Kennedy. The asymptotic behavior of feynman integrals. *Phys. Rev.*, D28:3073, 1983.

[Col98]      John Collins. Renormalization. *Cambridge University Press*, 1998.

[CP75]      John C. Collins and M. J. Perry. Superdense matter: Neutrons or asymptotically free quarks? *Phys. Rev. Lett.*, 34:1353, 1975.

[CR91]      J. R. Cudell and D. A. Ross. Theory and phenomenology of the gluon propagator from the dyson-schwinger equation in qcd. *Nucl. Phys.*, B359:247–261, 1991.

[Cre77]      Michael Creutz. Gauge fixing, the transfer matrix, and confinement on a lattice. *Phys. Rev.*, D15:1128, 1977.

[Cre80]      M. Creutz. Monte carlo study of quantized su(2) gauge theory. *Phys. Rev.*, D21:2308–2315, 1980.

[Cuc99]      Attilio Cucchieri. Infrared behavior of the gluon propagator in lattice landau gauge: The three-dimensional case. *Phys. Rev.*, D60:034508, 1999.

[DDFG$^+$98]      L. Del Debbio, M. Faber, J. Giedt, J. Greensite, and S. Olejnik. Detection of center vortices in the lattice yang-mills vacuum. *Phys. Rev.*, D58:094501, 1998.

[DDFGO97a]      L. Del Debbio, M. Faber, J. Greensite, and S. Olejnik. Center dominance and z(2) vortices in su(2) lattice gauge theory. *Phys. Rev.*, D55:2298–2306, 1997.

[DDFGO97b]      L. Del Debbio, M. Faber, J. Greensite, and S. Olejnik. Center dominance, center vortices, and confinement. 1997.

[DDFGO98]      L. Del Debbio, M. Faber, J. Greensite, and S. Olejnik. Center vortices and the asymptotic string tension. *Nucl. Phys. Proc. Suppl.*, 63:552–554, 1998.

[dFD99]  Philippe de Forcrand and Massimo D'Elia. On the relevance of center vortices to qcd. *Phys. Rev. Lett.*, 82:4582–4585, 1999.

[DZ89]  G. Dell'Antonio and D. Zwanziger. Ellipsoidal bound on the gribov horizon contradicts the perturbative renormalization group. *Nucl. Phys.*, B326:333–350, 1989.

[EKKL99]  J. Engels, O. Kaczmarek, F. Karsch, and E. Laermann. The quenched limit of lattice qcd at non-zero baryon number. *Nucl. Phys.*, B558:307–326, 1999.

[Eli75]  S. Elitzur. Impossibility of spontaneously breaking local symmetries. *Phys. Rev.*, D12:3978–3982, 1975.

[ELRT98]  M. Engelhardt, K. Langfeld, H. Reinhardt, and O. Tennert. Interaction of confining vortices in su(2) lattice gauge theory. *Phys. Lett.*, B431:141–146, 1998.

[ELRT00]  M. Engelhardt, K. Langfeld, H. Reinhardt, and O. Tennert. Deconfinement in su(2) yang-mills theory as a center vortex percolation transition. *Phys. Rev.*, D61:054504, 2000.

[ER00a]  M. Engelhardt and H. Reinhardt. Center projection vortices in continuum yang-mills theory. *Nucl. Phys.*, B567:249, 2000.

[ER00b]  M. Engelhardt and H. Reinhardt. Center vortex model for the infrared sector of yang-mills theory: Confinement and deconfinement. *Nucl. Phys.*, B585:591–613, 2000.

[FA02]  C. S. Fischer and R. Alkofer. Infrared exponents and running coupling of su(n) yang-mills theories. *Phys. Lett.*, B536:177–184, 2002.

[FAR02]  C. S. Fischer, R. Alkofer, and H. Reinhardt. The elusiveness of infrared critical exponents in landau gauge yang-mills theories. *Phys. Rev.*, D65:094008, 2002.

[Fey69]  Richard P. Feynman. Very high-energy collisions of hadrons. *Phys. Rev. Lett.*, 23:1415–1417, 1969.

[FGO98]  M. Faber, J. Greensite, and S. Olejnik. Casimir scaling from center vortices: Towards an understanding of the adjoint string tension. *Phys. Rev.*, D57:2603–2609, 1998.

[FP67]  L. D. Faddeev and V. N. Popov. Feynman diagrams for the yang-mills field. *Phys. Lett.*, B25:29–30, 1967.

[G$^+$87]      Rajan Gupta et al. The hadron spectrum on a 18**3 x 42 lattice. *Phys. Rev.*, D36:2813, 1987.

[GLR04]      Jochen Gattnar, Kurt Langfeld, and Hugo Reinhardt. Signals of confinement in green functions of su(2) yang- mills theory. 2004.

[GM64]      Murray Gell-Mann. A schematic model of baryons and mesons. *Phys. Lett.*, 8:214–215, 1964.

[GM84]      F. Gutbrod and I. Montvay. Scaling of the quark - anti-quark potential and improved actions in su(2) lattice gauge theory. *Phys. Lett.*, B136:411, 1984.

[GPP$^+$98]      L. Giusti, M. L. Paciello, S. Petrarca, B. Taglienti, and M. Testa. On the definition of gauge field operators in lattice gauge-fixed theories. *Phys. Lett.*, B432:196–202, 1998.

[Gre03]      J. Greensite. The confinement problem in lattice gauge theory. *Prog. Part. Nucl. Phys.*, 51:1, 2003.

[Gri78]      V. N. Gribov. Quantization of non-abelian gauge theories. *Nucl. Phys.*, B139:1, 1978.

[GW73]      D. J. Gross and Frank Wilczek. Asymptotically free gauge theories. i. *Phys. Rev.*, D8:3633–3652, 1973.

[Hei03]      Ulrich W. Heinz. The quark-gluon plasma at rhic. *Nucl. Phys.*, A721:30–39, 2003.

[Kap]      J. I. Kapusta. Finite temperature field theory. Cambridge Monographs On Mathematical Physics (1993) 219 p.

[Kap92]      David B. Kaplan. A method for simulating chiral fermions on the lattice. *Phys. Lett.*, B288:342–347, 1992.

[KLM$^+$94]      L. Karkkainen, P. Lacock, D. E. Miller, B. Petersson, and T. Reisz. The physical phase of dimensionally reduced gauge theories. *Nucl. Phys.*, B418:3–14, 1994.

[KLRS97]      K. Kajantie, M. Laine, K. Rummukainen, and Mikhail E. Shaposhnikov. 3d su(n) + adjoint higgs theory and finite-temperature qcd. *Nucl. Phys.*, B503:357–384, 1997.

[Kog79]      John B. Kogut. An introduction to lattice gauge theory and spin systems. *Rev. Mod. Phys.*, 51:659, 1979.

[L$^+$02]      K. Langfeld et al. Vortex induced confinement and the ir properties of green functions. 2002.

[Lan89]     N. P. Landsman. Limitations to dimensional reduction at high temperature. *Nucl. Phys.*, B322:498, 1989.

[Lan02]     K. Langfeld. From lattice gauge theory to the physics of confinement. *lecture notes.* 2002.

[LB88]      M. Le Bellac. From critical phenomena to gauge fiels. an introduction to the methods and applications of quantum field thoery. reprint 1997. 1988. PARIS, FRANCE: INTEREDITIONS (1988) 639 P. PARIS, FRANCE: ED. CNRS (1988) 639p.

[LB96]      M. Le Bellac. Thermal field theory. 1996. Cambridge Univesity Press (1996) 256 p.

[Lin79]     Andrei D. Linde. Phase transitions in gauge theories and cosmology. *Rept. Prog. Phys.*, 42:389, 1979.

[LMR92]     Pierre LaCock, David E. Miller, and Thomas Reisz. Dimensional reduction of su(2) gauge theory beyond the perturbative horizon. *Nucl. Phys.*, B369:501–518, 1992.

[LRG02]     K. Langfeld, H. Reinhardt, and J. Gattnar. Gluon propagators and quark confinement. *Nucl. Phys.*, B621:131–156, 2002.

[LRT98]     Kurt Langfeld, Hugo Reinhardt, and Oliver Tennert. Confinement and scaling of the vortex vacuum of su(2) lattice gauge theory. *Phys. Lett.*, B419:317–321, 1998.

[LS00a]     Kurt Langfeld and Alexandra Schafke. Vortex dominance of the 0+ and 2+ glueball mass in su(2) lattice gauge theory. *Phys. Lett.*, B493:350–355, 2000.

[LS00b]     Kurt Langfeld and Gwansoo Shin. Lattice yang-mills theory at finite densities of heavy quarks. *Nucl. Phys.*, B572:266–288, 2000.

[LSG91]     W. Lucha, F. F. Schoberl, and D. Gromes. Bound states of quarks. *Phys. Rept.*, 200:127–240, 1991.

[LSWP99]    Derek B. Leinweber, Jon Ivar Skullerud, Anthony G. Williams, and Claudio Parrinello. Asymptotic scaling and infrared behavior of the gluon propagator. *Phys. Rev.*, D60:094507, 1999.

[LTER99]    K. Langfeld, O. Tennert, M. Engelhardt, and H. Reinhardt. Center vortices of yang-mills theory at finite temperatures. *Phys. Lett.*, B452:301, 1999.

[Mac]       Gerhard Mack. Properties of lattice gauge theory models at low temperatures. DESY 80/03.

[Man76]     S. Mandelstam. Vortices and quark confinement in nonabelian gauge theories. *Phys. Rept.*, 23:245–249, 1976.

[Man79]     S. Mandelstam. Approximation scheme for qcd. *Phys. Rev.*, D20:3223, 1979.

[MM]        I. Montvay and G. Munster. Quantum fields on a lattice. Cambridge, UK: Univ. Pr. (1994) 491 p. (Cambridge monographs on mathematical physics).

[MMST93]    P. Marenzoni, G. Martinelli, N. Stella, and M. Testa. High statistics study of the gluon propagator in the landau gauge at beta = 6.0. *Phys. Lett.*, B318:511–516, 1993.

[MO87]      J. E. Mandula and M. Ogilvie. The gluon is massive: A lattice calculation of the gluon propagator in the landau gauge. *Phys. Lett.*, B185:127–132, 1987.

[MP79]      G. Mack and V. B. Petkova. Comparison of lattice gauge theories with gauge groups z(2) and su(2). *Ann. Phys.*, 123:442, 1979.

[MRR+53]    N. Metropolis, A. W. Rosenbluth, M. N. Rosenbluth, A. H. Teller, and E. Teller. Equation of state calculations by fast computing machines. *J. Chem. Phys.*, 21:1087–1092, 1953.

[Nad90]     Sudhir Nadkarni. The su(2) adjoint higgs model in three-dimensions. *Nucl. Phys.*, B334:559, 1990.

[NN93]      Rajamani Narayanan and Herbert Neuberger. Infinitely many regulator fields for chiral fermions. *Phys. Lett.*, B302:62–69, 1993.

[NO79]      Holger Bech Nielsen and P. Olesen. A quantum liquid model for the qcd vacuum: Gauge and rotational invariance of domained and quantized homogeneous color fields. *Nucl. Phys.*, B160:380, 1979.

[OS73]      Konrad Osterwalder and Robert Schrader. Axioms for euclidean green's functions. *Commun. Math. Phys.*, 31:83–112, 1973.

[OS75]      Konrad Osterwalder and Robert Schrader. Axioms for euclidean green's functions. 2. *Commun. Math. Phys.*, 42:281, 1975.

[OS78]      K. Osterwalder and E. Seiler. Gauge field theories on the lattice. *Ann. Phys.*, 110:440, 1978.

[Par75]      G. Parisi. Quark imprisonment and vacuum repulsion. *Phys. Rev.*, D11:970, 1975.

[Pol73]      H. David Politzer. Reliable perturbative results for strong interactions? *Phys. Rev. Lett.*, 30:1346–1349, 1973.

[Pol74]      H. David Politzer. Asymptotic freedom: An approach to strong interactions. *Phys. Rept.*, 14:129–180, 1974.

[Pol75]      Alexander M. Polyakov. Compact gauge fields and the infrared catastrophe. *Phys. Lett.*, B59:82–84, 1975.

[Pol78]      Alexander M. Polyakov. Thermal properties of gauge fields and quark liberation. *Phys. Lett.*, B72:477–480, 1978.

[Rei96]      H. Reinhardt. Emergence of the haar measure in the standard functional integral representation of the yang-mills partition function. *Mod. Phys. Lett.*, A11:2451–2462, 1996.

[Rei02]      H. Reinhardt. Topology of center vortices. *Nucl. Phys.*, B628:133–166, 2002.

[Rei03]      H. Reinhardt. On 't hooft's loop operator. *Phys. Lett.*, B557:317–323, 2003.

[Roe]      G. Roepstorff. Path integral approach to quantum physics: An introduction. Berlin, Germany: Springer (1994) 387 p.

[RS00]      Craig D. Roberts and Sebastian M. Schmidt. Dyson-schwinger equations: Density, temperature and continuum strong qcd. *Prog. Part. Nucl. Phys.*, 45:S1–S103, 2000.

[RSTZ02]      H. Reinhardt, O. Schroeder, T. Tok, and V. C. Zhukovsky. Quark zero modes in intersecting center vortex gauge fields. *Phys. Rev.*, D66:085004, 2002.

[RW94]      Craig D. Roberts and Anthony G. Williams. Dyson-schwinger equations and their application to hadronic physics. *Prog. Part. Nucl. Phys.*, 33:477–575, 1994.

[Sch99]      Martin Schaden. Equivariant gauge fixing of su(2) lattice gauge theory. *Phys. Rev.*, D59:014508, 1999.

[Sei78]      E. Seiler. Upper bound on the color confining potential. *Phys. Rev.*, D18:482–483, 1978.

[Sei82]   E. Seiler. Gauge theories as a problem of constructive quantum field theory and statistical mechanics. *Lect. Notes Phys.*, 159:1–192, 1982.

[Sha84]   B. Sharpe. Gribov copies and the faddeev-popov formula in lattice gauge theories. *J. Math. Phys.*, 25:3324–3330, 1984.

[Shu80]   Edward V. Shuryak. Quantum chromodynamics and the theory of superdense matter. *Phys. Rept.*, 61:71–158, 1980.

[Smi]     A. Smilga. Lectures on quantum chromodynamics. Singapore, Singapore: World Scientific (2001) 322 p.

[SS96]    H. Suman and K. Schilling. First lattice study of ghost propagators in su(2) and su(3) gauge theories. *Phys. Lett.*, B373:314–318, 1996.

[Sti86]   M. Stingl. Propagation properties and condensate formation of the confined yang-mills field. *Phys. Rev.*, D34:3863, 1986.

[Sus79]   Leonard Susskind. Lattice models of quark confinement at high temperature. *Phys. Rev.*, D20:2610–2618, 1979.

[Suz71]   M. Suzuki. *Prog. Theor. Phys.*, 48:1337, 1971.

[SY82]    B. Simon and L. G. Yaffe. Rigorous perimeter law upper bound on wilson loops. *Phys. Lett.*, B115:145, 1982.

[Tay71]   J. C. Taylor. Ward identities and charge renormalization of the yang- mills field. *Nucl. Phys.*, B33:436–444, 1971.

[Tep99]   Michael J. Teper. Su(n) gauge theories in 2+1 dimensions. *Phys. Rev.*, D59:014512, 1999.

[tH71a]   Gerard 't Hooft. Renormalizable lagrangians for massive yang-mills fields. *Nucl. Phys.*, B35:167–188, 1971.

[tH71b]   Gerard 't Hooft. Renormalization of massless yang-mills fields. *Nucl. Phys.*, B33:173–199, 1971.

[tH75]    Gerard 't Hooft. Gauge fields with unified weak, electromagnetic, and strong interactions. 1975. Rapporteur's talk given at Int. Conf. on High Energy Physics, Palermo, Italy, Jun 23-28, 1975.

[tH78]    Gerard 't Hooft. On the phase transition towards permanent quark confinement. *Nucl. Phys.*, B138:1, 1978.

[Tro59]   H. F. Trotter. On the product of semi-groups of operators. *Proc. Am. Math. Soc.*, 10:545–551, 1959.

[vB00]       Pierre van Baal. Qcd in a finite volume. 2000.

[Vra01]      Pavlos M. Vranas. Domain wall fermions and applications. *Nucl. Phys. Proc. Suppl.*, 94:177–188, 2001.

[vSAH97]     Lorenz von Smekal, Reinhard Alkofer, and Andreas Hauck. The infrared behavior of gluon and ghost propagators in landau gauge qcd. *Phys. Rev. Lett.*, 79:3591–3594, 1997.

[vSHA98]     Lorenz von Smekal, Andreas Hauck, and Reinhard Alkofer. A solution to coupled dyson-schwinger equations for gluons and ghosts in landau gauge. *Ann. Phys.*, 267:1, 1998.

[WA01]       Peter Watson and Reinhard Alkofer. Verifying the kugo-ojima confinement criterion in landau gauge qcd. *Phys. Rev. Lett.*, 86:5239, 2001.

[Weg71]      F. J. Wegner. Duality in generalized ising models and phase transitions without local order parameters. *J. Math. Phys.*, 12:2259–2272, 1971.

[Wil74]      Kenneth G. Wilson. Confinement of quarks. *Phys. Rev.*, D10:2445–2459, 1974.

[Wil03]      Anthony G. Williams. Nonperturbative qcd, gauge-fixing, gribov copies, and the lattice. *Prog. Theor. Phys. Suppl.*, 151:154–160, 2003.

[YM54]       Chen-Ning Yang and R. L. Mills. Conservation of isotopic spin and isotopic gauge invariance. *Phys. Rev.*, 96:191–195, 1954.

[Zwa91]      D. Zwanziger. Vanishing of zero momentum lattice gluon propagator and color confinement. *Nucl. Phys.*, B364:127–161, 1991.

[Zwa92]      Daniel Zwanziger. Critical limit of lattice gauge theory. *Nucl. Phys.*, B378:525–590, 1992.

[Zwa94]      Daniel Zwanziger. Fundamental modular region, boltzmann factor and area law in lattice gauge theory. *Nucl. Phys.*, B412:657–730, 1994.

[Zwe64]      G. Zweig. An su(3) model for strong interaction symmetry and its breaking. 2. 1964. CERN-TH-412.

# Danksagung

An erster Stelle gilt mein Dank Prof. Dr. Hugo Reinhardt, der es mir ermöglicht hat, in seiner Arbeitsgruppe diese Dissertation anzufertigen. Stets war er an meiner wissenschaftlichen Arbeit interessiert und hat sie durch aufschlußreiche Diskussionen gefördert.

Mein ganz besonderer Dank gilt Herrn Priv.-Doz. Dr. habil. Kurt Langfeld. Sein fortlaufender Strom an Ideen, sein Enthusiasmus und seine Begeisterung an dem Thema meiner Arbeit waren eine große Stütze. Die exzellente Zusammenarbeit mit ihm habe ich sehr genossen und werde sie vermissen.

Ein großes Dankeschön geht auch an Dipl.-Phys. Laurent Moyaerts für die gute Zusammenarbeit und für die Diskussionen über Gittereichtheorie und numerische Verfahren, die sehr fruchtbar waren.

Meinem langjährigen Zimmerkollegen Dr. Oliver Schröder danke ich für die sehr angenehme Atmosphähre, die vielen ausgiebigen Gespräche, die sich nicht nur auf Physik beschränkten, und für das akribische Austreiben des Fehlerteufels. Auch möchte ich mich bei Dr. Torsten Tok für seine zahlreichen Anmerkungen und für das Korrekturlesen meiner Arbeit bedanken.

Der gesamten Arbeitsgruppe danke ich für das kollegiale Verhältnis und für die angenehme und förderliche Atmosphähre. Unsere gemeinsammen Kaffeerunden (und die dabei stattfindenden Diskussionen), die Kneipentouren und die (fast) wöchentlichen Fußballspiele werden mir fehlen.

An meine Freunde Bastl, Chris, Udo, meine Mitbewohner der Zundel-WG und meinen Freundeskreis geht ein ganz herzliches Dankeschön für das Ertragen meines Quängelns, für die Toleranz und für die zahlreichen Einladungen zum Essen.

Abschließend möchte ich mich ganz besonders bei meinen Eltern und meiner Schwester bedanken. Ohne ihr Verständnis, Unterstützung und Geduld wäre mir diese Arbeit niemals möglich gewesen. Daher möchte ich ihnen meine Doktorarbeit widmen.

# Lebenslauf

**Persönliche Daten**

| | |
|---|---|
| **Name:** | Jochen Gattnar |
| **Geboren:** | 28.12.1970 |
| **Geburtsort:** | Ruit auf den Fildern |
| **Familienstand:** | ledig |
| **Anschrift:** | Friedrich-Zundel-Str. 4 |
| | 72074 Tübingen |

**Werdegang**

| | |
|---|---|
| 1976 - 1980 | Grundschule Bissingen-Teck |
| 1980 - 1990 | Ludwig-Uhland Gymnasium, Kirchheim-Teck |
| 22.05.1990 | Abitur |
| 1991 - 1995 | Studium der Physik (Diplom) |
| | Eberhard-Karls-Universität zu Tübingen |
| 1995 - 1996 | Studium der Physik |
| | University College Dublin |
| 1996 - 1999 | Studium der Physik |
| | Eberhard-Karls-Universität zu Tübingen |
| 1998 - 1999 | Diplomarbeit "*Das effektive Potential für den Ordnungsparameter des $SU(3)$ Yang-Mills Deconfinement-Phasenübergangs*" bei Prof. Dr. Hugo Reinhardt und Dr. habil. Michael Engelhardt am Institut für Theoretische Physik der Eberhard-Karls-Univeristät zu Tübingen |
| 12.07.1999 | Diplom in Physik |
| seit 1999 | Anfertigung der Dissertation "*Aspects of Confinement in Lattice Gauge Field Theory*" unter der Anleitung von Prof. Dr. Hugo Reinhardt und Priv.-Doz. Dr. habil. Kurt Langfeld |

**Akademische Lehrer:**

Alkofer, Baumann, Clement, Dittrich, Fischer, Güttinger, Kaul, Kern, Kley, Kramer, Langfeld, Lichte, Lutz, McLaughlin, Montwill, Müther, O'Sullivan, Pfister, Plies, Reinhardt, Ruder, Schwenk, Staudt, Wagner, Yserentant

# Publikationen

1. J. Gattnar, K. Langfeld, A. Schafke, H. Reinhardt
   *"Center Vortex Dominance After Dimensional
   Reduction of SU(2) Lattice Gauge Theory."*
   Phys.Lett.B489: 251-258, 2000

2. K. Langfeld, H. Reinhardt, J. Gattnar
   *"Gluon Propagators and Quark Confinement."*
   Nucl.Phys.B621: 131-156, 2002

3. K. Langfeld, H. Reinhardt, J. Gattnar
   *"Manifestation of Confinement in the Gluon
   Propagator."*
   Nucl.Phys.Proc.Suppl.106: 673-675, 2002

4. K. Langfeld, J.C.R. Bloch, J. Gattnar, H. Reinhardt
   *"Vortex Induced Confinement and the IR Properties
   of Green Functions."*
   Gargnano 2002, Quark confinement and the hadron spectrum, 297-299

5. Jochen Gattnar, Kurt Langfeld, Hugo Reinhardt
   *"Signals of Confinement in Green Functions of
   SU(2) Yang-Mills Theory."*
   Phys.Rev.Lett.93: 061601, 2004